Antifibrotic Drugs: New Candidates for the Treatment of Pulmonary Arterial Hypertension?

Inaugural Dissertation

Submitted to the

Faculty of Biology and Chemistry

in partial fulfillment of the requirements

for the - Dr. rer. nat -

of the Faculties of Biology and Chemistry

at the Justus Liebig University Giessen

by

Lu, Changwu

Of

Shandong, China

Giessen 2017

From the Institute of Pulmonary Pharmacotherapy

Chairman: Prof. Dr. rer. nat. Ralph Schermuly

from the Faculty of Medicine of the Justus Liebig University Giessen

First Supervisor and Committee Member: Prof. Dr. rer. nat. Michael Martin

Second Supervisor and Committee Member: Prof. Dr. rer. nat. Ralph Schermuly

Committee Members: ....
....

Date of Doctoral Defense:

Table of Contents

Table of Contents

Table of Contents

Table of Contents

Table of Contents

INTRODUCTION

1 INTRODUCTION

1.1 The definition of pulmonary hypertension

The first description of pulmonary hypertension (PH) was from autopsy specimens over a century ago by the German physician Ernst von Romberg [1]. The first clinical and hemodynamic study was published in 1951 by Dresdale [2]. Pulmonary hypertension is defined as a sustained elevation in mean pulmonary artery pressure (mPAP) of 25 mm Hg or more at rest, and it must be assessed by right heart catheterization. The pressure in a normal pulmonary artery is in the range of 14 ± 3 mm Hg with a normal upper limit of approximately 20 mm Hg at rest. The clinical significance of a mPAP of 21-24 mm Hg is unclear. People with a mPAP in this range are at risk of developing pulmonary arterial hypertension (PAH) and should be closely monitored. Furthermore, PH can be subclassified as precapillary (PAWP ≤15 mm Hg) or postcapillary (PAWP >15 mm Hg) according to the level of pulmonary artery wedge pressure (PAWP) [3].

1.2 The classification of pulmonary hypertension

Pulmonary hypertension was initially classified into primary PH and secondary PH based on the absence or presence of identifiable causes. With a better understanding of the disease, the classification of PH has gone through a series of changes based on mechanisms rather than associated conditions. According to the updated clinical classification of PH by the consensus in 5th World Symposium on Pulmonary Hypertension in 2013, PH was classified into five categories (Table 1, next page) that share similar pathophysiologic mechanisms, clinical presentations, and therapeutic approaches [3, 4].

PAH represents a subgroup of PH patients who are hemodynamically characterized by the presence of pre-capillary PH. These patients have a PAWP of ⩽15 mmHg and a pulmonary vascular resistance (PVR) of >3 Wood units (WU), without other causes of pre-capillary PH such as PH due to lung diseases, chronic thromboembolic pulmonary hypertension (CTEPH), or other rare diseases [5]. Pulmonary arterial hypertension has several subcategories that differ in etiology, though these categories share similar pathological and hemodynamic characteristics and terms of clinical management [5]. These pathological features include pulmonary arterial endothelial cell (EC) dysfunction, pulmonary artery EC and smooth muscle cell (SMC) proliferation, vasoconstriction, and in situ thrombosis [6, 7].

Table 1 Clinical classification of pulmonary hypertension

1. Pulmonary arterial hypertension (PAH)
1.1 Idiopathic 1.2 Heritable 1.2.1 BMPR2 mutation 1.2.2 ALK1, ENG, SMAD9, CAV1 and KCNK3 mutation 1.2.3 Unknown 1.3 Drugs and toxins induced 1.4 Associated with: 1.4.1 Connective tissue disease 1.4.2 HIV infection 1.4.3 Portal hypertension 1.4.4 Congenital heart disease 1.4.5 Schistosomiasis
1'. Pulmonary veno-occlusive disease and/or pulmonary capillary haemangiomatosis
1". Persistent pulmonary hypertension of the newborn
2. Pulmonary hypertension due to left heart disease
2.1 Left ventricular systolic dysfunction 2.2 Left ventricular diastolic dysfunction 2.3 Valvular disease 2.4 Congenital/acquired left heart inflow/outflow tract obstruction and congenital cardiomyopathies 2.5 Other
3. Pulmonary hypertension due to lung diseases and/or hypoxia
3.1 Chronic obstructive pulmonary disease 3.2 Interstitial lung disease 3.3 Other pulmonary diseases with mixed restrictive and obstructive patterns 3.4 Sleep-disordered breathing 3.5 Alveolar hypoventilation disorders 3.6 Chronic exposure to high altitude 3.7 Developmental lung diseases
4. Chronic thromboembolic pulmonary hypertension and other pulmonary artery obstructions
4.1 Chronic thromboembolic pulmonary hypertension 4.2 Other pulmonary artery obstructions
5. Pulmonary hypertension with unclear and/or multifactorial mechanisms
5.1 Haematological disorders: chronic haemolytic anaemia, myeloproliferative disorders and splenectomy 5.2 Systemic disorders: sarcoidosis, pulmonary histiocytosis and lymphangioleiomyomatosis 5.3 Metabolic disorders: glycogen storage disease, Gaucher disease and thyroid disorders 5.4 Others: tumoral obstruction, fibrosing mediastinitis, chronic renal failure, and segmental PH

BMPR2: bone morphogenic protein receptor type II; ALK1: activin receptor-like kinase 1; ENG: endoglin; CAV1: caveolin-1; KCNK3: potassium channel, two pore domain subfamily K, member 3. (Updated from Simonneau et al. 2013) [4].

1.3 The epidemiology of pulmonary arterial hypertension

Right heart catheterization is required for a reliable diagnosis of PH. This invasive examination procedure for epidemiology studies is not ethical or feasible which makes the incidence and prevalence of PH more difficult to study than that of systemic

hypertension. Large-scale, population-based epidemiology investigations must be based on echocardiography, although this is not the gold standard for diagnosing PH. According to the investigations and reports from registries, all age groups are affected by this condition, and it has rapidly growing importance in elderly people in countries with aging populations [6]. Present estimates suggest a PH prevalence of approximately 1% of the global population, which increases to 10% in individuals over 65 years old. This disease was estimated to affect 50 million to 70 million people worldwide in 2015 [6]. Thus, PH is a substantial global health issue [6].

Most of the registries for PAH are in developed countries [6]. The incidence of PAH in European countries ranges from 1.1 to 7.6 per million adults per year, and the prevalence of PAH is from 6.6 to 26.0 per million adults [6, 8-14]. The rough estimate for the global incidence of PAH is about five per million adults per year and the prevalence is approximately 15 per million adults. These numbers are generally underestimated because they do not include PAH associated with congenital heart disease, schistosomiasis, or HIV infection, which are prevalent in some countries of the world [6]. In addition, PAH affects young, female individuals [15]. Although female sex is a risk factor for this disease, females have better survival rates than males [15].

1.4 The pathology of pulmonary arterial hypertension

Pulmonary arterial hypertension has a multifactorial and complicated pathobiology [7]. The molecular mechanisms of PAH are still not clear, though the understanding has expanded significantly in recent years. Although the classification of PAH includes many different sub-categories, there is a common pathway which results from a combination of environmental factors and genetic predispositions. The different sub-categories of PAH are characterized by excessive pulmonary vasoconstriction and abnormal vascular remodeling processes that usually affect all vessel layers (Figure 1) [16, 17]. This vascular remodeling and its consequent pulmonary vascular obstruction lead to a progressive increase in pulmonary vascular resistance. This resistance increases right ventricular afterload, resulting in right ventricular hypertrophy and ultimately right ventricular failure and death.

The abnormalities of the pulmonary vasculature include (1) abnormal muscularization of distal precapillary arteries, (2) medial hypertrophy and thickness of large pulmonary muscular arteries, (3) loss of precapillary arteries, (4) neointimal formation, and (5) formation of angio-proliferative plexiform lesions in these vessels [16].

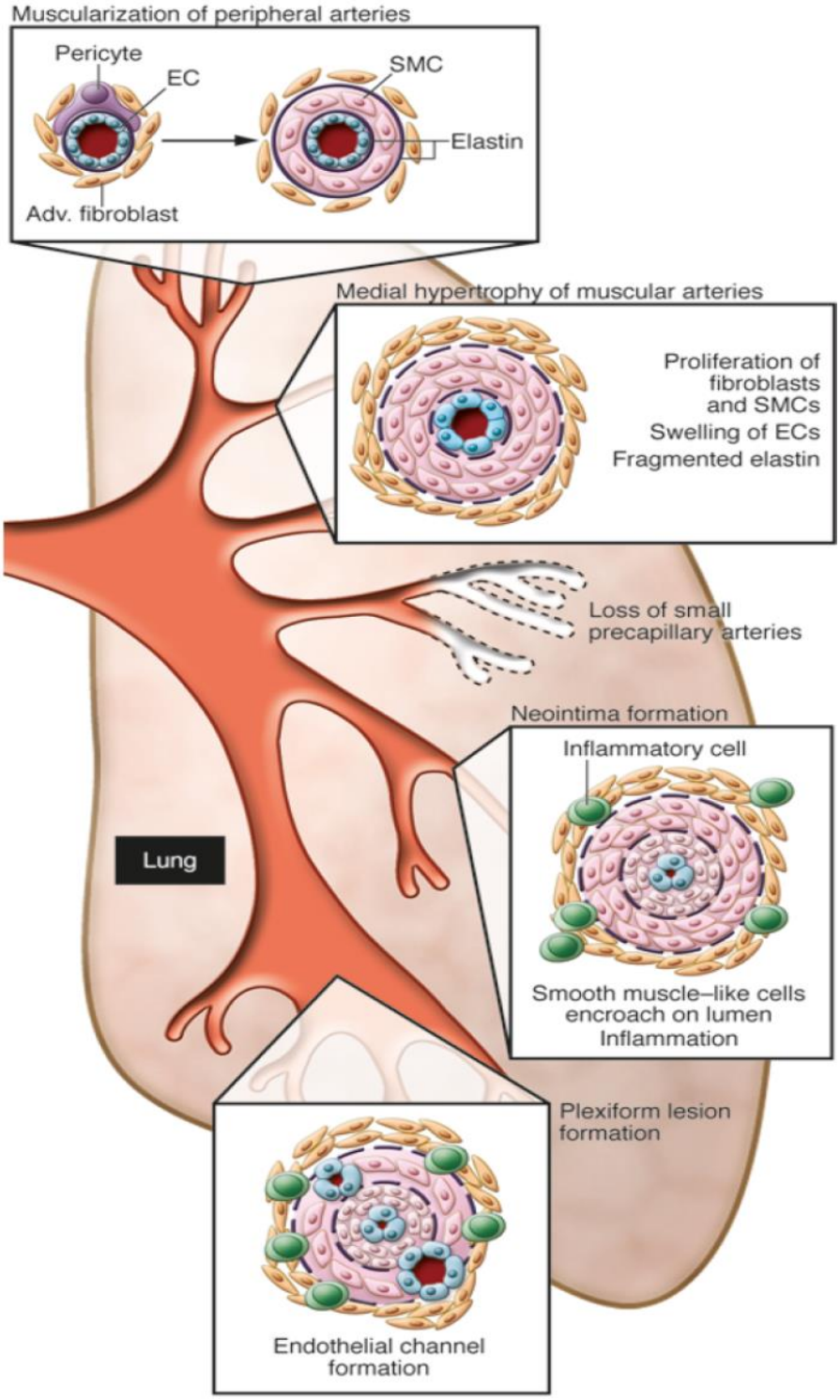

Figure 1. The pathobiology of pulmonary arterial hypertension.

Scheme is illustrating the different vascular abnormalities associated with PAH compared to normal pulmonary circulation and depicts the abnormalities throughout the pulmonary circulation (Rabinovitch, 2012) [16].

1.5 The histology of pulmonary arterial hypertension

The pathological changes associated with PAH predominantly occur in the small distal pulmonary arteries (<500 μm), and do not affect pulmonary veins [7]. The histological features of PAH include the infiltration of inflammatory or progenitor cells, in situ thrombosis, the occlusion of small arteries, intimal hyperplasia, medial hypertrophy, adventitial proliferation or fibrosis, and angio-proliferative plexiform lesions (Figure 2) [18].

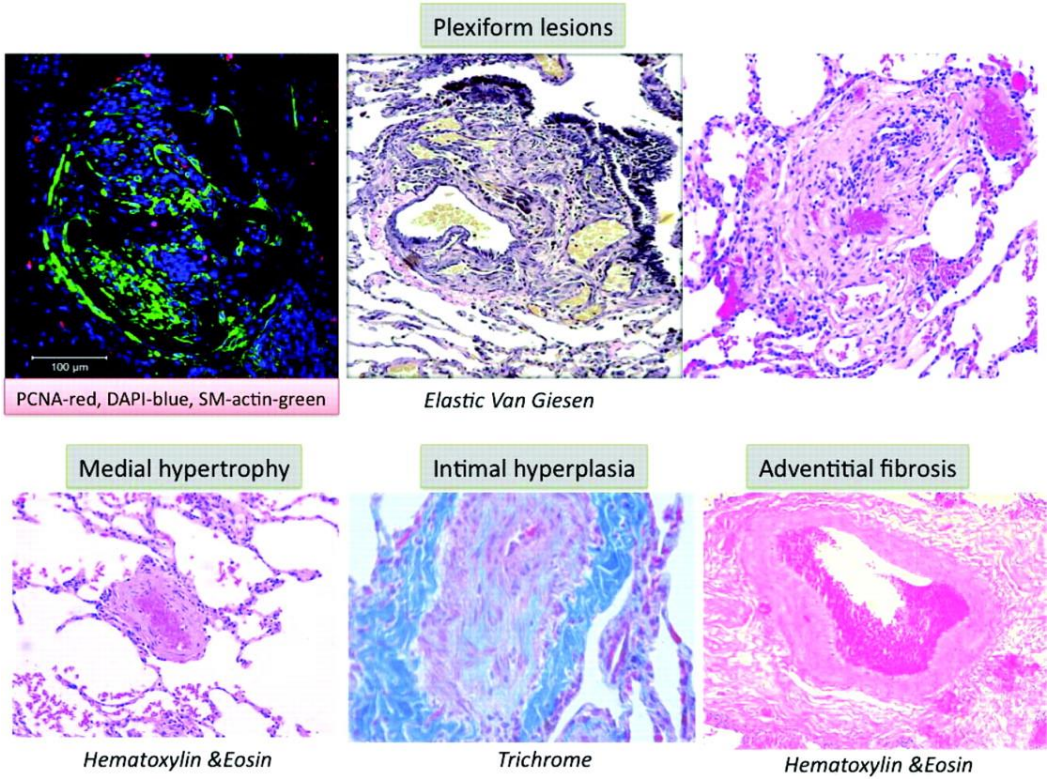

Figure 2. Histology of PAH.

Plexiform lesions are shown at the top. Evidence of cell proliferation is shown on the upper left; proliferating cell nuclear antigen (PCNA) is in red, smooth muscle (SM) actin is in green, and DAPI (4',6-diamidino-2-phenylindole) nucleus staining is in blue. Medial hypertrophy, intimal fibrosis, and adventitial proliferation are displayed at the bottom (Archer, 2010) [18].

1.6 Molecular mechanisms of pulmonary arterial hypertension

1.6.1 The imbalance of vasoactive mediators in the pathogenesis of pulmonary arterial hypertension

The regulation of vascular tone is maintained by the balance between vasodilators such as nitric oxide (NO) and prostacyclin, and vasoconstrictors such as thromboxane A2 and endothelin-1 (ET-1) [19]. Endothelial dysfunction due to inflammation or shear stress is a primary cause of persistent vasoconstriction as it disrupts this balance. Excessive vasoconstriction is the result of endothelial dysfunction leading to the chronically impaired production of vasodilators and antiproliferative agents such as NO

and prostacyclin, along with overexpression of vasoconstrictors and proliferative substances such as thromboxane A2 and ET-1.

1.6.1.1 Nitric oxide

Nitric oxide is synthesized in the endothelium by the endothelial NO synthase (eNOS), which catalyzes the oxidation of l-arginine to produce l-citrulline in the presence of oxygen, nicotinamide adenine dinucleotide phosphate (NADPH), and essential cofactors such as tetrahydrobiopterin (BH4). Once formed, NO diffuses from the endothelium to the vascular smooth muscle cell (SMC) and activates the sGC/cGMP pathway [20]. The activation of sGC converts guanosine 5'-triphosphate (GTP) to cyclic guanosine 3',5'-monophosphate (cGMP), which then activates downstream cGMP-dependent protein kinase G (PKG) and reduces intracellular calcium to induce vasodilation [20].

The critical role of NO in the development of PAH is supported by the evidence of reduced eNOS expression in the pulmonary vasculature in PAH patients [21]. Furthermore, eNOS-null mice are more susceptible to chronic hypoxia that triggers PH than wild-type mice, suggesting that NO acts as a vasodilator and inhibits SMC proliferation, platelet aggregation, and thrombosis in the blood vessel lumen [22].

1.6.1.2 Prostacyclin

Prostacyclin is a prostaglandin member of the eicosanoid family of lipid molecules. Prostacyclin is an effective vasodilator that can also attenuate vascular SMC proliferation, inhibit platelet aggregation, and exert anti-inflammatory and antithrombotic effects. Prostacyclin binds to its specific I-prostanoid receptor in the underlying SMCs to promote relaxation and subsequent vasodilation by activating adenylyl cyclase and increasing intracellular cAMP levels, which then activates protein kinase A (PKA) [23].

The level of prostacyclin decreases in patients with PAH [24], and the expression of prostacyclin receptors and synthases are reduced in these patients [25, 26]. Moreover, mice with prostacyclin receptor deficiency develop severe PAH and vascular remodeling after chronic hypoxia exposure [25]. This evidence indicates that prostacyclin plays an important role in the development of PAH.

1.6.1.3 Endothelin-1

Endothelin-1 is one of the most potent vasoconstrictors in biology [27]. There are two different G-protein–coupled receptors: endothelin receptor type A (ETA) and endothelin receptor type B (ETB) for ET-1 binding [27]. Endothelin receptor type A receptors are predominantly expressed on vascular smooth muscle cells, and they mediate

vasoconstriction, proliferation, hypertrophy, cell migration, and fibrosis. Endothelin receptor type B receptors are located on ECs and SMCs. Although their activation on SMCs results in vasoconstriction, ETB activation on endothelial cells produces vasodilation and anti-proliferation by increasing the production of NO and prostacyclin [28].

The level of ET-1 is elevated in patients with PAH and animals of the PAH model. Big ET-1 (precursor of ET-1) level in the plasma also increases in PAH patients [29-31]. In addition, the expression of constrictive ETA and ETB both increase on SMCs, and decreased expression of vasodilatory ETB has been found in ECs as PAH progresses [28]. An increasing number of translational therapies targeting the NO–sGC–cGMP pathway, prostacyclin pathway, and endothelin-1 pathway have been effective in the treatment of PAH in the clinic (Figure 3) [20], which confirms the importance of these three pathways in the development of PAH.

1.6.2 The role of growth factors in pulmonary arterial hypertension

Growth factors such as platelet-derived growth factor (PDGF), fibroblast growth factor (FGF), transforming growth factor β (TGFβ), vascular endothelial growth factor (VEGF), and hepatocyte growth factor (HGF) are involved in the remodeling process in PAH [7]. Growth factors are potent mitogens and chemoattractants for vascular cells, such as SMCs, fibroblasts, and ECs. Activation of cell surface tyrosine kinase receptors (TKR) initiates major intracellular signaling cascades. These signaling cascades control many cellular functions and processes, including cellular proliferation, migration, differentiation, resistance to apoptosis, and extracellular matrix deposition [17].

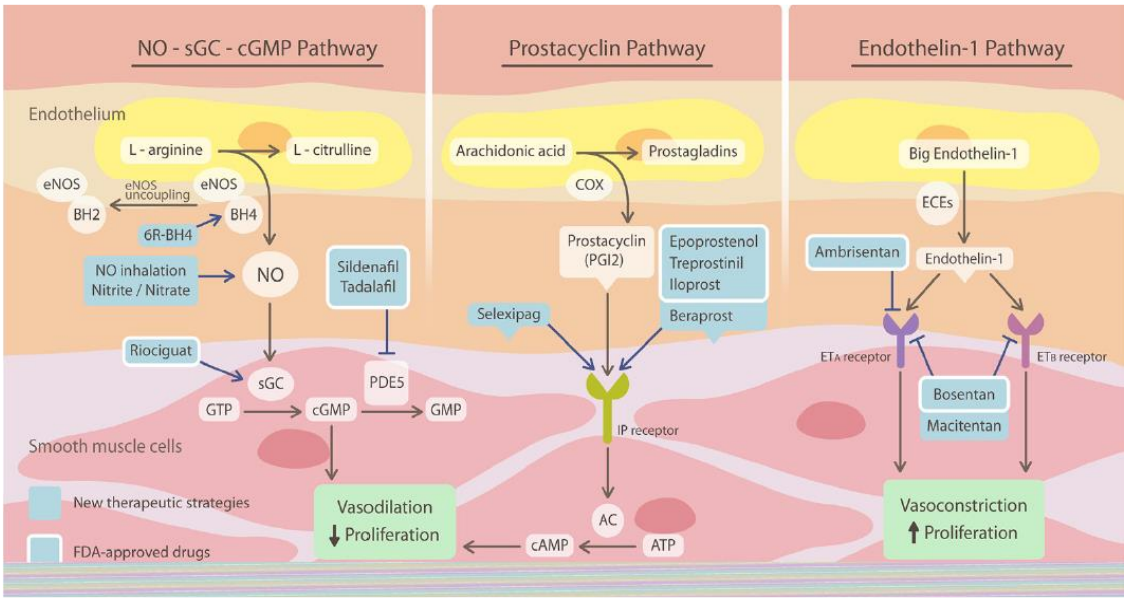

Figure 3. Classic vasodilator and vasoconstrictor systems and their translational therapies for PAH.

Nitric oxide activates the vasodilation and antiproliferation of SMC via a cGMP-dependent mechanism. Inhalation of NO, administration of nitrite or nitrate, sGC stimulator (riociguat), phosphodiesterase 5 (PDE5) inhibitors (sildenafil and tadalafil), and BH4 analog (6R-BH4) have been effective in the treatment of PAH. Prostacyclin activates vasodilation and inhibits proliferation of smooth muscle cells via a cAMP-dependent mechanism. Prostacyclin and its derivatives (epoprostenol, treprostinil, iloprost, and beraprost) and I-prostanoid (IP) receptor agonists (selexipag) provide therapeutic benefit in PAH, and ET-1 stimulates vasoconstriction and proliferation via activation of ETA and ETB receptors on SMC. In addition, ETA blocker (ambrisentan) and dual ET-1 blockers (bosentan and macitentan) are useful in the treatment of PAH; AC indicates adenylyl cyclase; BH2, dihydrobiopterin; COX, cyclooxygenase; ECEs, endothelin-converting enzymes; eNOS, endothelial NO synthase; FDA, Food and Drug Administration (Lai, 2014) [20].

1.6.2.1 Platelet-derived growth factor

Platelet-derived growth factor (PDGF) acts as a potent mitogen and chemoattractant for pulmonary artery smooth muscle cells (PASMCs). The expression of PDGF and its receptor is elevated in the lungs of patients with PAH, and PDGF receptor expression is increased in experimental PH models [32-35]. Imatinib, the first tyrosine kinase inhibitor (TKI) for the treatment of chronic myeloid leukemia (CML), reversed advanced pulmonary vascular disease in two animal models of PH by inhibiting PDGF signaling [36]. In a randomized, multicenter, placebo controlled phase III trial, imatinib demonstrated efficacy, improved exercise capacity and hemodynamics in patients with advanced PAH (IMPRES trial) [37].

1.6.2.2 Fibroblast growth factor

Fibroblast growth factor 2 (FGF2), also known as bFGF or FGF-β, is a member of the fibroblast growth factor family. Fibroblast growth factor 2 levels in plasma and urine are significantly elevated in patients with PAH [38]. Furthermore, hypoxia and shear-stress-induced FGF2 upregulation is observed in rat and ovine pulmonary arterial SMC [39, 40], and upregulation of FGF-2 occurs in lambs with PH [41], but not in hypoxic mice [42]. Fibroblast growth factor 2 small interfering RNA treatment prevents lung FGF2 production and almost reverses monocrotaline-induced PH in rats [43]. In addition, the pharmacological inhibition of FGF receptor 1 reverses established PH in the same model [43].

1.6.2.3 Hepatocyte growth factor

Hepatocyte growth factor is secreted by mesenchymal cells and it acts as a multi-functional cytokine, primarily on cells of epithelial origin; it signals these cells through tyrosine phosphorylation of its receptor, c-Met. Hepatocyte growth factor expression downregulates under hypoxia in vascular cells and organ culture systems [44], and HGF production is decreased in monocrotaline-induced PH in rats [45]. Moreover, HGF gene transfer inhibits vascular medial hyperplasia and matrix accumulation to attenuate the development of monocrotaline-induced PH in rats [45, 46]. This growth factor might have a protective role in pulmonary vascular remodeling, but more preclinical and clinical studies are required to confirm this.

1.6.2.4 Vascular endothelial growth factor

Vascular endothelial growth factor is a sub-family of the PDGF family which has five members: placental growth factor and VEGF A, B, C, and D. The expression of VEGF and VEGF receptor 2 (VEGFR-2) is upregulated in the plexiform lesions of patients with PAH [47, 48], indicating a role for VEGF in the pathogenesis of PAH. However, data from animal models have been inconsistent. Vascular endothelial growth factor is down-regulated in rats with monocrotaline-induced PH, but increased in rats with chronic hypoxic PH [49, 50]. The VEGFR-2 antagonist Sugen5416 is combined with chronic hypoxia in rats, and induces severe PH with angioproliferative lesions (plexiform lesions) [51]. Thus, the inhibition of VEGF plays a role in the development of PH. However, the inhibition of VEGF signaling (and others) by the multikinase inhibitor sorafenib in rats attenuates experimental PH (i.e. monocrotaline-induced or VEGFR inhibition combined with hypoxia) [52, 53]. The controversies regarding the role of VEGF in the pathogenesis of PH continue, as results from experiments that used VEGF treatment for rats with established PH show that it aggravated the disease [54]. However, gene-transfer-

mediated VEGF overexpression attenuates the development of experimental PH in rats (monocrotaline-induced, pulmonary fibrosis, and hypoxic models) [55-57].

1.6.2.5 Epidermal growth factor

Transforming growth factor alpha (TGF-α), a member of the EGF family, is a mitogenic polypeptide. Pulmonary overexpression of TGF-α results in vascular remodeling and the development of PH in mice [58]. The inhibition of the EGF receptors attenuates monocrotaline-induced PH in rats [59, 60], but it does not improve chronic hypoxia-induced PH in mice [59].

1.6.2.6 Transforming growth factor β

The TGF-β superfamily is involved in regulating homeostasis and multiple cellular functions, including proliferation, differentiation, apoptosis and endothelial mesenchymal transition (endo-MT) [61]. The TGF-β superfamily is comprised of a large series of cytokine growth factors. Transforming growth factor β members are cataloged into several subfamilies, including the prototypic TGF-β ligands, receptors, accessory molecules, activins, and the bone morphogenetic proteins (BMP) which are the largest of these groups [62]. Among them, BMP receptor 2 (BMPR2), activin receptor-like kinase 1 (ALK1), and endoglin (ENG) are recognized as causal factors in hereditary and associated forms of PAH [63]. Bone morphogenetic protein receptor 2 encodes a type 2 receptor for bone morphogenetic proteins involved in the control of vascular cell proliferation. Mutations in these receptors have been identified that account for approximately 75% of patients with a known family history of PAH, and up to 25% of apparently sporadic cases [64]. Bone morphogenetic protein receptor 2 is the major predisposing gene and BMPR2 defects in this gene are the major genetic determinant underlying PAH. Other genes related to TGF-β superfamily receptor signaling have been identified as rare causes of PAH. For example, ALK1 and ENG are present when PAH is associated with hereditary hemorrhagic telangiectasia [65, 66].

1.6.3 The role of inflammation in pulmonary arterial hypertension

Inflammation plays a prominent role in the initiation and progression of human PAH and in experimental models of PH [7, 67]. Monocytes, macrophages, T lymphocytes and dendritic cells are found in plexiform lesions and other vascular lesions of PAH-affected human lungs [68]. Furthermore, inflammation contributes to the growth of pulmonary plexiform lesions which are characteristic features of PAH [69]. The inflammatory cells and cytokines and chemokines which induced by these cells all regulate the growth, migration, and differentiation of all cell types, leading to vascular remodeling [67].

The circulating levels of monocyte chemoattractant protein 1, tumor necrosis factor (TNF), interleukin-1β (IL-1β), and interleukin-6 (IL-6) were increased in patients with idiopathic pulmonary arterial hypertension (IPAH) [70, 71]. Animal models also support the role of inflammatory cytokines in the initiation, development, and progression of PAH. Monocrotaline-treated (MCT) rats showed increased IL-1 expression in their lungs, and repeated injections of an IL-1 receptor antagonist reduced PH and right heart hypertrophy in this MCT model [72]. Increased IL-6 expression was also found in the MCT model, and rats injected with IL-6 developed PH [73, 74]. Furthermore, overexpression of IL-6-induced PH in mice [75], and IL-6-deficient mice were protected from hypoxia-driven lung inflammation and pulmonary vascular remodeling in this animal model [76]. Cytokines can be also used as biomarkers to diagnose PAH in patients.

1.6.4 Collagen deposition and fibrosis in pulmonary arterial hypertension

Excessive vascular collagen accumulation in the large pulmonary arteries of rats with hypoxic PH plays a role in decreased pulmonary vascular compliance [77], and the expression of collagen 1 in hypoxic mice prevents the mechanical properties of the extralobar pulmonary arteries from returning to normal after removal from hypoxic conditions [78]. In addition to the pathogenesis mentioned above, thrombosis, proteases, elastases, peroxisome proliferator-activated receptors (PPARs), and mitochondrial dysfunction are all involved in the initiation and development of PAH [7].

1.7 Treatment

Although there are several treatment options available, there is no cure for PAH. The treatment process of PAH patients cannot be considered solely as the prescription of drugs, as it is characterized by a complex strategy that includes the initial evaluation of severity and the subsequent response to treatment [5].

Treatment for PAH includes conventional therapy and specific drug therapy by vasodilators. Conventional therapy for PAH can include oral anticoagulation, diuretics, supplemental oxygen, and digoxin, and other cardiovascular drugs. Lung or heart-lung transplants are treatment options that are reserved for patients who are not improving with medical therapies [5].

Three separate signaling pathways involved in vascular dilation can be addressed with specific approved drugs for the specific drug therapy [79]. Prostacyclin (epoprostenol), prostacyclin analogs, and prostacyclin receptor agonists are applied to target the prostacyclin pathway. In addition, phosphodiesterase type 5 inhibitors and guanylate cyclase stimulators address the NO pathway and endothelium receptor

antagonists are applied to inhibit the endothelin pathway. The clinical experiences and meta-analysis show that combinations of therapies with existing drugs under different mechanisms of action maximize therapeutic benefits and minimize side effects [5].

To further improve symptoms and prognosis, in addition to these three well-known pathways, therapeutic strategies targeted at diverse pathobiological changes are being explored. The following compounds are under investigation for future use: TKIs, rho kinase inhibitors, VEGF receptor inhibitors, angiopoietin-1 inhibitors, and elastase inhibitors [5].

1.8 Animal models of pulmonary hypertension

To understand the pathophysiological mechanisms underlying the pathogenesis of PAH and to find an effective treatment for PAH, animal models are used to simulate the disease. There are several well-accepted animal models established that mimic the human situation, including MCT-induced PH, hypoxia-induced PH, and Sugen5416 plus chronic hypoxia exposure induced PH [80-83].

MCT-induced PH is the oldest model and it is still frequently investigated [83, 84]. However, the neointima lesions observed in patients with PAH are not formed in MCT-induced PH rats. Moreover, many agents that are not efficacious for PAH patients have been reported to prevent or cure vascular remodeling in this model [82]. Chronic hypoxia is the most commonly used physiological stimulus for PH development in animal models. This experimental model of PH represents group 3 of the PH classification. The main issue with this animal model is that remodeling is reversed after returning to normoxic conditions.

A rat model that mimics the pulmonary vascular changes as seen in human PAH, was recently developed. It is a combination of a single subcutaneous injection of the VEGF receptor inhibitor Sugen5416 together with exposure to chronic hypoxia (SuHx) for 3–5 weeks followed by re-exposure to normoxia [85]. The SuHx rat develop endothelial cell proliferation, an occlusion of small precapillary arterioles and vascular remodeling that does not reverse after being re-exposed to normoxia [86]. This model is relevant to human PAH because pulmonary hypertension is severe, progressive and refractory to treatment as it is in most PAH patients [81, 86].

1.9 Antifibrotic drug: Pirfenidone

Pirfenidone is an orally available pyridone analog [5-methyl-1-phenyl-2-(1H)-pyridone]; it is multifunctional with antifibrotic, anti-inflammatory, and antioxidant activities [87]. This drug was initially developed as an anti-inflammatory agent in 1967,

but the focus was then shifted to developing pirfenidone as an antifibrotic agent since it was found to have antifibrotic activity in a hamster model of bleomycin-induced lung fibrosis [87-89]. Pirfenidone also showed antifibrotic properties in several animal models of heart, liver, and renal fibrosis [89, 90].

Pirfenidone was first approved for idiopathic pulmonary fibrosis (IPF) treatment in Japan in 2008. However, it was not approved by the US Food and Drug Administration (FDA) in the United States of America (USA) due to conflicting results of phase III trials assessing the efficacy of pirfenidone from the SP3 trial in Japan and the multinational CAPACITY trials [91, 92]. Additional clinical evidence to support the use of pirfenidone in the USA was requested by the FDA. To assess and confirm the efficacy and safety of pirfenidone, the ASCEND study was performed in IPF patients. In this clinical trial, pirfenidone demonstrated remarkable efficacy in IPF treatment, including a significant reduction in the primary endpoint, a decline in forced vital capacity (FVC) over one year, less decline in the six-minute walk test distance, and improved progression-free survival. No side effects were reported related to respiratory symptoms or mortality [93-95]. The FDA granted pirfenidone (Esbriet) fast track status, priority review, orphan drug designation, and breakthrough therapy designation [96], and pirfenidone was approved on 15 Oct 2014 by the FDA [96]. In addition to its clinical indication for IPF, a randomized and placebo-controlled clinical trial showed that pirfenidone also has potential benefits for diabetic nephropathy [97].

The key target molecule and precise mechanism of action for pirfenidone are not clear, and further studies are needed to explore its precise mechanism of action. Pirfenidone appears to exert inhibitory effects on multiple pathways that lead to the development of IPF as shown in Figure 4 [87]. The antifibrotic efficacy of pirfenidone is likely due to the inhibition of TGF-β, which is an important pro-fibrotic cytokine and biomarker of lung fibrosis that is extensively involved in the development of lung fibrosis [98]. The mechanism of action for pirfenidone also includes suppression of inflammation by regulating the expression of pro-fibrotic factors and proinflammatory cytokines. Pirfenidone demonstrates attenuation of the expression of IL-1β, IL-6, and TNF-α to decrease the fibrotic response [87, 99]. A reduction in oxidative stress is another mechanism of pirfenidone for treating lung fibrosis. Misra’s research found that pirfenidone inhibited NADPH-dependent microsomal lipid peroxidation and scavenged hydroxyl radicals [100].

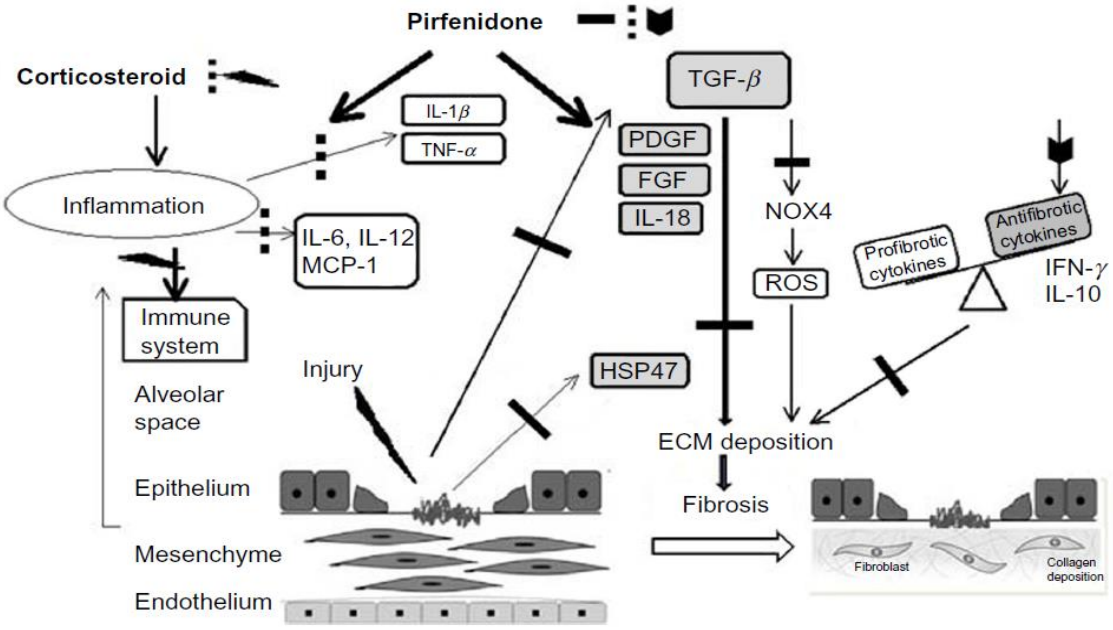

Figure 4. Potential mechanisms for the suppression of fibrogenesis by pirfenidone.

Notes: Pirfenidone may inhibit the production of pro-fibrotic cytokines, inflammatory cytokines, collagen-specific chaperone HSP-47, and reactive oxygen species, and stimulate the production of IFN-γ and IL-10. It has, however, limited suppressive activity for immunity, which is strongly suppressed by corticosteroids. ECM, extracellular matrix; FGF, fibroblast growth factor; HSP, heat shock protein; IFN, interferon; IL, interleukin; MCP, monocyte chemoattractant protein; NOX, NADPH oxidase isoform; PDGF, platelet-derived growth factor; ROS, reactive oxygen species; TGF, transforming growth factor; TNF, tumor necrosis factor (Takeda, 2014) [87].

1.10 Antifibrotic drug: Nintedanib

Nintedanib is a tyrosine kinase inhibitor (TKI) for the treatment of IPF and non-small-cell lung cancer from Boehringer Ingelheim, Germany. Nintedanib (formerly known by its development code BIBF 1120), is a small molecule that was originally designed as an ATP-competitive inhibitor of fibroblast growth factor receptor 1 (FGFR 1) and vascular endothelial growth factor receptor 2 (VEGFR 2) [101, 102]. Both of these tyrosine kinases receptors are pro-angiogenic, and BIBF1120 was selected as an antiangiogenic drug and developed for cancer therapy. Nintedanib is approved in Europe for non-small-cell lung cancer patients with advanced adenocarcinoma after first-line chemotherapy [103].

Studies also show that nintedanib is also a potent inhibitor of platelet-derived growth factor receptor (PDGFR)-α and β, and a new indication for nintedanib was appointed for its development as a potential treatment for IPF [103, 104]. Two phase III clinical trials, INPULSIS-1 and INPULSIS-2, showed that nintedanib slowed disease progression in

patients with IPF by reducing the annual rate of decline in forced vital capacity (FVC) [105].

Nintedanib is a small molecule that inhibits multiple receptor tyrosine kinases (RTKs) and non-receptor tyrosine kinases (nRTKs) [106]. Nintedanib inhibits the following RTKs: PDGFR α and β, FGFR 1-3, VEGFR 1-3, and Fms-like tyrosine kinase-3 (FLT3). Among them, FGFR, PDGFR, and VEGFR have been implicated in IPF pathogenesis [107]. Nintedanib binds competitively to the ATP binding pocket of these receptors and blocks intracellular signaling for the proliferation, migration, and transformation of fibroblasts, representing the essential mechanisms of IPF pathology. The following nRTKs were inhibited by nintedanib: Lck, Lyn, and Src kinases [106].

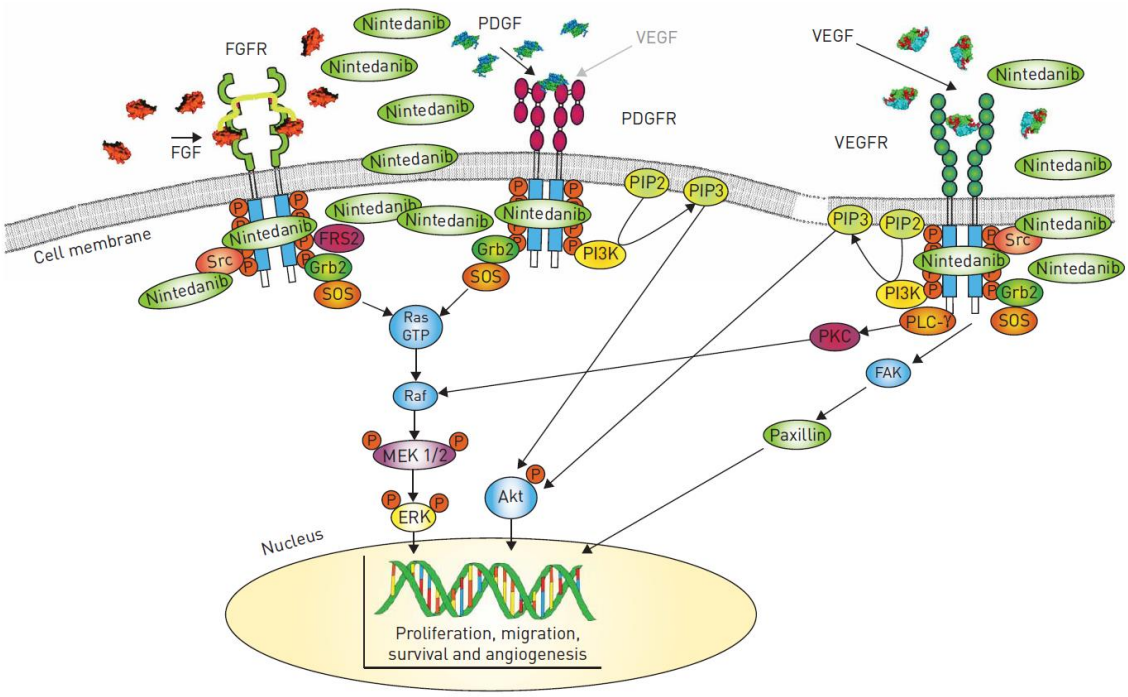

Figure 5. The pharmacology of nintedanib and the downstream signaling pathways.
FAK: focal adhesion kinase; FGF: fibroblast growth factor; FRS2: FGFR substrate 2; Grb2: growth factor receptor-bound protein 2; MEK1/2: mitogen-activated protein kinase 1/2; PDGF: platelet-derived growth factor; PI3K: phosphatidylinositol-4,5-bisphosphate 3-kinase; PIP2/3: phosphatidylinositol-2/3-phosphate; PKC: protein kinase C; PLC-γ: phospholipase C-γ; SOS: son of sevenless, a guanine nucleotide exchange factor that acts on the Ras GTPases (Wollin, 2015) [106].

2 AIMS OF THE STUDY

Pulmonary arterial hypertension is caused by an obliterative pulmonary vasculopathy that predominantly affects small pulmonary arteries. PAH is characterized by excessive vasoconstriction due to the dysregulation of vascular tone and thickening of vessel walls caused by the abnormal proliferation of vascular SMCs. Current pharmacotherapies which are approved for treatment of PAH focus on vasodilation, including substances like calcium channel blockers, prostacyclin, prostacyclin analogs, prostacyclin receptor agonists, phosphodiesterase type 5 inhibitors, soluble guanylate cyclase stimulators and endothelium receptor antagonists [79]. Although these therapeutic approaches relieve the pulmonary vasoconstrictive component of the disease and provide symptomatic relief with some amelioration in the prognosis, there is no strong evidence to support that these vasodilators have a direct antiproliferative effect on pulmonary vascular cells, and the underlying pathological pulmonary vascular and right ventricular remodeling is still progressing.

Future medical intervention strategies must therefore go beyond vasodilation, to target vascular remodeling in the pulmonary vasculature. There are several drug candidates that focus on vascular remodeling currently under investigation. These new therapeutic agents must be continuously explored because of the insufficient efficacy and poor tolerability of these compounds.

It was found found that PDGF-induced collagen synthesis is involved in pulmonary vascular remodeling [108]. The immunohistochemistry staining in figure 6 shows that collagen expression is higher in the smooth muscle cells from lung tissue of the PAH patient than that from lung tissue of the healthy donor. In experimental PAH, collagen deposition in the smooth muscle cells is increased compared to control (figure 6, next page).

AIM OF THE STUDY

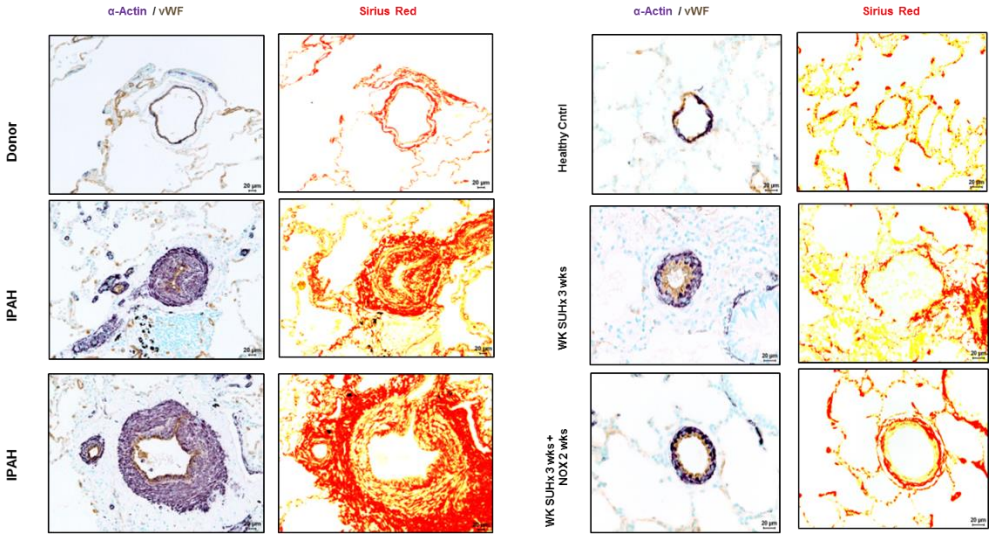

Figure 6. Collagen deposition in the SMC from IPAH and experimental PAH. (Unpublished data in our lab, staining by Ewa Bieniek)

Based on the antifibrotic effect of pirfenidone and nintedanib in experimental pulmonary fibrosis and IPF patients, the hypothesis of this study was that pirfenidone/nintedanib may inhibit collagen synthesis and the cell proliferation of PASMCs induced by growth factors in PH. Thus, the effects of pirfenidone and nintedanib were investigated on hemodynamics and pulmonary vascular remodeling in a rat model of experimental PAH induced by single injection of Sugen5416 and hypoxic exposure (SuHx). In addition, the downstream of effects on the cellular and molecular level were analyzed to explore the mechanism of action of pirfenidone and nintedanib. The following experiments were conducted:

1. The effect of pirfenidone on hPASMCs proliferation induced by PDGF-BB or multi-growth factors

2. The effect of pirfenidone on hPASMCs migration induced by PDGF-BB

3. The effect of pirfenidone on collagen expression and secretion

4. The effect of pirfenidone on mRNA expression of proinflammatory cytokines

5. An evaluation of the *in vivo* effects of pirfenidone in PAH rats, including indexes of right ventricular systolic pressure, right ventricle function and hypertrophy, vascular remodeling, collagen expression and inflammation

6. An investigation of the mechanism of action of pirfenidone

7. The effect of nintedanib on hPASMCs proliferation induced by PDGF-BB or multi-growth factors

8. The effect of nintedanib on hPASMCs migration induced by PDGF-BB

9. The effect of nintedanib on collagen expression and secretion

AIM OF THE STUDY

10. The effect of nintedanib and proinflammatory cytokines on mRNA expression

11. An evaluation of the *in vivo* effects of nintedanib on SuHx rats

12. An investigation of the mechanism of action of nintedanib

3 MATERIALS AND METHODS

3.1 Materials

3.1.1 Chemicals, reagents, kits

Product	Company
2-propanol	Sigma- Aldrich, Germany
Acetic acid	Sigma- Aldrich, Germany
Acrylamide	Roth, Germany
Ammonium persulfate (APS)	Sigma- Aldrich, Germany
Bovine serum albumin (2 mg/ml)	Bio-Rad, USA
Bovine serum albumin (20 mg/ml)	Sigma-Aldrich, USA
Bovine serum albumin powder	Serva, Germany
Bromophenol blue	Merck, Germany
Cell Proliferation ELISA, BrdU (colorimetric)	Roche, USA
DAB substrate kit	Vector, Germany
DC™Protein Assay	Bio-Rad, USA
DEPC water	Roth, Germany
Dimethyl sulfoxide (DMSO)	Sigma-Aldrich, USA
Disodium phosphate (Na_2HPO_4)	Roth, Germany
DNeasy Blood & Tissue Kit	Qiagen, Germany
Enhanced chemiluminescence (ECL) kit	Amersham, USA
Ethanol 70%	SAV LP, Germany
Ethanol 96%	Otto Fischhar, Germany
Ethanol 99.9%	Berkel AHK, Germany
Ethylenediaminetetraacetic acid (EDTA)	Sigma-Aldrich, USA
Glycerol	Sigma-Aldrich, USA
Glycine	Roth, Germany
Heparin	Ratiopharm, Germany
Hydrogen peroxide 30%	Vector, Germany
ImPRESEE Kit anti-rabbit Ig	Vector, Germany
iScript cDNA synthesis kit	Bio-Rad, USA
Isoflurane	Baxter, UK
iTaq SYBR Green Supermix	Bio-Rad, USA
Ketamine	Bela Pharm, Germany
Monopotassium phosphate (KH_2PO_4)	Roth, Germany

Nintedanib	Boehringer Ingelheim, Germany
Non-fat milk powder	Roth, Germany
Normal horse serum	Vector, Germany
Normal rabbit serum	Vector, Germany
Paraformaldehyde (PFA) 3.7%	Sigma-Aldrich, USA
Paraplast® Plus paraffin embedding medium	Sigma-Aldrich, USA
Pertex® mounting medium	Medite, Germany
PDGF-BB	PeproTech, USA
Pirfenidone	Roche, Swiss
Potassium chloride (KCl)	Sigma-Aldrich, USA
Positively charged glass slides	Langenbrinck, Germany
Precision Plus Protein Standards	Bio-Rad, USA
RIPA buffer	Santa Cruz, USA
RNAse-Away	Thermo Fisher, USA
RNeasy Plus Mini Kit	Qiagen, Germany
Saline (NaCl 0.9%)	B. Braun, Germany
SDS Solution, 20% w/v	AppliChem, Germany
SIRCOL collagen assay	Biocolor Ltd., UK
Sodium chloride (NaCl)	Sigma-Aldrich, USA
Sodium Orthovanadat (Na_3VO_4)	Sigma-Aldrich, USA
Sugen 5416	Tocris, UK
Tetramethylethylenediamine (TEMED)	Sigma-Aldrich, USA
Tissue-Tek® O.C. T™ Compound	Sakura, Japan
Tris Base	Roth, Germany
Tris-HCl	Roth, Germany
Triton-X100	Sigma-Aldrich, USA
Tween®20	Sigma-Aldrich, USA
UltraPure water	Cayman Europe, Estonia
Xylol (isomere) >98% pure, for histology	Roche, Germany
β-Mercaptoethanol	Sigma-Aldrich, USA

3.1.2 Cell culture medium

Name	Company
DPBS	PAN, Germany
Fetal bovine serum	Roth, Germany
Smooth Muscle Basal Medium (SmBM)	Lonza, Germany
Smooth Muscle Growth Medium-2 (SmGM-2) SingleQuot Kit Suppl. & Growth Factors	Lonza, Germany
Trypsin/EDTA	PAN, Germany

3.1.3 Antibodies

3.1.3.1 Primary antibodies

Table 2 Primary antibodies

Antibody (catalog number)	Host	Company
Akt (9272)	rabbit polyclonal antibody	Cell Signaling, USA
p-Akt (9271)	rabbit polyclonal antibody	Cell Signaling, USA
CD 68 (MCA341R)	mouse monoclonal antibody	Bio-Rad, USA
Collagen 1, (600-401-103-0.1)	rabbit polyclonal antibody	Rockland, USA
Pan-actin (4968)	rabbit polyclonal antibody	Cell Signaling, USA
PCNA(FL-261) (sc-7907)	rabbit polyclonal antibody	Santa Cruz, USA
PDGFR-β (958) (sc-432)	rabbit polyclonal antibody	Santa Cruz, USA
p-PDGFR-β (Tyr 1021)-R (sc-12909-R)	rabbit polyclonal antibody	Santa Cruz, USA
PI3 Kinase p85 (19H8), (4257)	rabbit polyclonal antibody	Cell Signaling, USA
p-PI3 Kinase p85/p55 (4228)	rabbit polyclonal antibody	Cell Signaling, USA

3.1.3.2 Secondary antibody

Horseradish peroxidase (HRP)–conjugated secondary antibody:

Sheep anti-rabbit IgG (1:50000) GE Healthcare, PA, USA

Donkey anti-mouse IgG (1:50000) GE Healthcare, PA, USA

3.1.4 Primers

Table 3 Primers for quantitative RT-PCR

Gene		Primer Sequence
Human IL-1β	Forward	5’ CAGACCTTCCAGGAGAATGAC 3’
	Reverse	5’ AGGTGGAGAGCTTTCAGTTCA 3’
Human IL-6	Forward	5’ ACAGACAGCCACTCACCTCTT 3’
	Reverse	5’ TGGAAGGTTCAGGTTGTTTTC 3’
Human HPRT	Forward	5’ TGACACTGGCAAAACAATGCA 3’
	Reverse	5’ GGTCCTTTTCACCAGCAAGCT 3’
Rat IL-1β	Forward	5’ GGCTTCCTTGTGCAAGTGTC 3’
	Reverse	5’ TGTCGAGATGCTGCTGTGAG 3’
Rat IL-6	Forward	5’ AGAGACTTCCAGCCAGTTGC 3’
	Reverse	5’ TGCCATTGCACAACTCTTTTCT 3’
Rat collagen 1a1	Forward	5’ GCTCCCCAGCTGTCTTATGG 3’
	Reverse	5’ CAATCCTCGAGCACCCTGAG 3’
Rat collagen 3a1	Forward	5’ GCTGGCATCAAAGGACATCG 3’
	Reverse	5’ GGGAGCCCTCAGATCCTCTT 3’
Rat HPRT	Forward	5’ ACAGGCCAGACTTTGTTGGAT 3’
	Reverse	5’ GGCCACAGGACTAGAACGTC3’

3.1.5 Equipments

Equipment	Company
Balance 1.0-3000g RP 3000	AugustSauter, Switzerland
Balance PCB 200-2 Precision	Kern, Germany
Balance XS205	MettlerToledo, Switzerland
BioDoc Analyzer	Biometra, USA
Cell culture incubator, Hera Cell	Heraeus, Germany
Centrifuge Roranta 460R	Hettich, Germany
Cytospin™ 4 Cytocentrifuge	Thermo Scientific, USA

Electrophoresis chamber	Bio-Rad, USA
Freezer (+4°C, -20 °C, -80 °C)	Bosch, Germany
Hypoxia Chambers	Bio Spherix, USA
Hypoxic gas (10% O_2) ventilation	Praxair, Germany
Infinite® 200 microplate reader	Tecan, Switzerland
Inolab PH meter	WTW, Germany
Light microscope DM IL	Leica, Germany
LightCycler® 480 Instrument	Roche, Germany
Liquidator 96	Steinbrenner, Germany
Live imaging microscope DMI6000 B	Leica, Germany
Microtome RM2165	Leica, Germany
Mounting bath HI1210	Leica, Germany
Mounting heating plate HI1220	Leica, Germany
Multifuge centrifuge	Heraeus, Germany
Mx3000P qPCR System	Stratagene, USA
Normoxic gas (21% O_2) ventilation	Praxair, Germany
Pipetboy and pipettes	Eppendorf, USA
Precellys®24 homogenizer	BertinTech., France
Rotator Staurt®SB3	Bibby Scientific, U.K.
Shaker	Bruker, Belgium
Thermocycler T3000	Biometra, USA
Vevo® 2100 system	VisualSonics, Canada
Vortex machine	VWR, Germany
Water bath for cell culture	HLC, Germany
Water bath for tubes	Medingen, Germany
Western blot unit	Bio-Rad, USA

3.1.6 Other materials

Materials name	**Company**
6-well, 24-well, 96-well microplate	Corning, USA
96er PCR-plate for LC480	Steinbrenner, Germany
AGFA cronex 5 medical X-ray film	AGFA, Belgium
Chromatography column	Bio-Rad, USA
Cover glass 60 x 24 (0.13-0.18 mm)	Langenbrinck, Germany
Falcon tubes	BD Biosciences, USA
Film cassettes	Kodak, USA

Filter tips (10, 100, 1000µl)	Nerbe plus, Germany
Gel blotting paper	Whatman, USA
Glass pipettes, cell culture dishes, plates	Sarstedt, Germany
Glass slides Super Frost® Plus	R.La ngenbrinck, Germany
Micro-Insert 4 Well	Ibidi, Germany
Needles 26-20G (0.45-0.9mm)	Microlance™ 3 BD, Ireland
Nitrocellulose membrane	Bio-Rad, USA
Precellys bead mill sample tube	Berlin Tech, France
Radiographic films hypersensitive	Amersham, USA
Radiographic films	Santa Cruz, USA
Scalpels	Feather, Japan
Shandon™ Single Cytoslides™	Thermo Scientific, USA
Syringes 1, 2, 5, 10, 25 ml	B. Braun, Germany
Tips (10, 100, 1000 µl)	Eppendorf, USA

3.1.7 Computer software

Software	**Company**
Fluorescence (LAS AF) Microscope Software	Leica, Germany
i-Control	Tecan, Austria
Leica Application Suite Advanced	Leica, Germany
Leica QWin Imaging Software	Leica, Germany
LightCycler® 480 Software	Roche, Germany
Magellan v.6.3	Tecan, Austria MS®
MxPro™ QPCR Software	Agilent Technologies, USA
Prism® v6.05	GraphPad statistics, USA

3.2 Methods

3.2.1 Human pulmonary artery smooth muscle cells culture

Pulmonary artery smooth muscle cells from healthy donors were purchased from Lonza (Basel, Switzerland). They were cultured on cell-culture dishes in smooth-muscle growth medium (SmGM-2) from Lonza (Basel, Switzerland) and incubated in a humidified atmosphere of 95% air and 5% CO_2 at 37°C.

3.2.1.1 Cryopreservation

At 80% confluency, cells were washed with DPBS buffer and trypsinization was performed by adding pre-warmed trypsin. Growth medium was added to stop the trypsin activity, and the cells were then centrifuged at 1,000 *rpm* and 20°C for five minutes. The

pellet was then resuspended in a cooled freezing cryopreservation medium (SmGM-2: DMSO, 9:1), kept in a cell-freezing container for 24 hours at -80°C, and later transferred to liquid nitrogen and stored for future use.

3.2.1.2 Seeding and splitting

The appropriate volume of medium was pre-incubated at 37°C and 5% CO_2 for 30 minutes. The cryopreserved cells were thawed and seeded to the plates containing a pre-incubated medium, and they were incubated at 37°C and 5% CO_2 until the cell confluency reached 80%. The cells were trypsinized and cell pellets were re-suspended in the fresh SmGM-2 growth medium, and the cell count and viability were determined using a hemocytometer and trypan blue. The cells were seeded at a seeding density of 3,500 cells/cm^2.

3.2.2 Cell proliferation assay

Pulmonary artery smooth muscle cells were plated in a 96-well plate with 4000 cells per well. After serum starvation for 24h, the cells were stimulated with human recombinant PDGF-BB or multiple growth factors (MGF) in the presence or absence of pirfenidone/nintedanib for 24h.The proliferation of hPASMCs was assayed with a kit from Roche (Basel, Switzerland) that monitors the incorporation of 5-bromo-2deoxyuridine (BrdU) into newly synthesized DNA; BrdU was detected using anti-BrdU–peroxidase conjugate in accordance with the manufacturer's instructions. After the reactions were stopped, absorbance at 450 nm was measured using a Tecan infinite multi-mode microplate reader, and the cell viability was checked using a WST-1 assay (Roche, Basel, Switzerland) and following the manufacturer's protocols.

3.2.3 Cell migration assays

Cell migration was performed with wound-healing assays. Pulmonary artery smooth muscle cells were digested with 0.05% trypsin and dispersed into homogeneous cell suspensions; they were plated in low 35-mm μ-dishes with culture inserts (Ibidi, Martinsried, Germany). Inserts were then removed with sterile forceps to create a wound field of approximately 500 μm. Cells were stimulated with 30 ng/ml of human recombinant PDGF-BB for migration in the presence or absence of pirfenidone or nintedanib for 24h. Migration was measured by photomicrography after cells were fluorescently labeled. The results are expressed as the number of migrated cells in this field.

3.2.4 Collagen assay

Pulmonary artery smooth muscle cells were plated in a 10-cm dish. After serum-starvation for 24h, the cells were stimulated with 30 ng/ml of human recombinant PDGF-BB in the presence or absence of pirfenidone or nintedanib for 72h. Collagen in the medium was measured using the Sircol soluble collagen assay (Biocolor, Newtownabbey, Northern Ireland) following the manufacturer's protocol. After isolation and concentration, 100 µl of the sample was added to 1 ml of the colorimetric reagent (the SR dye in picric acid) and agitated for 30 min followed by centrifugation at 12,000 *rpm* for 10 min. The SR dye was released from the pellet with the alkali reagent, and spectrophotometric readings were taken at 555 nm on a Tecan infinite multi-mode microplate reader.

3.2.5 Animals

Adult male 10-12-week-old CD rats with body weights between 200g and 250g were obtained from Charles River Laboratories. Animal study protocols (GI20/10, number 33/2013; GI20/10, number 47/2015) were approved by the University Animal Care Committee and the Federal Authorities for Animal Research of the Regierungspraesidium Giessen (Hessen, Germany). Rats were housed at room temperature (RT) with 12-hour light and dark cycles and free access to food and water.

3.2.5.1 Sugen5416 plus hypoxia induced PAH rat model

Sugen5416 was dissolved in DMSO at a concentration of 25 mg/ml. Adult rats (200-250 g in body weight) were selected in a randomized manner and subcutaneously injected with the Sugen5416 (20 mg/kg body weight) solution in the neck. Immediately after the injection, animals were exposed to hypoxia (10% O_2) in the ventilated hypoxia chamber for three weeks, followed by re-exposure to normoxia for another two weeks. Control animals, which were injected with the same volume of saline, were kept in normoxic conditions for the same duration. Hemodynamic studies and tissue freezing occurred at the end of treatment.

3.2.5.2 Experimental groups and treatment

Animals for the pirfenidone experiment were divided into three groups. Group I served as normal control rats, which were injected with sterile saline plus normoxia and were fed ad libitum with rodent laboratory chow. Group II served as PAH rats, which were injected with Sugen5416 plus hypoxia and were fed ad libitum with rodent laboratory chow. Group III served as the treatment group where hypoxia+Sugen5416 rats were fed with the same rodent laboratory chow with 0.5%(w/w) pirfenidone from day 21 to day 35.

Pirfenidone was mixed with the laboratory chow (the ratio is 0.5% weight of pirfenidone to 99.5% weight of chow) in a planetary mixer and was stored at 4°C.

Animals for the nintedanib experiment were also divided into three groups. Group I served as normal control rats; they received injections of sterile saline plus normoxia and received vehicle (methylcellulose) alone. Group II served as PAH rats that received injections of Sugen5416 plus hypoxia and were given vehicle (methylcellulose) alone. Finally, group III served as the treatment group where the hypoxia+Sugen5416 rats received nintedanib at 50mg/kg of their body weight from day 21 to day 35. Nintedanib was prepared fresh in methylcellulose at 50mg/ml and administrated *per os* with a gavage needle in the same manner.

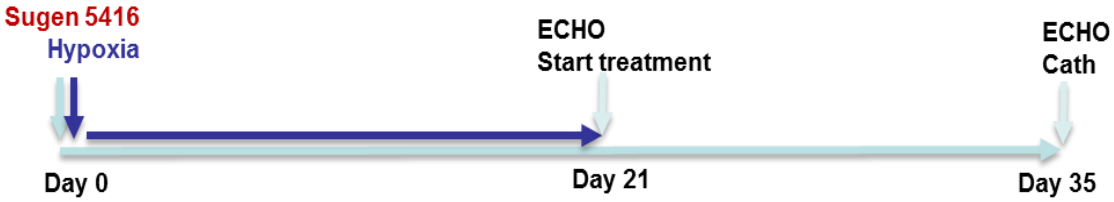

Figure 7. Schedule of treatment in PH rat model.

3.2.6 Echocardiography

The noninvasive measurement of several functional and morphometric parameters was performed by echocardiography, as described previously [109]. The rat was anesthetized with isoflurane and kept in a supine position on a heating platform. The limbs were tamped to ECG electrodes. Echocardiographic images were acquired with a VEVO 2100 high-resolution imaging system equipped with MicroScan linear array transducers, and the following parameters were analyzed:

-Right ventricle internal diameter (RVID) is the distance between the inner linings of the right ventricle free wall to the inner lining of the interventricular septum towards the right ventricle; it is measured in millimeters and serves as a parameter of right ventricle hypertrophy and dilatation.

-Stroke volume (SV) is the volume of blood ejected by the ventricle during each contraction.

-Cardiac output (CO) is the volume of blood ejected from the ventricle into the circulation per minute. Cardiac output equals SV multiplied by heart rate. The unit of measurement is liters/minute in humans and milliliters/minute in rodents.

-Cardiac index (CI) is the ratio of cardiac output per 100 grams of the body; it estimates the performance of cardiac output according to the size of the body.

3.2.7 Surgical preparation and hemodynamic measurements

At the end of treatment, the rats were anesthetized with isoflurane, followed by an intramuscular (*i.m.)* injection of heparin (50 IU/kg body mass) to measure the hemodynamic parameters. The rats were then tracheotomized and ventilated at a frequency of 60 breaths/min, with a positive end expiratory pressure of 1 cm H_2O throughout. Right ventricle systolic pressure (RVSP) is nearly equivalent to pulmonary artery systolic pressure in ideal conditions. To measure right ventricular systolic pressure (RVSP), a right heart catheter (PE 50 tube) was inserted through the right jugular vein, and to measure arterial pressure, a polyethylene catheter was inserted into the left carotid artery [110]. The computer software Labtech Notebook Runtime version 9.02 was used to record the pressure for five to ten minutes.

3.2.8 Lung tissue harvest and preparation

After the hemodynamic measurements, whole lungs were flushed through the pulmonary artery with saline to remove red cells. The right lobe was snap frozen in liquid nitrogen and stored at -80º C for molecular biology assessment, while left lobes were perfused under 22 cmH_2O of pressure through the pulmonary artery with 3.5 to 3.7 % formalin, and immersed in formalin for 24 hours. Formalin-fixed lung tissue samples were transferred to embedding cassettes and stored in phosphate-buffered saline (PBS). The dehydration was performed overnight in the Leica ASP300S tissue processor. The next day, the lung tissues were embedded in 65°C warmed paraffin with a heated Leica paraffin embedding module. The paraffin-embedded lung tissues were then cooled for hardening on a Leica cooling plate, sectioned to three-µm thick sections on the Leica fully-automated rotation microtome, and mounted on positively charged glass slides. Finally, lung tissue sections were dried on a Leica heating plate at 40°C and incubated at 37° C (for 12 hours) in a drying oven.

3.2.9 Medial wall thickness, neointima/media ratio and occlusion of vessels

To assess pulmonary vascular remodeling, the medial wall thickness was determined, and the neointima/media wall ratio analysis was performed as previously published and described [109]. The media wall thickness of pulmonary vessels is defined as the distance between the internal elastic lamina and external elastic lamina. The neointima wall thickness of pulmonary vessels is defined as the distance between the internal elastic lamina and lumen. Vessels were assessed for occlusive lesions and scored as: no evidence of neointimal formation (open), partial (<50%) luminal occlusion, and full-luminal occlusion (closed). To measure the medial wall thickness, neointima/media ratio and occlusion of vessels, van Gieson's staining was used. The three-µm lung tissue

sections were deparaffinized and rehydrated. After overnight staining in Resorcin-Fuchsin, the slides with the tissue sections were washed with water. The sections were immersed in Weigert's working solution of hematoxylin for five minutes, which was prepared by mixing an equal volume of Weigert's Iron Hematoxylin A and Weigert's Iron Hematoxylin B. The sections were washed with running water and then with aqua dest. After washing, the slides were immersed in Van Gieson solution for 10 minutes. The sections were dehydrated and immersed in xylol and coverslipped with mounting medium (Pertex®). Vessels with an outer diameter of 20 to 50µm were used for analysis. Elastic fibers and cell nuclei were stained dark blue or dark brown by the iron-hematoxylin stain, and collagen and muscle fibers were stained red by the van Gies counterstain. The cytoplasm was stained yellow due to counterstain. Finally, a light microscope with Leica Qwin V3 computer-assisted image analysis software was used for analysis.

3.2.10 Immunohistochemistry

The three-µm section of lung tissue was deparaffinized in xylene and rehydrated in a series of grade-decreasing ethanol solutions followed by PBS. Antigen retrieval was achieved with a citrate buffer 20 times for 20 minutes. The endogenous peroxidase activity of the tissue was blocked using a freshly prepared solution of 30% hydrogen peroxide (H_2O_2) and methanol in a 1:1 ratio. The slides were then incubated again in proteinase K at RT for 15 minutes. After washing, the slides were incubated with 10% BSA, and then washed with 1x PBS and incubated with 2.5% normal horse serum for 30 minutes. The slides were incubated with the primary antibody CD68 (1:100) or PCNA (1:100) overnight at 4°C. After washing with 1x PBS, the corresponding secondary antibody conjugated with HRP was applied for 30 min. After washing, the color was developed with the NovaRED substrate, followed by counterstaining with hematoxylin and dehydration. The procedure was completed by covering the slide with mounting medium and pulling the coverslip. The positive cells appeared brown or red in the light microscope and were examined under a Leica DM 2500 microscope using Leica QWin V3 imaging software.

3.2.11 Polymerase chain reaction (PCR)

3.2.11.1 RNA isolation

The total RNA from the hPASMCs and lung tissue were isolated by using the Qiagen RNeasy Mini kit. The procedures were followed according to the manufacturer’s instructions. For hPASMCs, the cell medium was aspirated and cells were washed twice

with DPBS. Then, 350µL of Buffer RLT+β-ME was applied to the cell-culture dish for five minutes. Cell lysate was scraped and collected for next step. For lung tissue, appropriate amount of tissue (30mg) and beads, and 600µL of RLT+β-ME were added to a homogenizing tube and homogenized twice for 40 seconds in a rotor-stator homogenizer. The tubes were then centrifuged for three minutes at the maximum speed (14,000 *rpm*) and the supernatant was collected for next procedure.

Cells lysate or supernatants from tissue were centrifuged for two minutes at 13,600 *rpm* in an QIAshredder spin column. An equal volume of 70% ethanol was added to the previous supernatant, mixed well, and transferred into an RNeasy mini column and centrifuged at 10,000 *rpm* for 20 seconds. Three hundred and fifty µL of Buffer RW1 was added to the RNeasy mini column and centrifuged at 10,000 *rpm* for 20 seconds. The flow through was discarded, and 80µL of DNase+RDD buffer was added to the RNeasy mini column and incubated at RT for 15 minutes. Three hundred and fifty µL of Buffer RW1 was added and centrifuged at 10,000*rpm* for 20 seconds, and the flow through was discarded. In addition, 500µL of RPE buffer was added and centrifuged at 10,000 *rpm* for 20 seconds. The flow through was discarded. For elution, 50µL of RNase-free water was added directly to the membrane and centrifuged at 10,000 *rpm* for one minute. The quality and concentration of total RNA was measured with a NanoDrop spectrophotometer and the RNA was stored at -80°C.

3.2.11.2 Reverse transcription - polymerase chain reaction (RT-PCR)

cDNA was synthesized by RT-PCR using the Bio-Rad iScript cDNA synthesis kit according to the manufacturer's instructions. One µg of RNA in 20 µl of the master mix was used per reaction (Table 4). The reverse transcription was performed in a thermocycler and the program is shown in Table 5. The cDNA was stored at -20°C.

Table 4 RT-PCR components

Components	Volume per reaction
5x iScript reaction mix	**4 µl**
iScript reverse transcriptase	**1 µl**
RNA (1µg)	**up to the concentration**
Nuclease-free water	**to the final volume (20 µl)**
Total mix volume	**20 µl**

Table 5 RT-PCR thermocycler program

Program	Temperature	Time
Annealing	**25°C**	**5 min**
Incubation	**42°C**	**30 min**
Thermal inactivation of reverse transcriptase	**85°C**	**5 min**
Hold at	**4°C**	

3.2.11.3 Quantitative real-time polymerase chain reaction (qPCR)

The exon-spanning primer pairs for human and rat genes were designed using the NCBI/ Primer-BLAST and are shown in Table 3. The product size is within the range of 100 bp - 300 bp. Furthermore, qPCR was performed on a Mx3000P® QPCR system machine using an iTaq™ SYBR® Green Supermix kit and procedures were followed according to manufacturer's instructions (Table 6, 7). The nuclease free water was used as negative control instead of cDNA.

Table 6 Quantitative PCR reaction components

qRT- PCR reaction component	Volume per reaction
cDNA template	2 µl
Forward primer 10 µM	0.5 µl
Reverse primer 10 µM	0.5 µl
iTaq SYBR Green supermix (2X)	10 µl
Nuclease-free water	6 µl
Total volume	20 µl

Table 7 Quantitative PCR program

	Temperature	Time	Cycle
Activation	**95°C**	**10 min**	**1**
Denaturation	**95°C**	**30 sec**	**40**
Annealing	**58°C**	**30 sec**	
Extension	**72°C**	**30 sec**	
Denaturing	**95°C**	**1 min**	
Dissociation curve	**55-95°C**	**indefinite**	**1**
Hold	**4°C**	**indefinite**	**1**

The dissociation curve was generated by MxPro™ QPCR software and used to ensure single product amplification. The threshold cycle (Ct values) was determined for each gene. The Ct values of the target genes were normalized to that of the housekeeping hypoxanthine-guanine phosphoribosyl transferase (*HPRT*) using the formula $\Delta Ct = Ct_{reference} - Ct_{target}$. The ΔCt of the control sample was then subtracted from a treated sample, providing the ΔΔCt. mRNA expression was analyzed with the $2^{-\Delta\Delta CT}$ method that represents the fold change of the treated target gene relative to the control. Each reaction was run in duplicate and repeated three times independently.

3.2.12 Western blotting

3.2.12.1 Protein isolation

The total protein was extracted in RIPA buffer (containing 1x TBS, 1% Nonidet P-40, 0.1% SDS, 0.5% sodium deoxycholate, and 0.004% sodium azide) according to the manufacturer's instructions. Proteinase inhibitor cocktail, sodium orthovanadate, and PMSF were added to RIPA immediately before use. In addition, 100 mg of lung tissue

was homogenized in 600 µl of RIPA or 1×10^6 hPASMCs in 300 µl of RIPA was centrifuged at 12,000 *rpm* for 30 minutes at 4°C and the supernatants were kept at -80°C.

Table 8 RIPA buffer recipe

Component of RIPA	Final concentration
RIPA buffer	**1x**
Protease inhibitor cocktail	**1x**
Sodium orthovanadate	**1%**
PMSF	**1%**

3.2.12.2 Protein concentration measurement

Protein concentration was determined with a Bio-Rad DC protein assay according to the manufacturer's instructions for the microplate assay protocol. This assay method is a well-documented Lowry assay with slight improvements. The assay is based on the reaction of protein with an alkaline copper tartrate solution and Folin reagent. There are two steps which lead to color development: the reaction between protein and copper in an alkaline medium (Reagent A) and the subsequent reduction of Folin (Reagent B) reagent by the copper-treated protein. A series of bovine serum albumin (BSA) concentration, 0.25- 0.5- 1- 2 mg/ml, was used as a standard for the protein from cell lysates, and 1.25- 2.5- 5- 10- 20 mg/ml, were used as a standard for the protein from tissue lysates. The protein samples were pre-diluted to the range of the standard and the protein concentration of each sample was estimated in duplicate. After developing the blue color, samples were measured at 750 nm using a Tecan microplate reader. The final protein concentration was calculated with accompanying Magellan™ software using the linear regression method.

3.2.12.3 SDS-polyacrylamide gel electrophoresis (SDS-PAGE)

Protein samples with equal concentration were mixed with 5× SDS gel loading buffer at a ratio of 4:1 (v/v) and denatured at 100°C for five minutes.

Table 9 5×SDS gel-loading buffer recipe

5×SDS gel-loading buffer component	Final concentration
Tris-HCl (2 M, pH 6.8)	**375 mM**
SDS	**10% (w/v)**
Glycerol	**50% (v/v)**
β-Mercaptoethanol	**12.5% (v/v)**
Bromophenol blue	**0.02% (w/v)**

Polyacrylamide gels were prepared according to the following procedure: The space between the glass plates was filled with separating gel mixture, and 2-propanol was

poured on top of this mixture until the gels polymerized. After 30 minutes, water from the resolving gel was removed and a 6% stacking gel solution was added. A comb was inserted, and polymerization lasted 30 minutes. The protocols for the SDS-PAGE gels are listed in table 10 and table 11. Finally, protein samples or dual protein markers were loaded into the lanes of SDS-PAGE gel and run at 100-130V for two hours to separate. The buffers are listed in table 12.

Table 10 Separation gel (8% and 10%)

Gel components	Final concentration	
	8%	10%
Tris-Cl (1.5 M, pH 8.9)	375 mM	375 mM
Acrylamide 30% (w/v)	8% (w/v)	10% (w/v)
SDS 10% (w/v)	0.1% (w/v)	0.1% (w/v)
APS 10% (w/v)	0.05% (w/v)	0.05% (w/v)
TEMED	0.1% (w/v)	0.1% (w/v)
Water up to the final volume		

Table 11 Stacking gel (6%)

Gel components	Final concentration
Tris-Cl (0.5 M, pH 6.8)	125 mM
Acrylamide 30% (w/v)	6% (w/v)
SDS 10% (w/v)	0.1% (w/v)
APS 10% (w/v)	0.05% (w/v)
TEMED	0.1% (w/v)
Water up to the final volume	

Table 12 Running buffer recipe

Running buffer component	Final concentration
Tris-HCl	25 mM
Glycine	192 mM
SDS	0.1% (w/v)

3.2.12.4 Transfer of proteins and staining

The proteins that were separated with the SDS-PAGE were transferred to a nitrocellulose membrane at 100V for one hour using a blotting apparatus. The membranes were blocked with 5% non-fat milk for one hour at RT and probed with primary antibodies (diluted in TBST with 5% BSA) at 4°C overnight. After washing three times with TBS containing 0.1% Tween-20, horseradish peroxidase (HRP)-conjugated secondary antibodies (diluted in TBST with 5% BSA) were applied for one hour at RT. After washing, the blots were developed using an enhanced chemiluminescence (ECL)

kit. The blots were captured by X-ray films and the intensity of bands was quantified by densitometry. The antibodies are listed in table 2.

Table 13 Blotting buffer recipe

Running buffer component	Final concentration
Tris-HCl	50 mM
Glycine	40 mM
Methanol	20% (w/v)

Table 14 TBST buffer (pH 7.6) recipe

TBST buffer (pH 7.6) component	Final concentration
Tris-HCl	20 mM
NaCl	150 mM
Tween	0.1% (v/v)

3.2.13 Statistics

GraphPad Prism® v6.05 was used for all statistical analysis, and data are expressed as means ± SEM when appropriate. Significance was assessed using unpaired t tests (when two groups analyzed) or one-way ANOVA-Newman-Keuls tests (for more than two groups); $P < 0.05$ was considered significant.

4 RESULTS

4.1 The effect of PDGF-BB on proliferation of human pulmonary arterial smooth muscle cells

Growth factors such as PDGFs are potent mitogens and chemoattractants for vascular cells. These growth factors play important roles in the remodeling process of PAH development by controlling many cellular functions and processes, including cellular proliferation, migration, and extracellular matrix deposition [7,17].

A pilot experiment for PDGF-BB induced hPASMCs proliferation was conducted with different concentrations ranging from 0 to 100ng/ml. In this experiment, PDGF-BB induced the proliferation of hPASMCs in a dose-response manner (Figure 8). Based on this pilot study, 30ng/ml was used as the concentration for PDGF-BB in the following *in vitro* experiments.

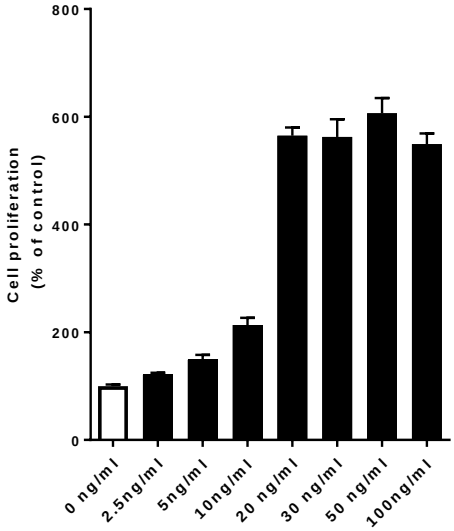

Figure 8. The effect of PDGF-BB on proliferation of human pulmonary arterial smooth muscle cells.

Human PASMCs proliferation was induced by PDGF-BB incubation for 24hours with different concentrations ranging from 0 ng/ml to 100 ng/ml. The proliferation of hPASMCs was assayed by the incorporation of BrdU into newly synthesized DNA. Results are expressed as mean ± SEM; n=6. PDGF, platelet derived growth factor.

4.2 The effect of pirfenidone on the proliferation of human pulmonary arterial smooth muscle cells

To determine the effect of pirfenidone on growth-factor-induced hPASMCs proliferation, PDGF-BB and multi-growth factors (MGF, including FBS, hEGF, hFGF-B, and insulin) were employed to stimulate the proliferation of hPASMCs. As shown in figure

9A, PDGF-BB induced proliferation of hPASMCs was inhibited by pirfenidone in a dose-response manner. However, hPASMCs proliferation which was induced by MGF was only inhibited by the high dose of pirfenidone (1mg/ml), and not the low or middle dose (Figure 9B). The viability of hPASMCs was also checked with the WST-1 kit and no cell toxicity was observed after pirfenidone incubation. Therefore, the inhibitory effect of proliferation for pirfenidone was not due to cytotoxicity.

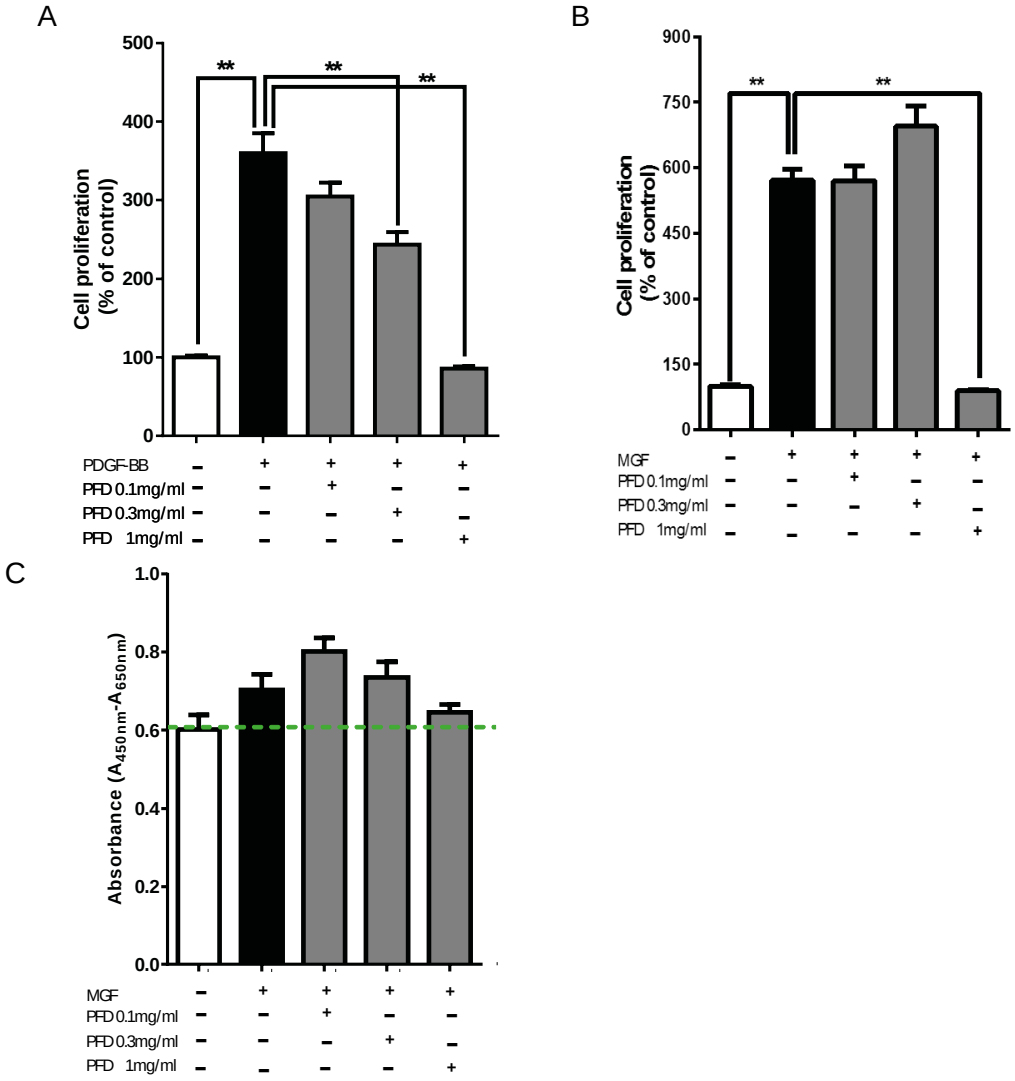

Figure 8. The effect of pirfenidone on the proliferation of human pulmonary arterial smooth muscle cells.

Human PASMCs was stimulated by 30ng/ml of PDGF-BB (A) or MGF (B) for 24hours to induce proliferation in the absence or presence pirfenindone. The proliferation of hPASMCs was assayed by the incorporation of BrdU into newly synthesized DNA. C, the viability of hPASMCs was checked by WST-1 method after 24 hours of pirfenidone incubation. Results are expressed as mean ± SEM; n=3 independent experiments; **P<0.01. PDGF, platelet derived growth factor; PFD, pirfenidone; MGF, multiple growth factors (including FBS, hEGF, hFGF-B, and insulin).

4.3 The effect of pirfenidone on the PDGF-BB-induced migration of human pulmonary arterial smooth muscle cells

The role of pirfenidone on cell migration was investigated by incubating hPASMCs with PDGF-BB in the absence and presence of pirfenidone (0.1, 0.3, 1mg/ml) for 24 hours, after which the cell migration was counted. As shown in figure 10, PDGF-BB significantly induced hPASMCs migration compared to the control group, and the high dose of pirfenidone inhibited PDGF-BB induced hPASMCs migration. However, the middle and low dose of pirfenidone did not demonstrate any inhibitory effect on hPASMCs migration.

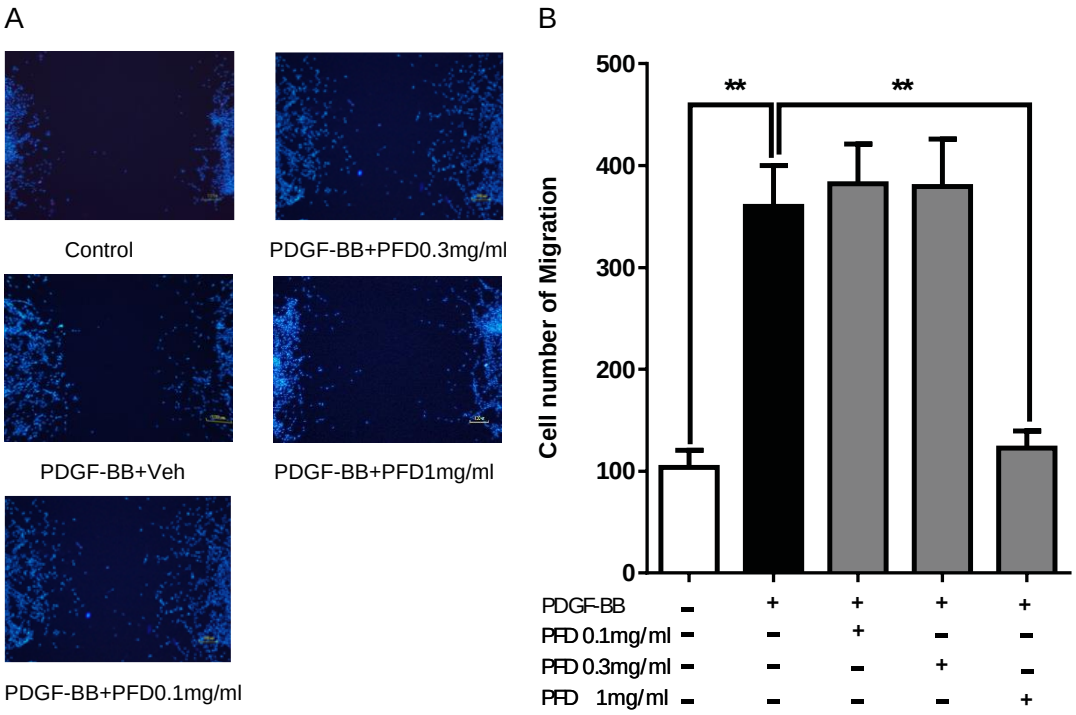

Figure 9. Effect of pirfenidone on PDGF-BB–induced migration of human pulmonary arterial smooth muscle cells.

A, representative picture of hPASMCs migration, scale bars = 100μm; B, cell number of hPASMCs migration. Human PASMCs were stimulated with 30 ng/ml of PDGF-BB for 24h to induce migration in the absence or presence of pirfenidone. Migration result was expressed as the number of migrated cells. Results are expressed as mean ± SEM; n=3-5 independent experiments. **P<0.01. PDGF, platelet derived growth factor; PDF, pirfenidone.

4.4 The effect of pirfenidone on PDGF-BB-induced collagen synthesis and the secretion of human pulmonary arterial smooth muscle cells

To investigate the effect of pirfenidone on collagen deposition in hPASMCs, the collagen I protein expression was investigated in the hPASMCs homogenate by western

blot and the collagen secretion of hPASMCs in the medium was observed with the Sircol method. Collagen I protein level was increased in PAMSCs after PDGF-BB incubation for 24 hours, and this increase was attenuated by pirfenidone, as shown in figure 11A. Moreover, collagen in the medium significantly increased after PDGF-BB incubation for 72 hours, and pirfenidone incubation decreased the content of collagen in the medium in a dose response manner (Figure 11B). The alteration in levels of collagen protein in the culture medium is consistent with the levels of intracellular collagen 1 protein, suggesting that collagen is secreted into extracellular space.

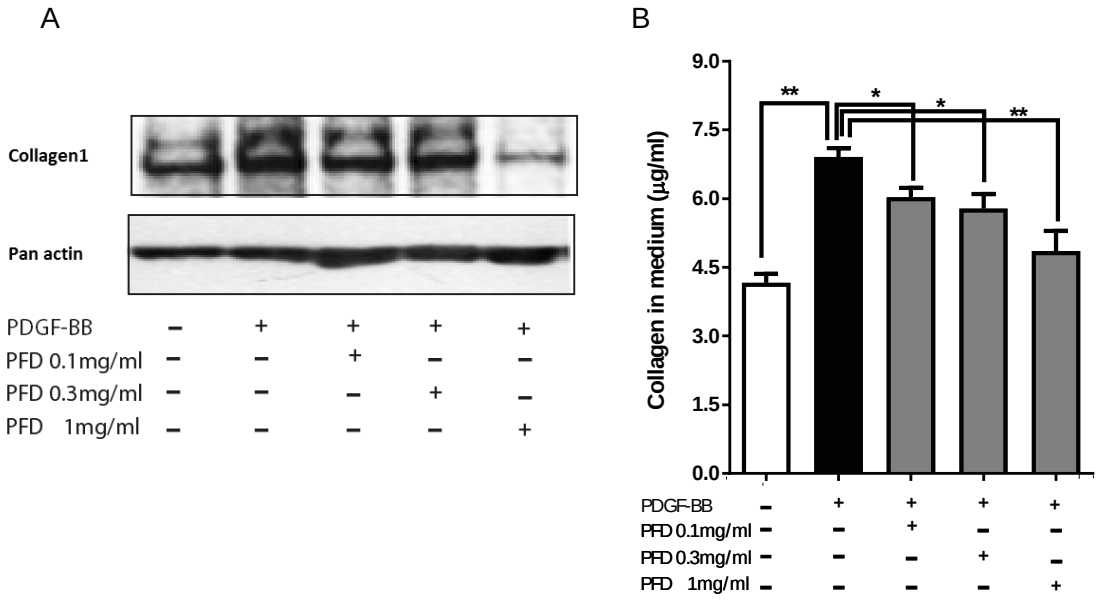

Figure 10. The effect of pirfenidone on PDGF-BB induced collagen synthesis and the secretion of human pulmonary arterial smooth muscle cells.

Human PASMCs were incubated with 30ng/ml of PDGF-BB in the absence and presence pirfenidone. A, representative western blot picture of collagen1. The total protein was extracted from hPASMCs 24 hours after incubation and collagen1 expression was checked by western blot. B, the soluble collagen1 level in the medium. The collagen secretion of hPASMCs in the medium was measured by the Sircol method 72 hours after incubation. Results are expressed as mean ± SEM; n=3~5 independent experiments, *P<0.05, **P<0.01. PDGF, platelet derived growth factor; PFD, pirfenidone.

4.5 The effect of pirfenidone on interleukin mRNA expression in human pulmonary arterial smooth muscle cells

Since accumulating evidence indicates that inflammation is involved in the development of PAH, the efficacy of pirfenidone for PDGF-BB-induced inflammatory cytokine interleukins mRNA expression was investigated. As shown in figure 12, the

increased levels of IL-1β and IL-6 induced by PDGF-BB were blocked by pirfenidone in a dose-response manner.

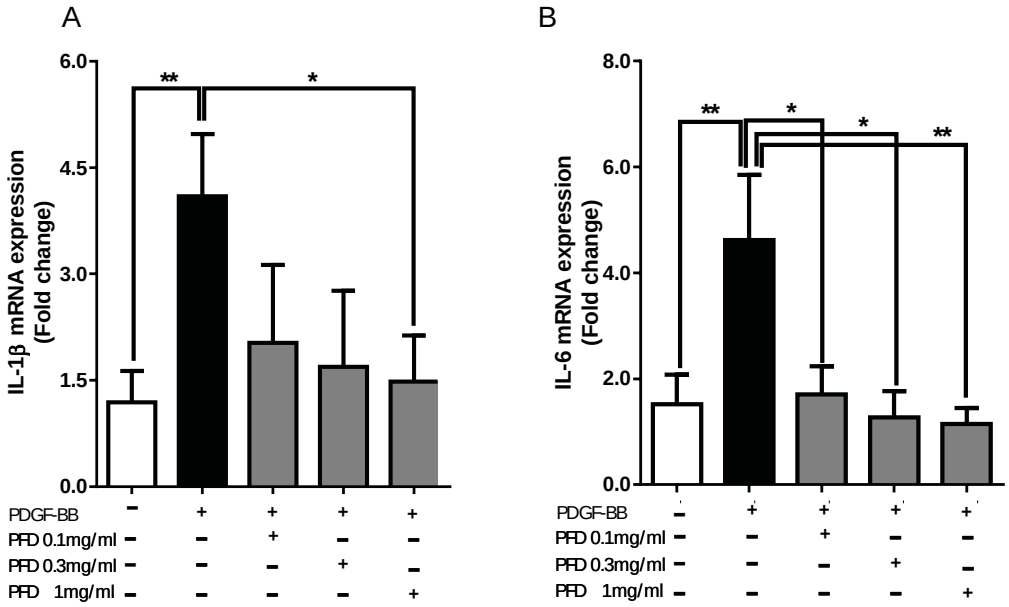

Figure 11. The effect of pirfenidone on the PDGF-BB-induced mRNA expression of interleukins in human pulmonary arterial smooth muscle cells.

A, IL-1β mRNA expression; B, IL-6 mRNA expression. Human PASMCs were incubated with 30ng/ml of PDGF-BB in the absence and presence pirfenidone for 24 hours. The RNA was isolated from the hPASMCs homogenate, cDNA was synthesized by RT-PCR and measured by qPCR. The results are expressed as mean ± SEM; n=3 independent experiments, *P<0.05; **P<0.01. PDGF, platelet derived growth factor; PFD, pirfenidone; IL, interleukin.

4.6 The effect of pirfenidone on the phosphorylation of PDGFRβ, PI3K, and AKT in human pulmonary arterial smooth muscle cells

Although pirfenidone was approved for IPF treatment in clinics in 2008, the precise action of mechanism is still unknown. To explore the mechanism of pirfenidone on hPASMCs' collagen synthesis, proliferation, and migration, the phosphorylation of the PDGFR-β, PI3K, and Akt signaling pathway was examined. As shown in figure 13, PDGF-BB stimulation led to obvious phosphorylation of PDGFR-β, PI3K, and Akt in hASMCs. Pirfenidone inhibited all the phosphorylation that was induced by PDGF-BB.

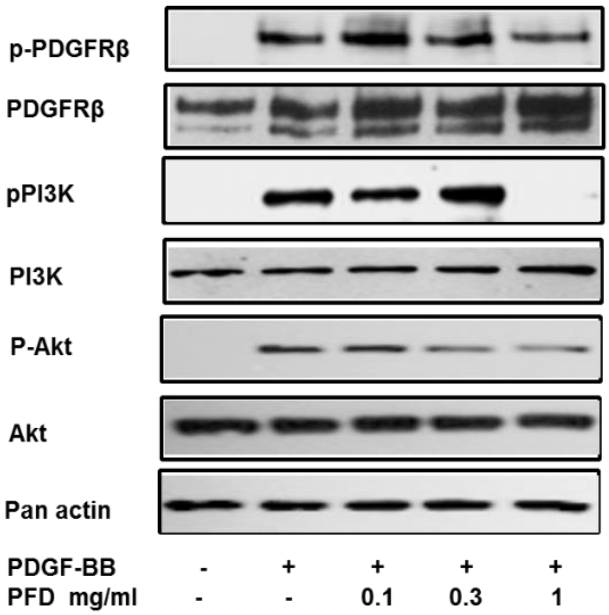

Figure 12. The effect of pirfenidone on the phosphorylation of PDGFR-β, PI3K, and Akt in human pulmonary arterial smooth muscle cells.

Human PASMCs were stimulated with 30ng/ml of PDGF-BB in the absence and presence of pirfenidone. The total protein was extracted from hPASMCs homogenate and checked by western blot. The total and phosphorylation of PDGFR-β and PI3K expression were assayed 15 mins after stimulation; the total and phosphorylation of Akt expression were checked 30 mins after stimulation. n=3 independent experiments. PDGF, platelet derived growth factor; PFD, pirfenidone.

4.7 The effect of pirfenidone on right ventricular systolic pressure and hypertrophy in SuHx rats

Considering the promising *in vitro* effects of pirfenidone, the SuHx rat's model of PH was employed to investigate the efficacy of pirfenidone *in vivo*. After injection of the VEGF receptor inhibitor with exposure to chronic hypoxia for three weeks followed by re-exposure to normoxia for another two weeks, rats exhibited significantly elevated right ventricular systolic pressure (RVSP) compared to normoxic control rats, as shown in figure 14 A. Pirfenidone reduced this elevated RVSP to 40.5 ± 4.2 mmHg ($p<0.05$, versus vehicle, Figure 14A).

The Fulton index, which is defined as RV/(LV+Septum), and right ventricular internal diameter (RVID) were examined to demonstrate the RV hypertrophy and dilatation. The Fulton index, a marker for right ventricular hypertrophy, significantly increased in PAH model rats (Figure 14B), and was lower in the pirfenidone treatment group ($p<0.01$, versus vehicle-treated rats, Figure 14B). Furthermore, RVID in SuHx rats also

significantly increased compared to normoxia control rats and was reduced to 4.36 ± 0.20 mm by treatment of pirfenidone ($p<0.05$, versus vehicle-treated rats, Figure 14C).

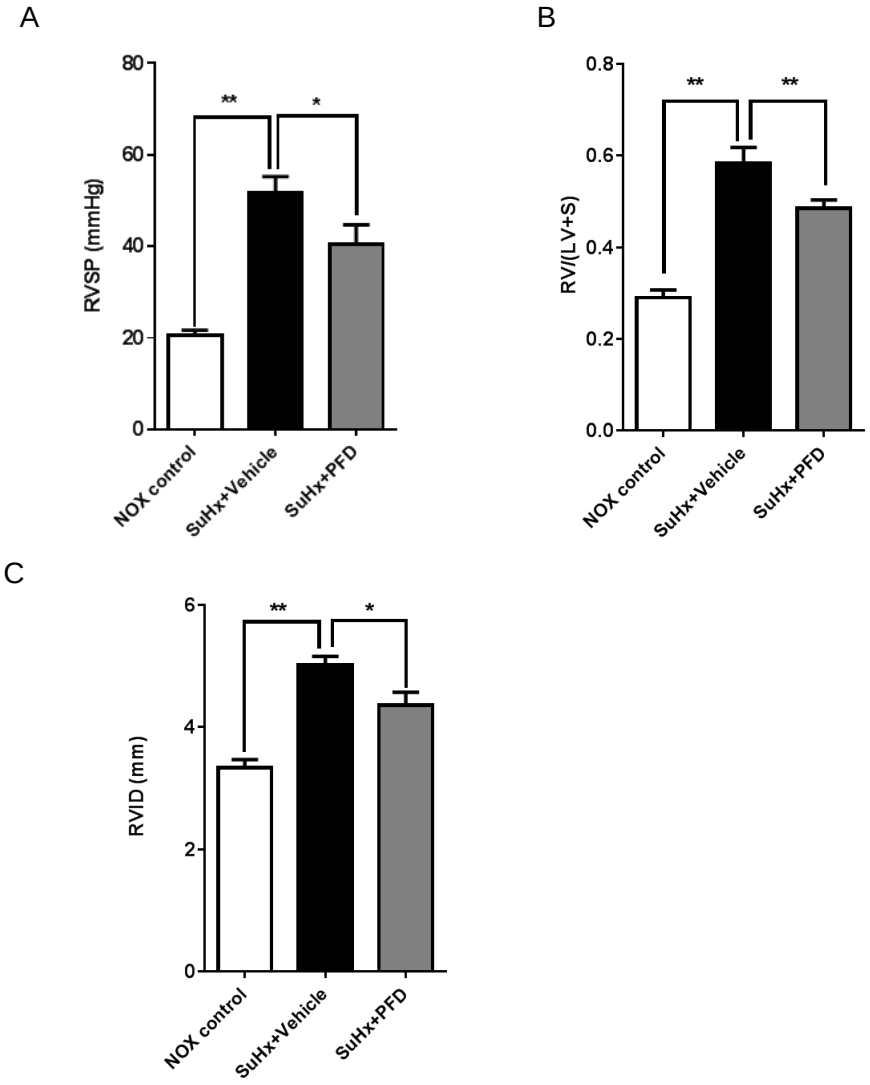

Figure 13. The effect of pirfenidone on RV systolic pressure and hypertrophy in SuHx rats. A, right ventricle systolic pressure; B, ratio of RV to left ventricular, RV/(LV+S); C, right ventricle internal diameter of different group. SuHx rats model was induced by subcutaneously injection with Sugen5416 and exposure to hypoxia for three weeks, followed by re-exposure to normoxia for another two weeks. Control animals, which were injected with the same volume of saline, were kept in normoxic conditions for the same duration. SuHx rats were either fed standard chow or 0.5% pirfenidone mixed in chow from day 21 to day 35. Control animals received standard diet. The results are expressed as mean ± SEM, n=6~8 rats per group, *P<0.05 and **P<0.01. PFD, pirfenidone; NOX, normoxia; RVSP, right ventricle systolic pressure; RVID, right ventricle internal diameter; RV, right ventricle; LV, left ventricle; S, septum.

4.8 The effect of pirfenidone on right ventricle function in SuHx rats

RESULTS

Right ventricle function is impaired in PH patients. Stroke volume, cardiac output (CO), and cardiac index (CI) were measured to evaluate the function of the right ventricle in experimental PAH. Consistent with the results of RV hypertrophy, SuHx rats showed RV dysfunction with decreased stroke volume, cardiac output, and cardiac index. Moreover, pirfenidone improved the RV function by increasing the stroke volume, cardiac output, and cardiac index of the right ventricle (all p<0.01, versus vehicle Figure 15A, B, and C).

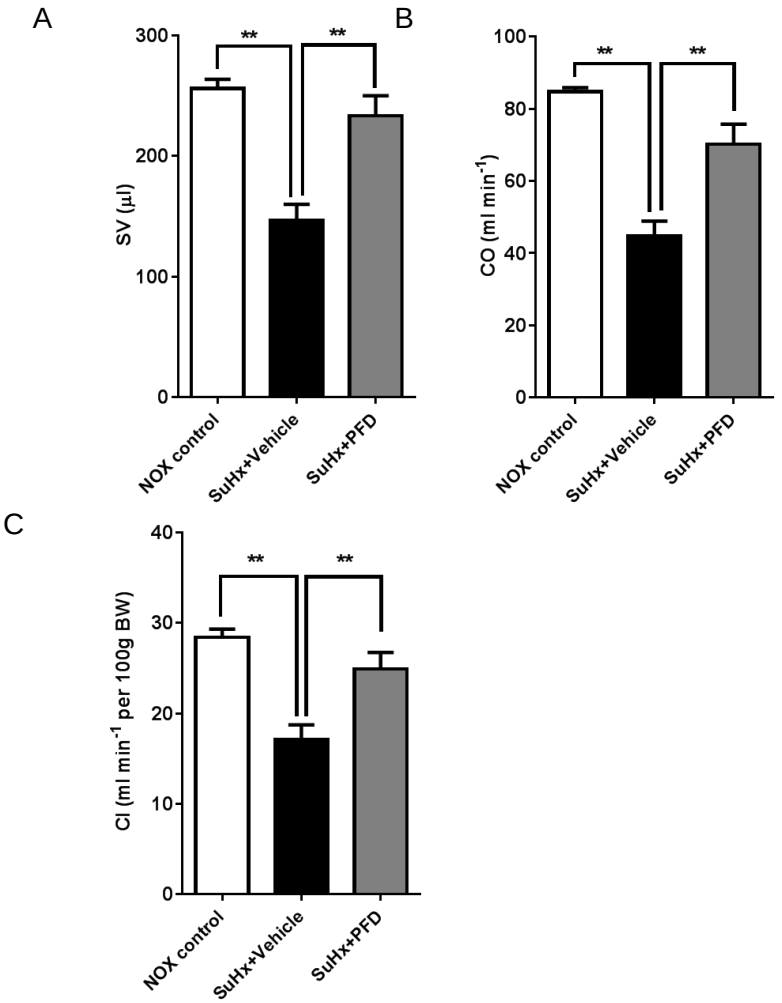

Figure 14. The effect of pirfenidone on RV function in SuHx rats.

A, stroke volume; B, cardiac output; and C, cardiac index of different groups. SuHx rats model was induced by injection with the Sugen5416 and hypoxia exposure for three weeks, followed by re-exposure to normoxia for another two weeks. Control animals, which were injected with saline, were kept in normoxic conditions. SuHx rats were either fed standard chow or 0.5% pirfenidone mixed in chow from day 21 to day 35. Control animals received standard diet. The results are expressed as mean ± SEM, n=6~8 rats per group, *P<0.05, **P<0.01. PFD, pirfenidone. NOX, normoxia; SV, stroke volume; CO, cardiac output; CI, cardiac index.

4.9 The effect of pirfenidone on vascular remodeling in SuHx rats

Neointima formation, media wall hypertrophy, and occlusion in small pulmonary vessels are key features of vascular remodeling in the development of PH. Similar to RV function and hypertrophy, the SuHx animal model demonstrated severe vascular remodeling which was shown by an increased neointima to media wall ratio and media wall thickness of the small pulmonary vessels (20-50 μm in diameter). The proportion of fully closed arteries was also remarkably increased and non-occlusion vessels were significantly decreased in SuHx rats. Pirfenidone attenuated the development of vascular remodeling and decreased the neointima to media wall ratio ($p<0.01$, versus vehicle; Figure 16A) and the media wall thickness ($p<0.05$, versus to vehicle, Figure 16B). The ratio of fully closed arteries was decreased, and the ratio of non-occlusion vessels was elevated after treatment by pirfenidone ($p<0.05$ or $p<0.01$, versus to vehicle, Figure 16C).

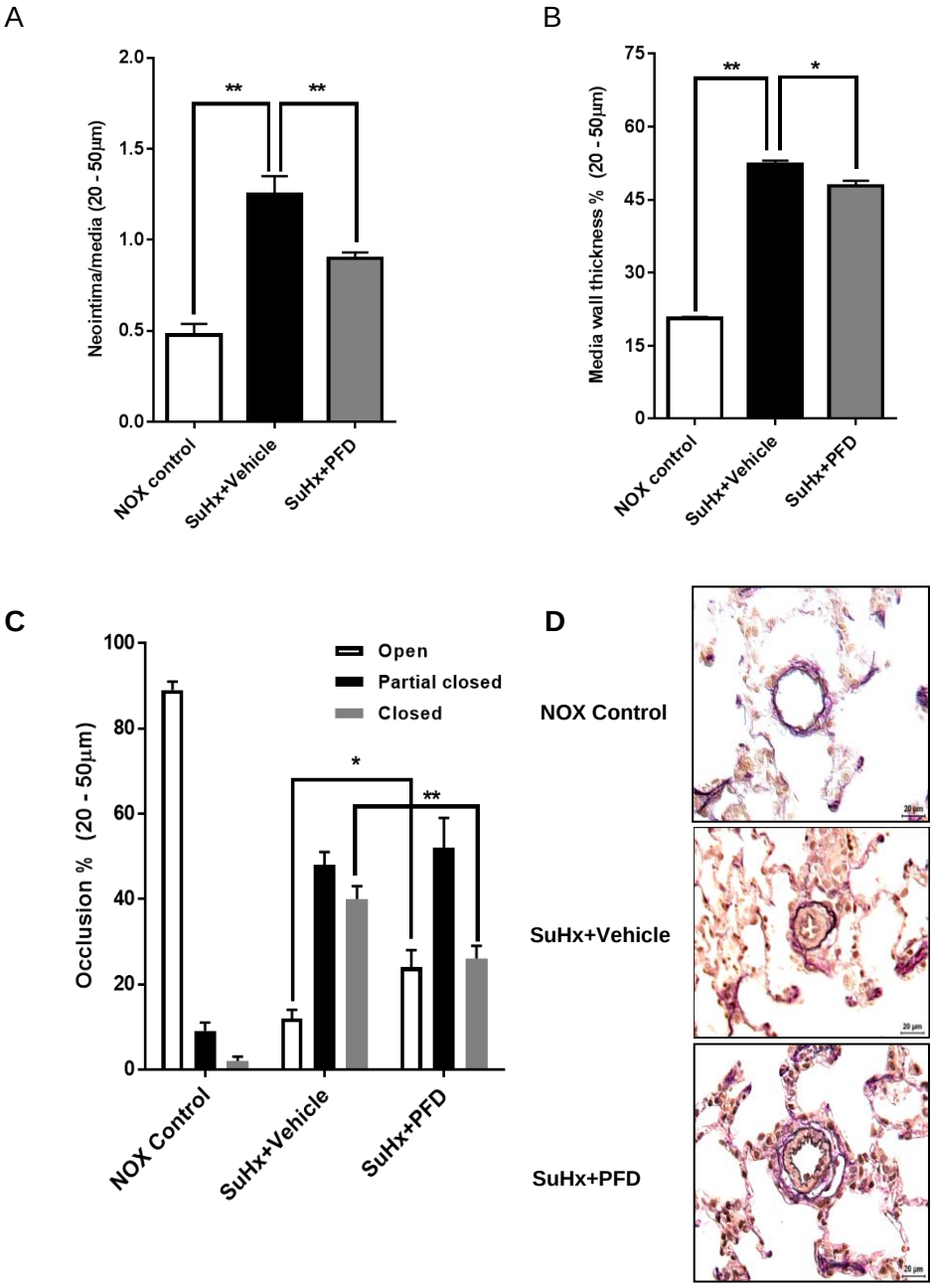

Figure 15. The effect of pirfenidone on vascular remodeling in SuHx rats.

A, neointima/media wall ratio; B media wall thickness; C, occlusion of vessels (20-50 μm in diameter) of different groups; D, representative images for vascular remodeling, scale bars=20μm. SuHx rats model was induced by subcutaneously injection with the Sugen5416 and exposure to hypoxia for three weeks, followed by re-exposure to normoxia for another two weeks. Control animals, which were injected with the same volume of saline, were kept in normoxic conditions for the same duration. SuHx rats were either fed standard chow or 0.5% pirfenidone mixed in chow from day 21 to day 35. Control animals received standard diet. The results are expressed as mean ± SEM, n=6~8 rats per group, *P<0.05 and **P<0.01. PFD, pirfenidone. NOX, normoxia.

4.10 The effect of pirfenidone on pulmonary vascular cell proliferation in SuHx rats

The proliferating cell nuclear antigen is a key factor in DNA replication and cell cycle regulation. To further evaluate the inhibitory effect of pirfenidone on vascular cell proliferation in the development of vascular remodeling, immunohistochemical staining for PCNA was performed. Immunohistochemistry results demonstrate that significantly increased PCNA positive cells were detected in vessels from SuHx rats. In addition, the PCNA positive cells remarkably decreased after treatment with pirfenidone ($p<0.01$, versus to vehicle, Figure 17B)

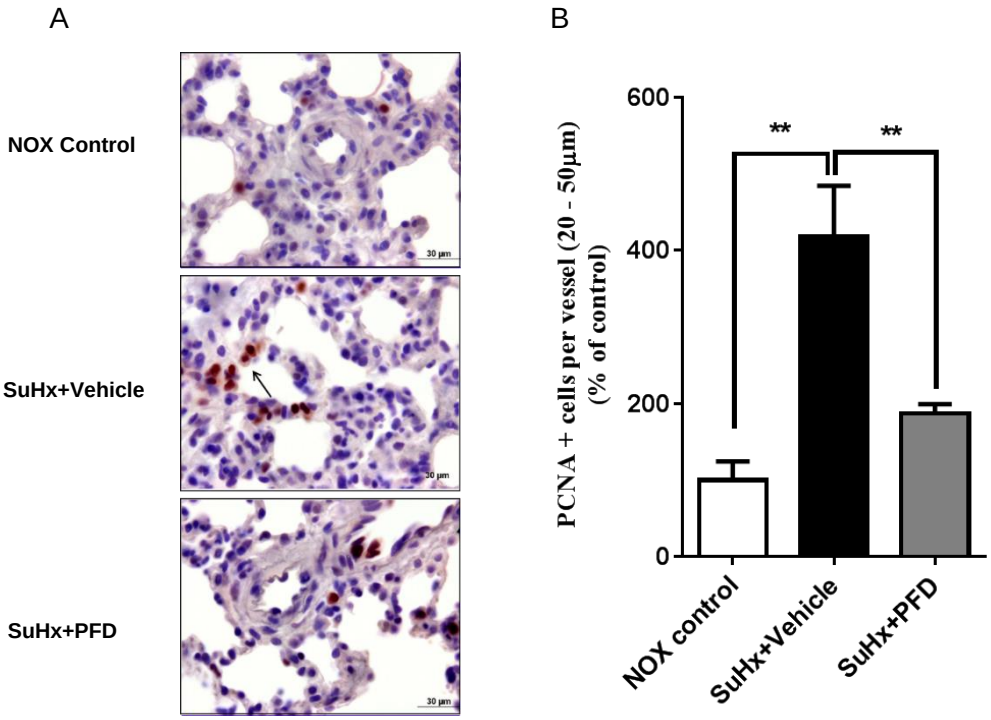

Figure 16. The effect of pirfenidone on pulmonary vascular cell proliferation.

A, representative images of PCNA staining, where the arrow indicates the PCNA positive cell scale bars=20μm; B, PCNA positive cells per vessels (20-50 μm in diameter). SuHx rats model was induced by subcutaneously injection with the Sugen5416 and exposure to hypoxia for three weeks, followed by re-exposure to normoxia for another two weeks. Control animals, which were injected with the same volume of saline, were kept in normoxic conditions for the same duration. SuHx rats were either fed standard chow or 0.5% pirfenidone mixed in chow from day 21 to day 35. Control animals received standard diet. The results are expressed as mean ± SEM, n=6 rats per group, **P<0.01. PCNA, proliferating cell nuclear antigen; PFD, pirfenidone. NOX, normoxia.

4.11 The effect of pirfenidone on collagen expression in lung tissue of SuHx rats

RESULTS

The antifibrotic effect of pirfenidone was measured by assessing the collagen level on mRNA and protein expression. The mRNA expression of collagen 1a1 and 3a1 were both elevated in the lung tissue from SuHX rats, and this increased mRNA expression was reversed by pirfenidone, as shown in figure 18. Likewise, a higher protein expression of collagen 1 was detected in SuHx rat compared to the normoxia controls, and pirfenidone treatment significantly attenuated the collagen 1 expression (P<0.05 versus vehicle, Figure 18D).

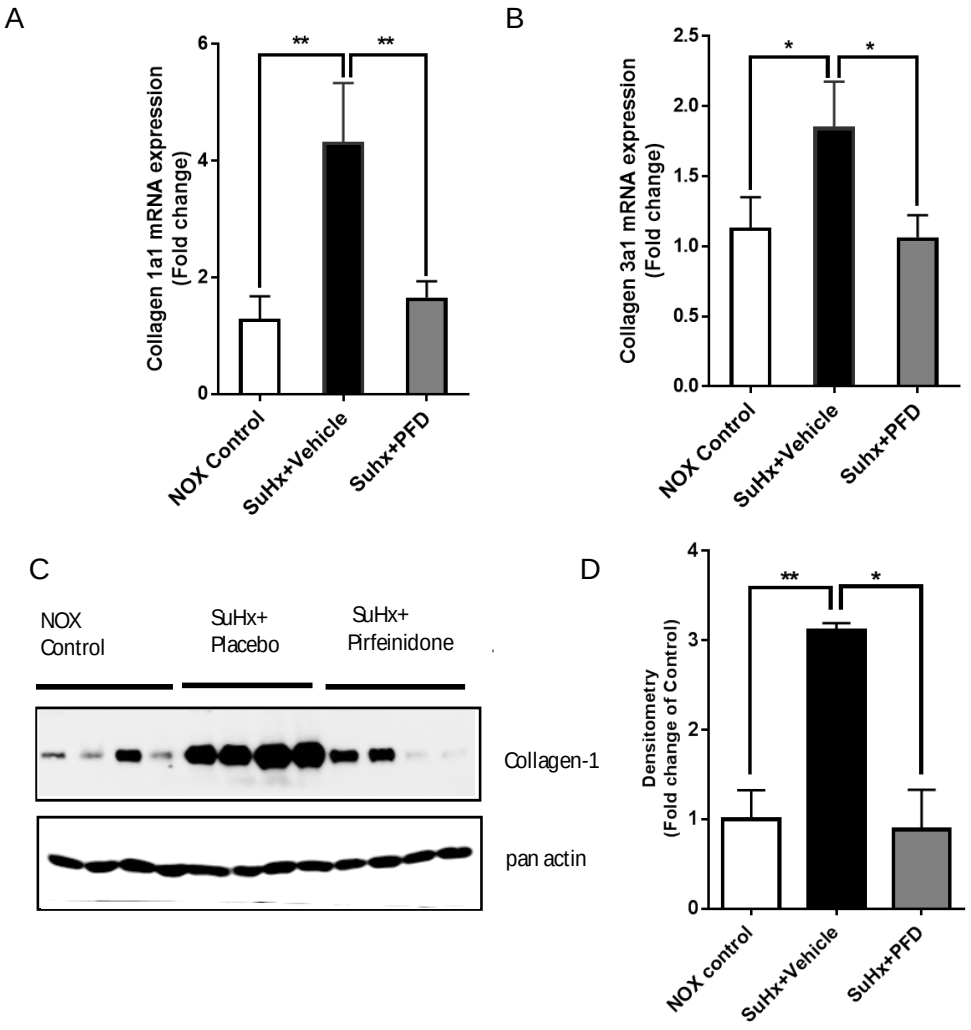

Figure 17. The effect of pirfenidone on interleukin mRNA expression lung tissue of in SuHx rats.

The protein and mRNA were extracted from lung tissue and collagen expression was checked by qPCR and western blot. A, collagen 1a1 mRNA expression; B, collagen 3a1 mRNA expression; C, western blots against collagen 1 with pan-actin as a loading control; D, densitometric quantification of phosphorylation collagen 1 expression is shown as a ratio by normalization to pan-actin in a bar graph. *P<0.05, **P<0.01. n=4~6 in each group. Values are expressed as mean ± SEM. PFD, pirfenidone; NOX, normoxia.

4.12 The effect of pirfenidone on inflammation in small pulmonary vessels of SuHx rats

The anti-inflammatory effect of pirfenidone was assessed by detecting macrophage infiltration in the small pulmonary vessels. Macrophage infiltration in the vessels was detected by immunochemical staining with CD68, a valuable marker to identify macrophages. More CD68 positive cells were present in the small pulmonary vessels, and pirfenidone treatment significantly decreased this macrophage infiltration in the vessels ($P<0.05$ versus vehicle, Figure 19B).

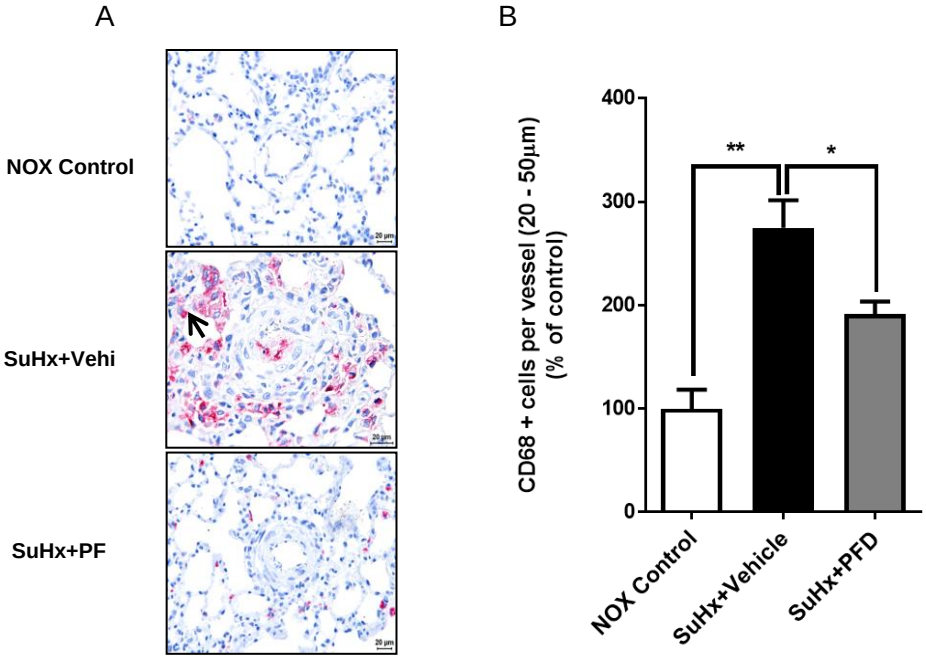

Figure 18. The effect of pirfenidone on inflammation in small pulmonary vessels of SuHx rats.

A, representative images of CD68 staining, where the arrow indicates the CD68 positive cell, scale bars=20µm; B, CD68 positive cells per vessels (20-50 µm in diameter). SuHx rats model was induced by subcutaneously injection with the Sugen5416 and exposure to hypoxia for three weeks, followed by re-exposure to normoxia for another two weeks. Control animals, which were injected with the same volume of saline, were kept in normoxic conditions for the same duration. SuHx rats were either fed standard chow or 0.5% pirfenidone mixed in chow from day 21 to day 35. Control animals received standard diet. The results are expressed as mean ± SEM, n=6 rats per group, *P<0.05 and **P<0.01. PFD, pirfenidone; NOX, normoxia.

4.13 The effect of pirfenidone on interleukin mRNA expression in lung tissue of SuHx rats

Interleukin mRNA expression in lung tissue was measured by RT-PCR as another index for the anti-inflammation efficacy of pirfenidone. Levels of IL-1β and IL-6 mRNA

from SuHx rats were much higher than those of normoxia control rats. As shown in figure 20, IL-1β and IL-6 expression were inhibited by pirfenidone treatment (both P<0.05 versus Vehicle).

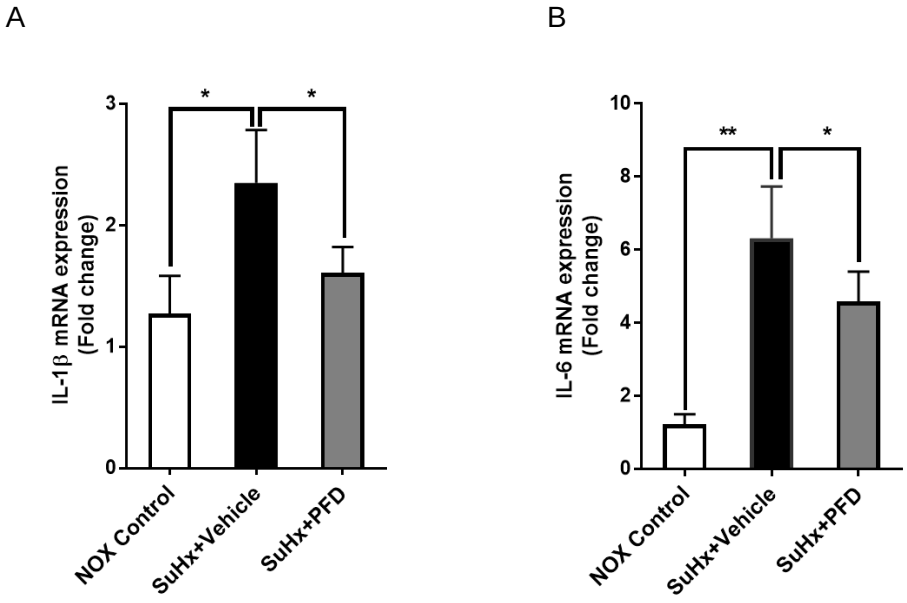

Figure 19. The effect of pirfenidone on interleukin mRNA expression in lung tissue of SuHx rats.

A, IL-1β mRNA expression; B, IL-6 mRNA expression. The mRNA was extracted from lung tissue and interleukin expression was checked by qPCR. SuHx rats model was induced by subcutaneously injection with the Sugen5416 and exposure to hypoxia for three weeks, followed by re-exposure to normoxia for another two weeks. Control animals, which were injected with the same volume of saline, were kept in normoxic conditions for the same duration. SuHx rats were either fed standard chow or 0.5% pirfenidone mixed in chow from day 21 to day 35. Control animals received standard diet. The results are expressed as mean ± SEM, n=6 in each group, *P<0.05 and **P< 0.01. PFD, pirfenidone; NOX, normoxia; IL, interleukin.

4.14 The effect of pirfenidone on the phosphorylation of PDGFR-β and AKT in lung tissue of SuHx rats

The *in vitro* data demonstrated that pirfenidone inhibited all phosphorylation of PDGFR-β, PI3K, and AKT that was induced by PDGF-BB. To elucidate the mechanism of pirfenidone acting on PAH development, the PDGFR-β and AKT signaling pathway in the lung tissue was investigated further. The Western blot results demonstrated a higher level of PDGFR-β and AKT phosphorylation in the lung tissue lysate of SuHx rats than in normoxia controls. The phosphorylation of both PDGFR-β and AKT was inhibited by pirfenidone, as shown in figure 21 (both p<0.05).

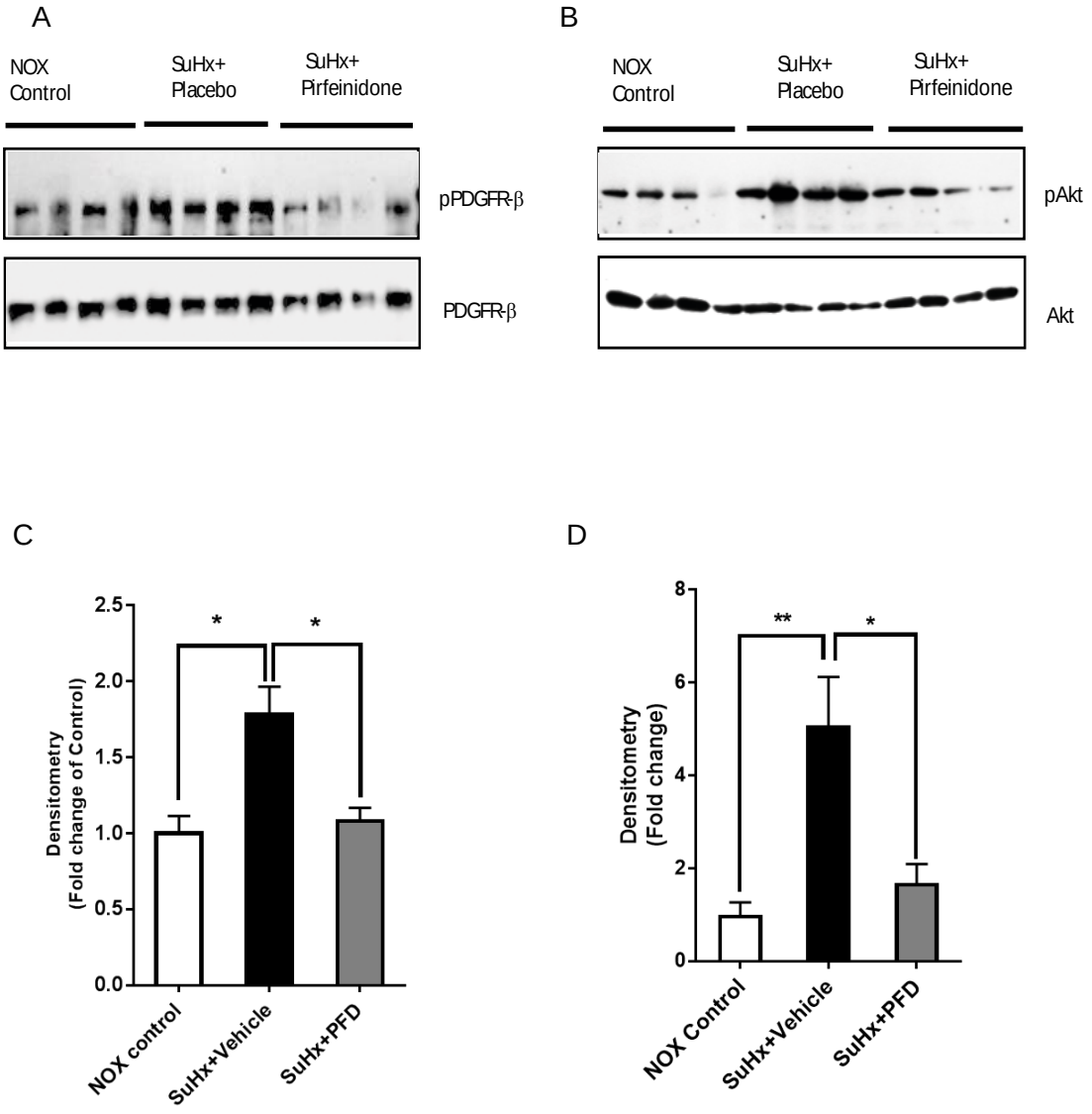

Figure 20. The effect of pirfenidone on the phosphorylation of PDGFR-β and Akt in lung tissue of SuHx rats.

A, western blots against pPDGFR-β with PDGFR-β as a loading control; B, western blots against pAkt with Akt as a loading control; C, densitometric quantification of phosphorylation PDGFR-β expression is shown as a ratio by normalization to PDGFR-β in a bar graph; D, densitometric quantification of phosphorylation Akt expression is shown as a ratio by normalization to Akt in a bar graph. The protein was extracted from lung tissue and PDGFR-β and Akt expression was checked by western blot. SuHx rats model was induced by subcutaneously injection with the Sugen5416 and exposure to hypoxia for three weeks, followed by re-exposure to normoxia for another two weeks. Control animals, which were injected with the same volume of saline, were kept in normoxic conditions for the same duration. SuHx rats were either fed standard chow or 0.5% pirfenidone mixed in chow from day 21 to day 35. Control animals received standard diet. Values are expressed as means ± SEM, n=4 in each group, *P<0.05, **P<0.01. PFD, pirfenidone; NOX, normoxia.

4.15 The effect of nintedanib on the proliferation of human pulmonary arterial smooth muscle cells

In addition to Pirfenidone, another drug (nintedanib) was approved for IPF treatment. The effects of nintedanib were investigated *in vitro* as well as those of pirfenidone. To determine the effect of nintedanib on growth-factor-induced hPASMCs proliferation, PDGF-BB and multi-growth factors (MGF) were employed to stimulate the proliferation of hPASMCs. As shown in figure 22 (next page), the proliferation of hPASMCs, induced by PDGF-BB, was inhibited by nintedanib in a dose-response manner, and nintedanib did not show inhibitory effects on multiple-growth-factor-induced cell proliferation. The viability of hPASMCs was also determined using a WST-1 kit, and no cytotoxicity was observed after nintedanib incubation. These findings demonstrate that the inhibitory effect of hPASMC proliferation for nintedanib did not result from cytotoxicity.

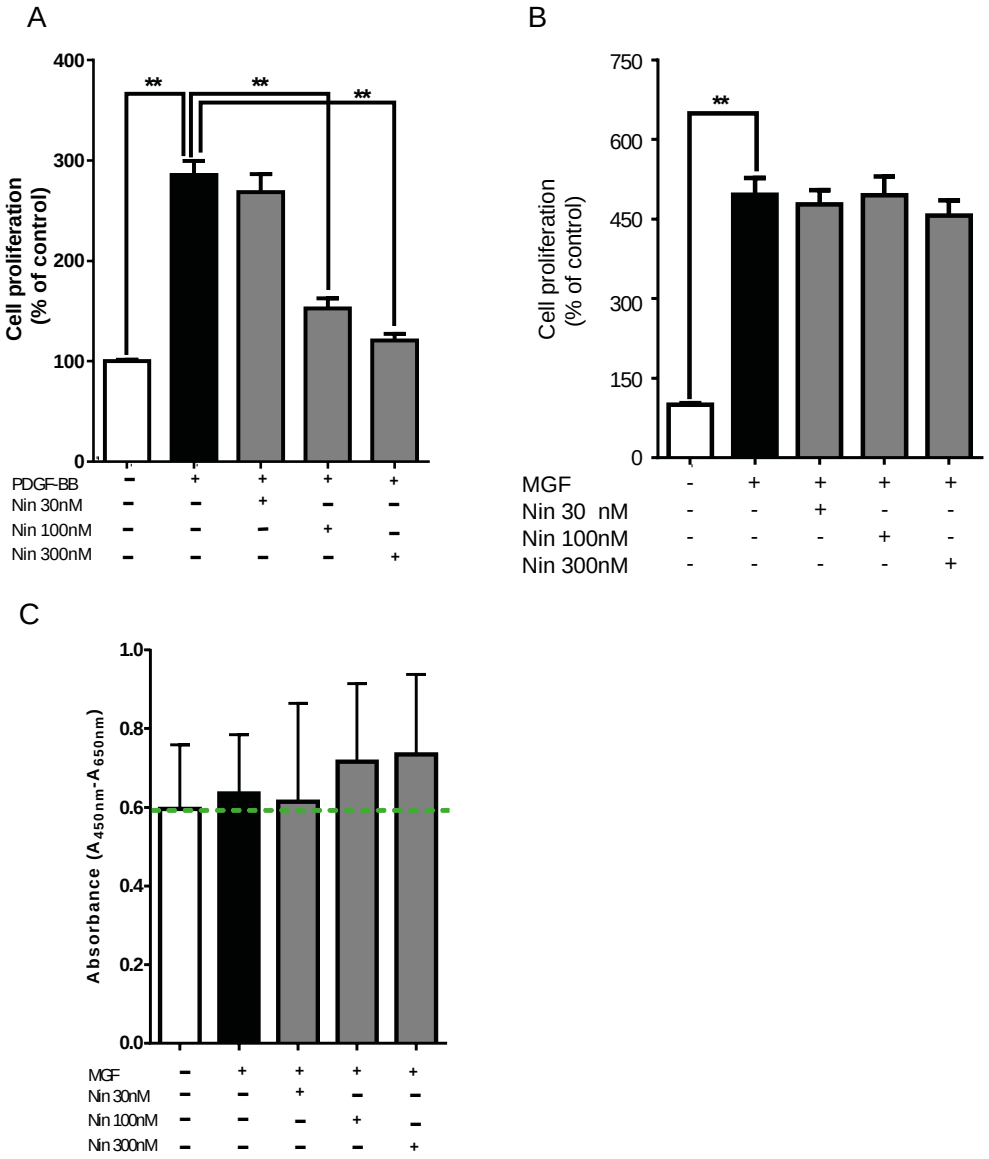

Figure 21. The effect of nintedanib on the proliferation of human pulmonary arterial smooth muscle cells.

Human PASMCs was induced by 30ng/ml of PDGF-BB (A) or MGF (B) for 24hours to induce proliferation in the absence or presence nintedanib. The proliferation of hPASMCs was assayed by the incorporation of BrdU into newly synthesized DNA. C, the viability of hPASMCs was checked by WST-1 method after 24 hours of nintedanib incubation. Results are expressed as mean ± SEM; n=3 independent experiments; **P<0.01. PDGF, platelet derived growth factor; Nin, nintedanib; MGF, multiple growth factors (including FBS, hEGF, hFGF-B, and insulin).

4.16 The effect of nintedanib on the PDGF-BB–induced migration of human pulmonary arterial smooth muscle cells

To investigate the role of nintedanib on PDGF-BB–induced cell migration, hPASMCs with PDGF-BB were also incubated in the absence and presence of nintedanib for 24

hours, after which the cell migration was counted. As shown in figure 23, the PDGF-BB-induced migration of cells was inhibited by nintedanib in a dose-response manner.

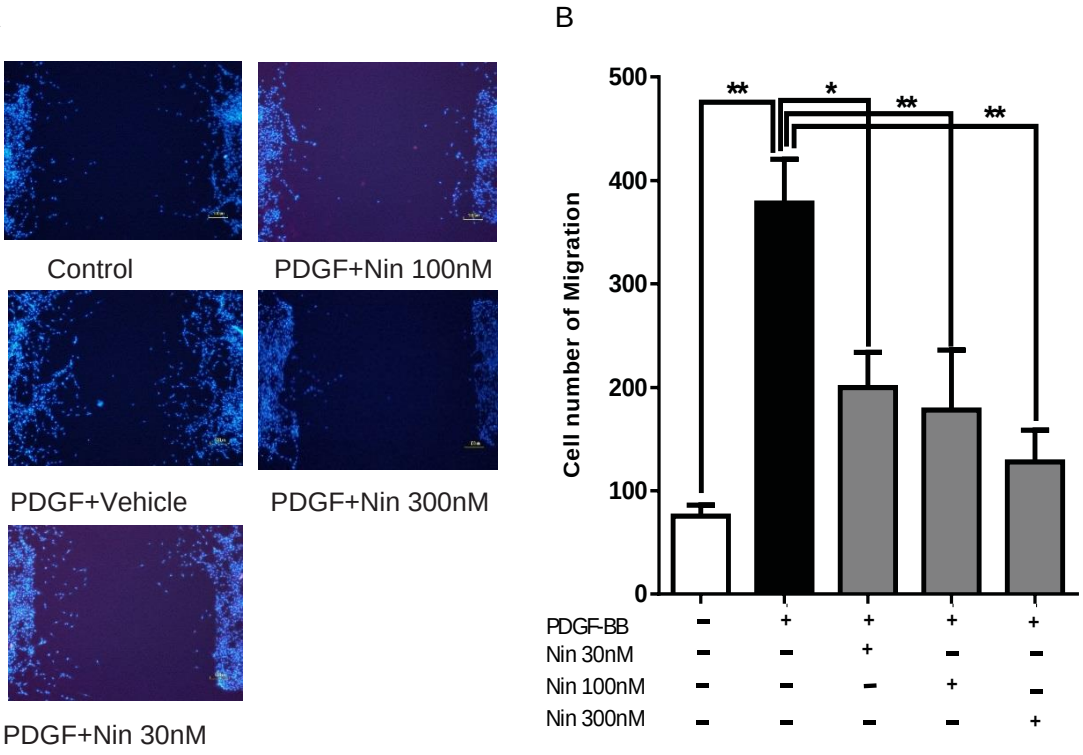

Figure 22. The effect of nintedanib on the PDGF-BB-induced migration of human pulmonary arterial smooth muscle cells.

A, representative picture of hPASMCs migration, scale bars = 100μm; B, cell number of hPASMCs migration. Human PASMCs were stimulated with 30 ng/ml of PDGF-BB for 24h to induce migration in the absence or presence of nintedanib. Migration result was expressed as the number of migrated cells. Results are expressed as means ± SEM; n=3-5 experiments, *P<0.05, **P<0.01. PDGF, platelet derived growth factor; Nin, nintedanib.

4.17 The effect of nintedanib on PDGF-BB-induced collagen synthesis and secretion in human pulmonary arterial smooth muscle cells

To further investigate the effect of nintedanib on collagen deposition, collagen I protein expression in hPASMCs homogenate was measured by western blot and collagen secretion in the medium with the Sircol method. The increased collagen I protein level, which was induced by PDGF-BB, was attenuated by nintedanib as shown in figure 24A. In parallel, nintedanib incubation decreased the content of collagen in the medium in a dose-response manner (Figure 24B).

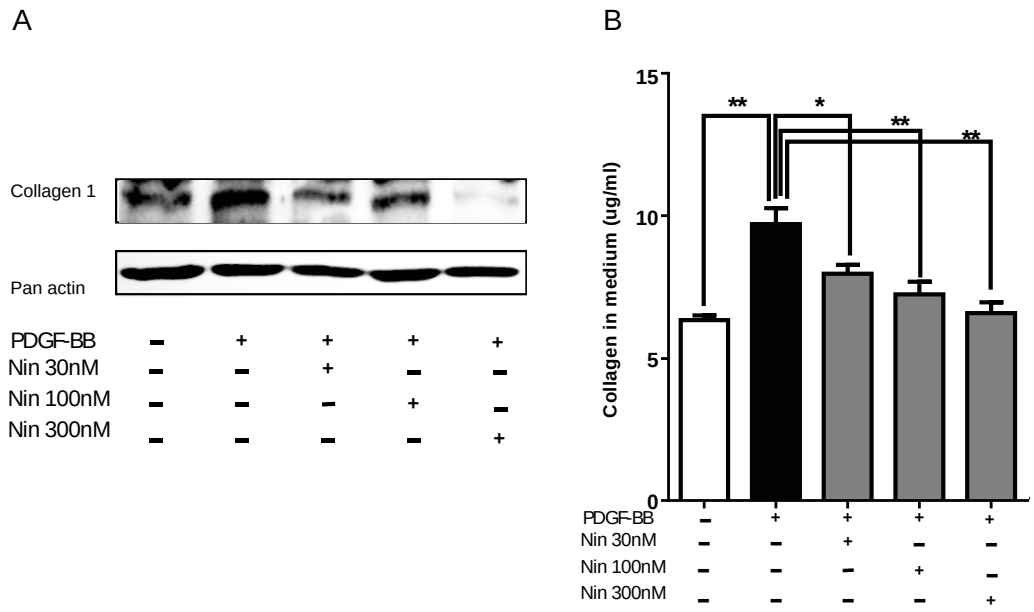

Figure 23. The effect of nintedanib on PDGF-BB-induced collagen synthesis and the secretion of human pulmonary arterial smooth muscle cells.

Human PASMCs were incubated with 30ng/ml of PDGF-BB in the absence and presence nintedanib. A, representative western blot picture of collagen1. The total protein was extracted from hPASMCs after 24hours incubation and collagen1 expression was checked by western blot. B, the soluble collagen1 level in the medium. The collagen secretion of hPASMCs in the medium was measured by the Sircol method 72 hours after incubation. Results are expressed as means ± SEM; n=3~5 experiments. *P<0.05, **P<0.01. PDGF, platelet derived growth factor; Nin, nintedanib.

4.18 The effect of nintedanib on interleukin mRNA expression in human pulmonary arterial smooth muscle cells

To investigate the efficacy of nintedanib on PDGF-BB-induced inflammatory cytokine expression, interleukin mRNA expression was examined. As shown in figure 25, increases in levels of IL-1β and IL-6 induced by PDGF-BB were blocked by the presence of nintedanib.

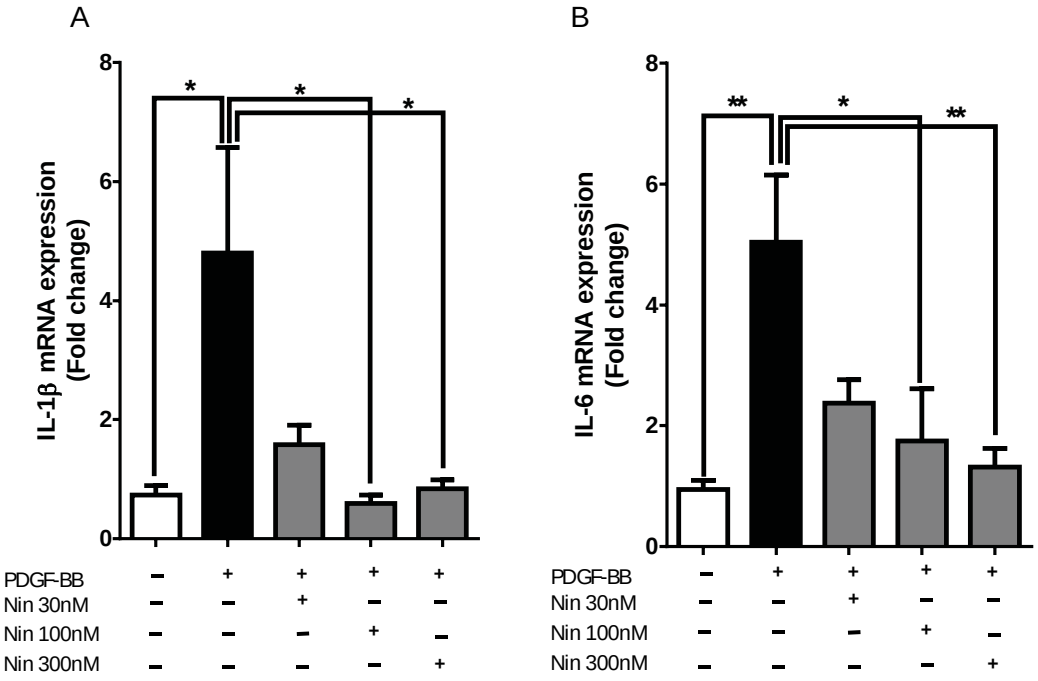

Figure 24. The effect of nintedanib on the PDGF-BB-induced mRNA expression of interleukins in human pulmonary arterial smooth muscle cells.

A, IL-1β mRNA expression, B, IL-6 mRNA expression. Human PASMCs were incubated with 30ng/ml of PDGF-BB in the absence and presence nintedanib. The RNA was isolated from the hPASMCs homogenate, cDNA was synthesized by RT-PCR and measured by qPCR. Results are expressed as means ± SEM; n=3 independent experiments, *P<0.05, *P<0.01. PDGF, platelet derived growth factor; Nin, nintedanib; IL, interleukin.

4.19 The effect of nintedanib on the phosphorylation of PDGFRβ, PI3K, and AKT in human pulmonary arterial smooth muscle cells

To investigate the role of nintedanib on PDGF-BB-induced increases in collagen synthesis, proliferation, and migration, the phosphorylation of PDGFR-β, PI3K, and Akt signaling pathway was examined. As shown in figure 26, nintedanib reversed the PDGF-BB-induced increases in the phosphorylation of PDGFRb, PI3K, and Akt.

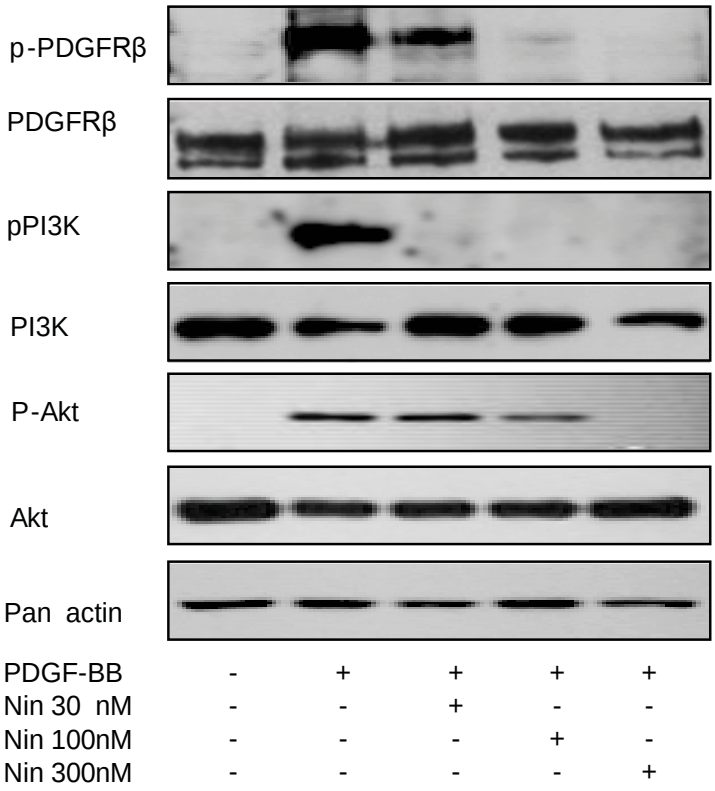

Figure 25. The effect of nintedanib on the phosphorylation of PDGFR-β, PI3K, and Akt in human pulmonary arterial smooth muscle cells.

Human PASMCs were incubated with 30ng/ml of PDGF-BB in the absence and presence nintedanib. The total protein was extracted from hPASMCs homogenate and checked by western blot. The total and phosphorylation of PDGFR-β and PI3K expression were assayed 15 minutes after stimulation with PDGF-BB; the total and phosphorylation of Akt expression were analyzed 30 minutes after stimulation with PDGF-BB. n=3 independent experiments. PDGF, platelet derived growth factor; Nin, nintedanib.

4.20 The effect of nintedanib on right ventricle systolic pressure and hypertrophy in SuHx rats

Based on the promising *in vitro* results of nintedanib, the efficacy of nintedanib was also investigated with the SuHx rat model. The RVSP in SuHx rats was significantly elevated compared to normoxia control rats, as shown in figure 27A. Nintedanib did not show any inhibitory effects on RVSP, which was unexpected. The Fulton index and RVID in SuHx rats were also increased compared to normoxia control rats (Figure 27B and C), and there were no changes in RV hypertrophy after treatment with nintedanib.

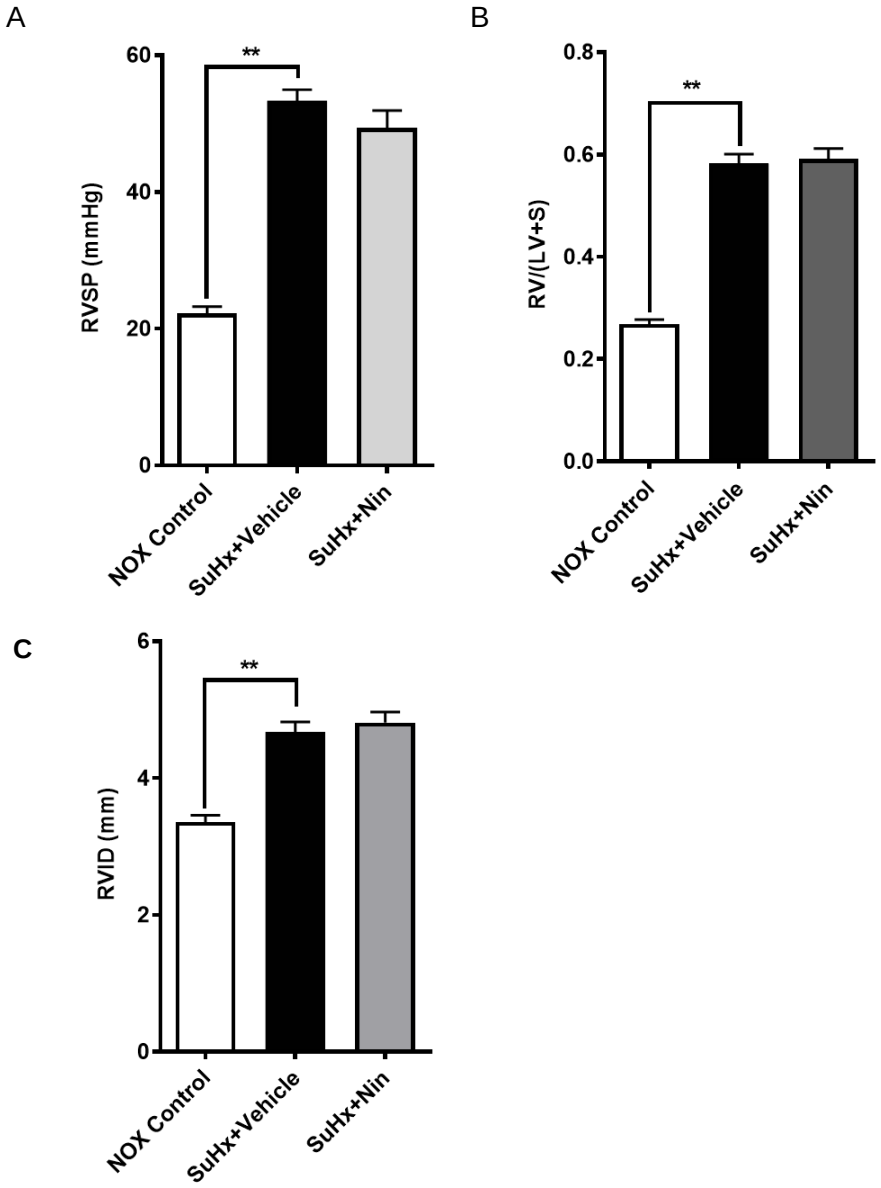

Figure 26. The effect of nintedanib on hemodynamics in SuHx rats.

A, right ventricle systolic pressure; B, ratio of RV to left ventricular, RV/(LV+S); C, right ventricle internal diameter of different group. SuHx rats model was induced by subcutaneously injection with the Sugen5416 and exposure to hypoxia for three weeks, followed by re-exposure to normoxia for another two weeks. Control animals, which were injected with the same volume of saline, were kept in normoxic conditions for the same duration. SuHx rats were either vehicle or 50mg/kg nintedanib from day 21 to day 35. Control animals received vehicle only. Results are expressed as mean ± SEM, n=6~10 rats per group, **P< 0.01. Nin, nintedanib; NOX, normoxia; RVSP, right ventricle systolic pressure; RVID, right ventricle internal diameter; RV, right ventricle; LV, left ventricle; S, septum.

4.21 The effect of nintedanib on RV function in SuHx rats

RESULTS

SuHx rats demonstrated impaired RV function, and nintedanib did not improve the SV, CO, or CI of the right ventricle (all p>0.05, versus to vehicle Figure 28A, B and C).

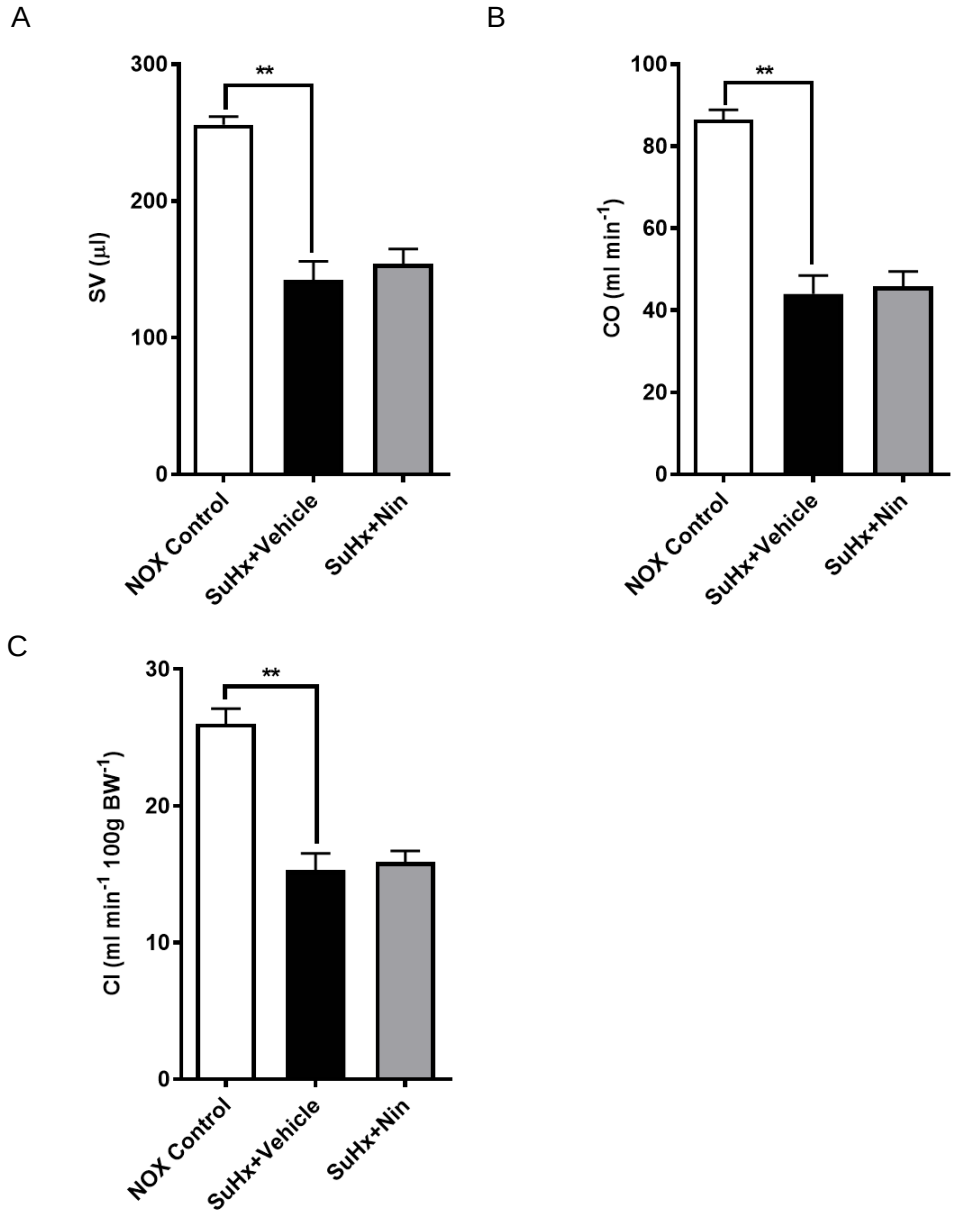

Figure 27. The effect of nintedanib on RV function in SuHx rats.

A, stroke volume; B, cardiac output; C, cardiac index of different group. SuHx rats model was induced by subcutaneously injection with the Sugen5416 and exposure to hypoxia for three weeks, followed by re-exposure to normoxia for another two weeks. Control animals, which were injected with the same volume of saline, were kept in normoxic conditions for the same duration. SuHx rats were either vehicle or 50mg/kg nintedanib from day 21 to day 35. Control animals received vehicle only. The results are expressed as mean ± SEM, n=6~10 rats per group, **P<0.01. Nin, nintedanib; NOX, normoxia; SV, stroke volume; CO, cardiac output; CI, cardiac index.

4.22 The effect of nintedanib on vascular remodeling in SuHx rats

SuHx rats demonstrated severe vascular remodeling, including an increased neointima to media wall ratio, media wall thickness, and occlusion of small pulmonary vessels. The neointima to media ratio was slightly decreased by treatment with nintedanib without statistical significance (P>0.05). Nintedanib did not demonstrate any effects on the media wall thickness or the occlusion of vessels, as shown in figure 29.

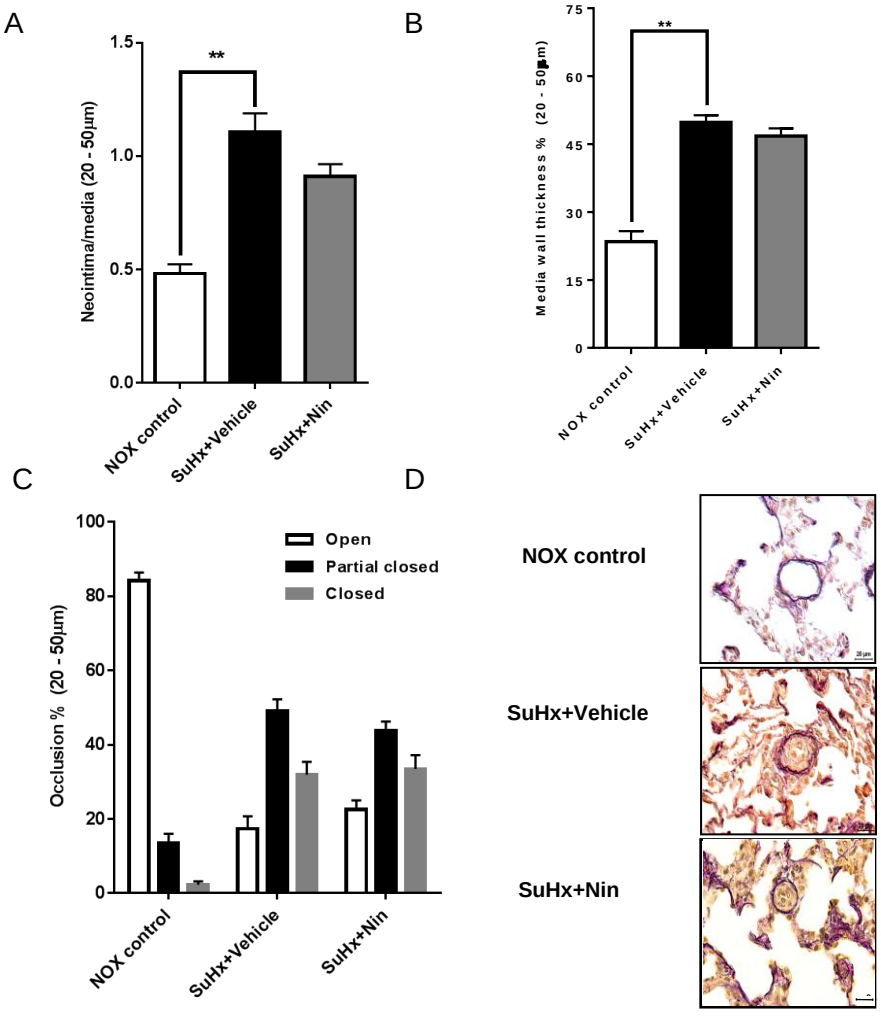

Figure 28. The effect of nintedanib on vascular remodeling in SuHx rats.

A, neointima/media wall ratio; B, media wall thickness; C, occlusion of vessels (20-50 μm in diameter) from different groups, scale bars=20μm; D, representative images for vascular remodeling. SuHx model was induced by Sugen5416 injection and exposure to hypoxia for three weeks, followed by re-exposure to normoxia for another two weeks. Control animals, which were injected with saline, were kept in normoxic conditions. SuHx rats were either vehicle or 50mg/kg nintedanib from day 21 to day 35. Control animals received vehicle only. The results are expressed as mean ± SEM, n=6~10 rats per group, **P<0.01. NOX, normoxia; Nin, nintedanib.

5 DISCUSSION

Pulmonary arterial hypertension is characterized by excessive vasoconstriction due to the dysregulation of vascular tone and vascular remodeling caused by abnormal proliferation, migration, and resistance to apoptosis of vascular cells. Currently approved agents for PAH treatment are primarily vasodilators [79]. These therapeutic approaches relieve the pulmonary vasoconstrictive component of the disease and provide symptomatic relief with some improvement in prognosis. However, these is no strong evidence to support that these vasodilators have a direct antiproliferative effect on PAMSCs, and the underlying pathological pulmonary vascular and right ventricular remodeling still progresses.

In this study, two antifibrotic drugs, pirfenidone and nintedanib, were administered in a well-recognized animal model of PAH to investigate the efficacy of these two compounds in the development of PAH. The novel findings of the present study are as follows: (1) The elevated RVSP in SuHx rats was attenuated by treatment with pirfenidone, but not with nintedanib. (2) Right ventricular function in SuHx rats was ameliorated with the treatment of pirfenidone, but not with nintedanib. Consistent with RV function, RV hypertrophy in the SuHx rat model was decreased by pirfenidone treatment, but not by nintedanib. (3) Pirfenidone inhibited the development of pulmonary vascular remodeling and the progression of occlusion lesions in the SuHx model, but nintedanib did not demonstrate the inhibitory effects on these indexes. (4) Pirfenidone attenuated pulmonary vascular cells proliferation and inflammation infiltration in SuHx rats; (5) Pirfenidone decreased collagen 1 expression by inhibiting phosphorylation of PDGFR-β and AKT in the lung tissue from SuHx rat. (6) Both pirfenidone and nintedanib reversed the proliferation of PASMCs which was induced by growth factors. (7) The migration of PASMCs that was induced by PDGF-BB was attenuated by both pirfenidone and nintedanib. (8) The collagen synthesis and secretion that was induced by PDGF-BB in PASMCs were inhibited by pirfenidone and nintedanib. (9) Both pirfenidone and nintedanib prevented the increased mRNA level of IL-1β and IL-6, which was induced by PDGF-BB. (10) The phosphorylation of PDGFR-β, PI3K, and AKT, which was induced by PDGF-BB in PASMCs, was inhibited by pirfenidone and nintedanib in vitro.

5.1 Pirfenidone improved vascular remodeling

In the present study, SuHx rats were employed as a PAH model to investigate the efficacy of pirfenidone and nintedanib. The SuHx rat model is a relatively new animal model for PAH, and it is well accepted for mechanism studies and drug research and

development. This model demonstrates severe changes in the pulmonary vasculature that closely mimic the vascular changes found in patients with severe PAH. In these patients, two major characteristic vascular changes are medial wall thickening due to PASMCs proliferation, and plexiform lesions which consist of PASMCs migration and a hyper-proliferative endothelium [111-114]. Plexiform lesions are identified as the pathological hallmark of PAH from different etiologies, though classical animal models other than the SuHx model of PH do not show this patho-histological feature [68, 69]. Furthermore, the SuHx model is refractory to treatment as it is in most PAH patients, while with the MCT-induced PAH, it is relatively easy to improve or cure the vascular remodeling due to the acute or subacute nature of this model, which is not similar to patients with PAH [82, 115]. Therefore, SuHx rats were selected as the experimental PAH model for this study.

The process of vascular remodeling is central to the pathobiology of PAH. This process involves structural and functional changes to the normal architecture of pulmonary artery (PA) walls that lead to abnormal muscularization of PAs, medical hypertrophy, neointima formation, and formation of plexiform lesions. This study found that the increased media wall thickness in the SuHx model was suppressed by pirfenidone. The development of occlusive lesions and neointima formation were also inhibited by pirfenidone. However, nintedanib failed to show beneficial effects on the process of vascular remodeling in SuHx model.

Proliferation, migration, collagen deposition, and resistance to apoptosis of medial cells contribute to the development of vascular remodeling [116]. To explore the mechanism of action for pirfenidone on vascular remodeling, pulmonary artery cells proliferation and migration, and collagen deposition were investigated. The principal cells in the media of pulmonary vessels are PASMCs, and evidence shows that medial hypertrophy, the most consistent pathological finding in PAH, is mainly due to PASMCs proliferation and the remodeling of extracellular matrix (ECM) proteins [116, 117]. In this research, PASMCs were employed to investigate the effect of pirfenidone or nintedanib in these *in vitro* experiments.

In addition, PDGF-BB was selected as the stimulator for PASMCs because: 1) the PDGF ligand and receptor and PDGF signaling are increased or upregulated in the patients of PAH as well as experimental PAH animals [32-36], 2) the inhibition of PDGFR improves the survival in MCT-induced PAH rats [36, 52], and PDGFR inhibitor imatinib demonstrates significant improvements in exercise capacity and hemodynamics in patients with advanced PAH in the IMPRES clinical phase III trial [37]. 3) In addition,

among the growth factors which play a role in the development of PAH, PDGF-BB is one of the most potent mitogens and chemoattractants for SMCs [116, 118]. Together, these data support the concept that PDGF and the PDGF signaling pathway are increased and promote pulmonary vascular remodeling in PAH. Based our experiment for effect of different concentration PDGF-BB on PASMCs (Figure 8), 30ng/ml was used as the concentration of PDGF-BB to follow experiments on PASMC proliferation and migration, and collagen synthesis and secretion.

5.1.1 Pirfenidone inhibited human PASMCs proliferation

The proliferation of vascular smooth muscle cells, a prominent feature of PAH, is a critical event in progressive media wall thickening, which leads to vascular remodeling. Moreover, PCNA plays an essential role in nucleic acid replication and repair machinery, and is considered a marker of cell proliferation. Pulmonary artery cells proliferation was measured by PCNA staining. There were less PCNA positive pulmonary vessel cells found in the pirfenidone-treated rats than in the vehicle-treated rats due to pirfenidone's inhibition of proliferation. To confirm the proliferative inhibitory effect of pirfenidone on pulmonary artery cell proliferation, PASMCs proliferation induced by growth factors was employed. Similar to *in vivo* results, pirfenidone demonstrated a dose-response inhibitory effect on PAMSCs proliferation, which was induced by PDGF-BB. The high dose of pirfenidone (1mg/ml) even prevented the PASMCs proliferation that was induced by multiple growth factors. The previous study of pirfenidone discovered that pirfenidone could inhibit the proliferation of many different cells, including lung fibroblasts [119], leiomyoma cells [120], pterygium fibroblasts [121], renal fibroblasts [122], cardiac fibroblasts [123], hepatic stellate cells [124] and lens epithelial cells [125]. This is the first time that pirfenidone was shown to inhibit the proliferation of PASMCs.

The mechanism that pirfenidone uses to inhibit DNA synthesis and cell proliferation is still not clear, but it does not relate to cytotoxic effects on the cells [120] because the cytotoxicity by was determined with a WST-1 assay, and no cytotoxic effect of pirfenidone was detected.

5.1.2 Pirfenidone attenuated PASMCs migration

Migration plays an important role in physiologic processes including wound healing and immune function [126], and it contributes to disease processes such as inflammation [127], tumor growth, and metastasis [128]. Since the migration of PASMCs occurs during the processes of development, vascular injury, and vascular remodeling, it is possible that PASMCs migration plays a role in the abnormal muscularization of distal pulmonary

arteries, neointima formation, and the formation of plexiform lesions [114]. A recent study clarified the role of PASMCs proliferation and migration in neointima formation [129, 130]. As shown in figure 10, the increased migration that was induced by PDGF-BB was attenuated by the high concentration of pirfenidone. This result is consistent with the *in vivo* data showing that increased neointima was inhibited by pirfenidone treatment and that the occlusion of vessels decreased.

5.1.3 Pirfenidone decreased the deposition of collagen

Thickening of the PA wall is not only the result of PASMCs proliferation, as it is also due to extracellular matrix (ECM) production and collagen deposition. In Wanli's research, they found a PDGF-activated TGF-β1 signaling pathway in PASMCs, which led to the phosphorylation of Smad2/3 and an increase in collagen synthesis [108]. The present *in vitro* study shows that pirfenidone attenuated the PDGF-BB-induced collagen synthesis and secretion of PASMCs. The *in vivo* study also showed that the mRNA and protein level of collagen in lung tissue increased in the SuHx rat model, and both mRNA and protein expression decreased after treatment with pirfenidone. Although the exact mechanism of pirfenidone for IPF treatment is not yet clear, the antifibrotic activity is like achieved via suppression of TGF-β[87]. A recent investigation found that pirfenidone suppressed the mRNA expression of collagen and inhibited the activation of TGF-β-related Smad pathways both *in vitro* (fibroblasts and retinal pigment epithelial cells) and *in vivo* [131, 132]. It is assumed that pirfenidone inhibited the signaling pathway of TGF-β/Smad to suppress the collagen synthesis and deposition in the SuHx model by attenuating the phosphorylation of PDGFRβ to decrease the activity of the TGF-β1 signaling pathway (Figure 21).

5.2 Pirfenidone decreased right ventricle systolic pressure

Pulmonary artery pressure (PAP) is the product of cardiac output (CO) and pulmonary vascular resistance. The biggest determinant of pulmonary vascular resistance is abnormal vascular remodeling in the small pulmonary arterioles [17]. This abnormal vascular remodeling includes medial hypertrophy, intima hyperplasia, and the occlusion of small vessels which reduces the luminal area of the small pulmonary arteries and results in vascular pulmonary resistance. Through the coupling of pulmonary artery pressure with the structural changes in the pulmonary vascular wall, and decreased vascular remodeling by pirfenidone treatment, pirfenidone significantly reduced RVSP in SuHx rats. RVSP is almost equivalent to PAP in ideal conditions.

DISCUSSION

Research shows that RhoA/Rho-kinase-mediated vasoconstriction is the main cause of persistent PAP elevation [133, 134]. Fasudil, the Rho kinase inhibitor, improved hemodynamics by reducing pulmonary vascular resistance and mean PAP in the experimental model of PAH and in patients with PAH [135-137]. Furthermore, both pirfenidone and fasudil demonstrated an inhibitory effect on the RhoA/Rho pathway in the human retinal pigment epithelial cell line, ARPE-19 [138]. The reduction of RVSP in the present investigation may be not only due to improvement in pulmonary vascular remodeling, might be also associate with a reduction in pulmonary vascular vasoconstriction by inhibiting the RhoA/Rho pathway. However, this requires further investigation.

5.3 Pirfenidone improved right ventricle function and hypertrophy

Sustained elevated pressure has a devastating effect on the right ventricle, as PH provides an excessive burden on the right ventricle from the increased work to overcome the elevated downstream pressure. Over time, this results in right ventricle hypertrophy, right ventricle dysfunction, and right-sided heart failure consecutively [112]. Right ventricle failure is a major cause of dysfunction or death in patients with PAH. In addition, right ventricle function is the most important determining index of the prognosis of PAH, although the main pathology is vascular remodeling in the pulmonary vasculature.

In line with the result of the reduction in RVSP and improvement in pulmonary vascular remodeling, the right ventricle function also improved. Stroke volume, CO, and CI all significantly increased after treatment with pirfenidone compared to the vehicle. In this study, pirfenidone reduced right ventricle hypertrophy; this was demonstrated by decreased right ventricle internal diameter and the Fulton index, which are the markers of right ventricle hypertrophy. These data show that right ventricle hypertrophy was attenuated along with the improvement of right ventricle function after the reduction of right ventricle systolic pressure by pirfenidone treatment.

5.4 Pirfenidone suppressed expression of inflammatory markers

Inflammation underlies a wide variety of physiological and pathological processes. Increasing evidence indicates that inflammation is a major pathogenic component of vascular remodeling. Inflammatory processes are involved in the initiation and development of human PAH as well as in experimental models of PAH. Tuder's investigation found that an increased number of macrophages are present in the plexiform lesion of the patients with PAH [68], and in the chronic hypoxia and MCT-induced PH animal models [139, 140]. In addition, macrophage infiltration and activation

may induce the release of IL-1β, IL-6, monocyte chemotactic protein-1 (MCP-1), and TNF-α, which all play an important role in the pathogenesis of PAH [71, 141]. In the present study, macrophage (CD68 positive cells) accumulation was identified in the pulmonary vessels of the SuHx model rats. This study also demonstrates that the mRNA level of IL-1β and IL-6 are significantly elevated in SuHx lung tissue and in PASMCs after PDGF-BB stimulation.

Pirfenidone was initially designed as an anti-inflammatory agent, though the focus was later shifted to an anti-fibrotic agent [87]. Pirfenidone can modulate the expression of proinflammatory cytokines in addition to the effect of inhibiting pro-fibrotic factors [87]. The anti-inflammatory activity of pirfenidone has been demonstrated in a septic shock model [142] and a bleomycin-induced lung fibrosis model in mice [143]. Moreover, pirfenidone suppressed the production of TNF-α by post-transcriptional regulation of the TNF-α gene and enhanced the production of IL-10 in this septic shock mice model [142]. The proinflammatory cytokines in the lung tissue, such as IL-1β, IL-6, and MCP-1, were all inhibited by pirfenidone in this bleomycin-induced lung fibrosis model [143]. In addition, Gurujeyalakshmi reported that pirfenidone suppressed the mRNA level of PDGF-A and PDGF-B in bleomycin-induced lung fibrosis in hamsters [144]. This present study demonstrated that pirfenidone inhibited macrophage infiltration and accumulation. Consistent with the previous study on the effect of pirfenidone on inflammation, IL-1β and IL-6 mRNA expression was suppressed by pirfenidone in the lung tissue of SuHx rats and in PASMCs after PDGF-BB stimulation. The effect of pirfenidone on vascular remodeling is at least partly through inhibiting the inflammatory activity to achieve.

5.5 Pirfenidone inhibited PDGFRβ-PI3K-AKT signaling pathway

Growth factors, including PDGF [32, 36], EGF [60], and VEGF [145], have been implicated in the abnormal proliferation and migration of pulmonary artery vascular cells during vascular remodeling in patients with PAH and in experimental animal models of PAH. These growth factors act as potent mitogens and chemoattractants for SMCs, fibroblasts, and ECs by binding to receptor tyrosine kinases (RTKs) as extracellular stimuli to stimulate several intracellular signaling pathways including MAP kinase, protein kinase C, Rho/Rho A kinase, and phosphoinositide 3-kinase (PI3K) /Akt pathway [146]. The PI3K/Akt signaling pathway acts an important role in vascular development and normal vascular function.

PI3K is a heterodimeric enzyme that consists of one 85-kDa regulatory subunit and one 110-kDa catalytic subunit [147] and acts as a major signaling pathway component downstream of RTKs [148, 149]. PI3K catalyzes the production of phosphatidylinositol-

3, 4, 5-triphosphate, which activates essential downstream targets, such as serine/threonine kinase Akt [150]. The PI3K-Akt pathway regulates multiple cellular processes, including cell proliferation, migration, growth, and survival [149]. Although PI3K is well characterized as a major regulator of Akt activation in response to a variety of ligands, recent studies have found a diverse group of tyrosine and serine/threonine kinases that activate Akt directly to promote its pro-proliferative signaling functions [151, 152].

The importance of PI3K/Akt signaling in normal vascular development is exemplified by gene knockout studies. Mice models have an endothelial-specific knockdown of phosphatase and a tensin homolog (PTEN), and an inhibitor of PI3K/Akt; they exhibit increased angiogenesis [153]. Akt-1 gene knockout mice demonstrate delayed vessel maturation and increased vascular permeability [154].

In addition to the important role in normal vascular development and function, the PI3K/Akt pathway participates in vascular remodeling and the development of various vascular pathologies. Goncharova's study showed that PDGF-BB stimulates PASMCs proliferation and migration by activating the PI3K/Akt signaling cascade, demonstrating that PI3K/Akt signaling is both necessary and sufficient to mediate human pulmonary vessel SMCs proliferation and migration [155]. Furgeson et al. demonstrated that the inactivation of PTEN in SMCs promotes a pro-inflammatory phenotype and enhances neointima formation [156]. Both the inhibitors of PI3K and Akt attenuated hypoxia-induced pulmonary artery remodeling in rats. However, the Akt inhibitor triciribine blocked all manifestations of PH in vivo except elevated PAP, whereas PI3K inhibitor LY294002 alone suppressed a subset of endpoints [157]. The author speculated that this finding may be due to an Akt-independent pathway [157]. However, other investigations found that the PI3K inhibitor wortmannin [158] and Akt1 [159] knockout inhibited pulmonary vascular remodeling and decreased PAP by involving a PI3K/Akt signaling hypoxia-induced PAH animal model. In the present study, pirfenidone abolished the phosphorylation of Akt and PDGFRβ that was activated in SuHx rats. In addition, the *in vitro* data show that phosphorylation of PDGFRβ, PI3K, and Akt that was induced by PDGF-BB were all inhibited by pirfenidone. It is possible that the effect of pirfenidone on hemodynamics and vascular structure changes partly due to the inhibition of PI3K/Akt signaling cascade.

Previous studies from our lab have found that PFDGFR inhibitor imatinib reverses pulmonary hemodynamics and structural changes of the pulmonary artery in the animal model of PAH. Clinical trials also show that imatinib improves hemodynamics in patients

with PAH. Based on these data that pirfenidone inhibited PDGFRβ phosphorylation *in vitro* and *in vivo*, the inhibition of the PDGFRβ pathway is another mechanism of action for the efficacy of pirfenidone.

5.6 The effects of nintedanib on SuHx rats

Nintedanib demonstrated a potent inhibitory effect on PASMCs proliferation and migration induced by PDGF-BB. The PDGF-BB-induced collagen synthesis and secretion was also reversed by nintedanib. Furthermore, *in vitro* data shows that nintedanib inhibited inflammation and reversed the phosphorylation of PDGFRβ, PI3K, and Akt. Nintedanib seems to have a strong potent inhibitory effect compared to pirfenidone according to the *in vitro* data from this present investigation.

Nintedanib is an inhibitor of the receptor tyrosine kinases PDGFR-α/β with half maximal inhibitory concentration (IC_{50}) values of 59 and 65 nmol/L[101], and the IC_{50} for imatinib on PDGFR is in the range of 100nmol/L[160]. According to the available data, imatinib improved hemodynamics and vascular remodeling by regulating PDGF signaling. Nintedanib was expected to have similar effects and be a novel therapeutic approach for the patients with PAH. However, nintedanib did not demonstrate any effect on hemodynamics; there was a tendency to decrease vascular remodeling, but no statistical significance was achieved by nintedanib treatment.

Dasatinib, another TKI, demonstrated potent inhibition of PDGF-induced responses in vascular SMC [161]. However, clinical reports show that dasatinib induces severe precapillary PH fulfilling the criteria of PAH during dasatinib treatment for chronic myeloid leukemia (CML), and dasatinib induced PAH was completely resolved or partially reversed after withdrawal of TKI [162-164]. There are several hypotheses about the opposite effect of dasatinib and imatinib on PAH. Dumitrescu et al. speculated that Src inhibition may play a role in the development of dasatinib-associated PAH, because the main known difference in the kinase profile between dasatinib and imatinib is the additional inhibition of Src family kinases. Dasatinib inhibits PDGF-induced proliferation and the migration of vascular smooth muscle cells by inhibiting PDGFR activity and PDGF-dependent Src activation downstream of the PDGFR [161], which is beneficial in PAH. However, Src family kinases are required for the degradation of activated PDGFRs [165]. Thus, inhibition of Src might lead to increased signaling by PDGF.

An additional explanation may be related to off-target kinase inhibition. These mechanisms may influence pulmonary vascular wall integrity, leading to (peri)-vascular edema and increased PVR [163]. David *et al.* have similar views on dasatinib-associated PAH, which may due to the less specific target profile of dasatinib compared to imatinib,

allowing the additional inhibition of Src and Eph receptor[162, 166]. Nintedanib also inhibits nonreceptor tyrosine kinases of the Src family with IC_{50} values of 156 nmol/L for Src, 16 nmol/L for Lck, and 195 nmol/L for Lyn [101]. Therefore, the benefits of nintedanib on PAH through the inhibition PDGF signaling may be abolished by the suppression of the Src pathway or off-target kinase inhibition.

A recent investigation found elevations in markers of endothelial dysfunction and vascular damage in the serum of CML patients treated with dasatinib, when compared with CML patients treated with imatinib [167]. This investigation showed that dasatinib treatment causes pulmonary EC dysfunction *in vivo* and *in vitro*, and induces apoptosis in cultured human pulmonary ECs through mitochondrial ROS production, independent of its action on Src family kinases. The pretreatment of rats with dasatinib exaggerates the response to MCT administration and exposure to chronic hypoxia, which are two inducers of pulmonary vascular remodeling. It is believed that increased susceptibility to PAH development is due to pulmonary vascular damage, induction of endoplasmic reticulum stress, and mitochondrial ROS production caused by dasatinib.

The previous study demonstrated that nintedanib induced apoptosis in human umbilical vascular endothelial cells, human umbilical artery smooth muscle cells, and bovine retinal pericytes [101]. It was expected that nintedanib may also induce apoptosis in PASMCs and vascular endothelial cells, which might counteract the inhibition of PDGF signaling to cancel out the therapeutic benefits of nintedanib on PAH. Furthermore, the VEGF receptor 2 blockade (subcutaneous injection of Su5416 with IC_{50} 1.23μmol/L) is the ‘first hit’ that causes lung vascular endothelial cell apoptosis, and chronic hypoxia acts as the ‘second hit’ in this SuHx model. Nintedanib is an inhibitor of VEGFR subtypes with an IC_{50} of 13-34nmol/L. Theoretically, nintedanib can also be a harmful ‘hit’ by inducing vascular endothelial cells apoptosis to initiate the development of PAH. However, the role of VEGF is complex and inconsistent in pre-clinical data, and sorafenib attenuates the development of experimental PH (in both MCT and SuHx model) by inhibition of VEGF signaling [52, 53]. Since VEGF signaling plays a complex role in pulmonary pathophysiology, whether nintedanib can induce apoptosis in PASMCs or ECs via VEGF signaling is currently unknown and further study is required.

5.7 Limitations of this study

All three layers of the vessel wall are involved in the process of vascular remodeling. In addition to PASMCs, endothelial cells, fibroblasts, inflammatory cells, and platelets also play significant roles in PAH [111]. For example, EC apoptosis has been implicated as an initiating event in experimental PAH, leading either directly to the degeneration of

pre-capillary arterioles or to the selection of hyperproliferative, apoptosis-resistant, endothelial cells that may contribute to angioproliferative plexiform lesions. This study focused on PASMCs, and the effects of pirfenidone on ECs and other types of cells should be investigated in future experiments.

The net balance between apoptosis and proliferation determines the growth of PASMCs. Furthermore, the inhibition of apoptosis in PASMCs is involved in the development and progression of pulmonary arterial medial hypertrophy [168]. The effect of pirfenidone on the induction and enhancement of PASMCs apoptosis was not investigated. Previous studies of pirfenidone have either demonstrated no effect on apoptosis [132] or reduced apoptosis [89, 169]. Pirfenidone probably would not increase apoptosis to against the apoptosis-resistant phenomenon during the vascular remodeling process, which is required future research to investigate.

Since nintedanib did not show efficacy in RVSP, RV function, hypertrophy, or vascular remodeling in the SuHx rat model, further *in vivo* study of nintedanib on inflammation, collagen expression, and vascular proliferation was not performed although nintedanib demonstrated potent effects on PASMCs proliferation, migration, and other functional processes that were induced by PDGF-BB *in vitro*. The effect of nintedanib on EC apoptosis and the consequence of Src inhibition were not investigated, which may be a reason against benefits from inhibition PDGF signaling pathway.

5.8 Conclusion

In summary, this is the first paper to describe the successful therapeutic use of pirfenidone in a well-accepted animal model of PAH. Pirfenidone significantly attenuated PAP and vascular remodeling, and effectively improved RV function and RV hypertrophy. Although the key target molecule for pirfenidone is not yet clear and further research is needed to elucidate its precise mechanism of action, pirfenidone appears to exert inhibitory effects on multiple pathways that lead to the development of PAH. The multifunctional activity of pirfenidone includes suppression of inflammation, proliferation, migration, and collagen deposition of PASMCs by acting on the PDGF and PI3K/Akt signaling cascade. Pirfenidone has been prescribed to IPF patients since 2008 and has been well tolerated without severe side effects, and its clinical development as a new indication for PAH and PH due to lung disease through vascular remodeling might be imminent.

PDGF-BB-induced PASMCs proliferation, migration, and inflammation, and collagen synthesis and phosphorylation of PDGF/PI3K/Akt signaling were inhibited or reversed

by nintedanib in an *in vitro* study. Nintedanib demonstrated potent inhibitory effects on the PDGF signaling pathway, but did not show therapeutic effects on the SuHx rat model.

6 Summary

Pulmonary hypertension, defined by an mPAP of 25 mm Hg or more at rest, is a severe, progressive disease with no cure. In addition, PAH is characterized by an angioproliferative vasculopathy, mainly in the small pulmonary arteries, which results in progressive pulmonary vascular remodeling, increased pulmonary vascular resistance, and right ventricle dysfunction and failure. The proliferation, migration, and collagen synthesis of PASMCs play critical roles in pulmonary vascular remodeling.

Current pharmacotherapies that are approved for PAH treatment are focused on vasodilators. These therapeutic approaches relieve the pulmonary vasoconstrictive component of the disease and provide symptomatic relief with some amelioration in the prognosis. However, there is no strong evidence supporting that these vasodilators have a direct antiproliferative effect on PAMSCs, and the underlying pathological pulmonary vessels and right ventricle remodeling still progress. Therefore, future medical intervention strategies must go beyond vasodilation, for the medicine targeting vascular remodeling processes in pulmonary vasculature to have great potential therapeutic value and a promising future.

Both pirfenidone and nintedanib were approved for treatment IPF in 2014 by the FDA, ending an era without effective pharmacologic therapy for IPF. Based on the antifibrotic effect of pirfenidone and nintedanib in experimental pulmonary fibrosis and IPF patients, it was hypothesized that pirfenidone may inhibit collagen synthesis and the cell proliferation of PASMCs induced by growth factors in PH. Thus, the effects of pirfenidone and nintedanib on proliferation, migration, collagen synthesis, and inflammation in vitro were investigated. The efficacy of pirfenidone and nintedanib on hemodynamics and pulmonary vascular remodeling were also investigated in a PAH animal model.

An *in vitro* cellular study showed that both pirfenidone and nintedanib inhibited proliferation, migration, inflammation, collagen synthesis, and collagen secretion that was induced by PDGF. The PDGF-induced phosphorylation of PDGFRβ/PI3K/Akt signaling was also inhibited by these two compounds.

Given the promising *in vitro* effects, an experimental PAH rat model (SuHx) induced by a Sugen5416 injection and three weeks of hypoxia exposure was employed to evaluate the efficacy of pirfenidone and nintedanib in vivo. Pirfenidone treatment decreased the elevated RVSP, improved impaired RV function, and inhibited RV hypertrophy in SuHx rats. The pulmonary vascular remodeling in SuHx rats was also ameliorated after treatment with pirfenidone. To explore the mechanism of action for pirfenidone on vascular remodeling, vascular cells proliferation, collagen deposition, and

inflammation were investigated. Pirfenidone decreased vascular cells proliferation and collagen deposition, and suppressed inflammation by inhibiting phosphorylation of the PDGFRβ/Akt pathway. However, nintedanib did not demonstrate therapeutic effects on vascular remodeling, RVSP, RV function, or hypertrophy in the SuHx model.

In summary, this is the first paper to describe the successful therapeutic use of pirfenidone in a well-accepted animal model of PAH. Pirfenidone significantly attenuated PAH and the vascular remodeling, and effectively improved RV function and RV hypertrophy. Pirfenidone appears to exert inhibitory effects on multiple pathways that lead to the development of PAH, which includes the suppression of inflammation, proliferation, migration, and collagen deposition of PASMCs by acting on PDGF and the PI3K/Akt signaling cascade. The clinical development of pirfenidone as a new indication for PAH and PH due to lung disease through the improvement of vascular remodeling might be imminent. Nintedanib demonstrated potent inhibitory effects on cellular function in vitro, but did not show therapeutic effects in the SuHx rat model.

7 ZUSAMMENFASSUNG

De Lungenhochdruck (PAH) ist eine schwere, fortschreitende Erkrankung ohne Aussicht auf Heilung. PAH ist charakteriziert durch eine überwiegend in den kleinen Lungenarterien ablaufende angioproliferative Vaskulopathie, welche zu fortschreitenden Lungengefäßumbauprozessen, gesteigertem Lungengefäßwiderstand gefolgt von einer rechten Kammerdysfunktion und Kammerversagen, führt. Die Proliferation, Migration und Kollagensezernierung von glatten pulmonalen arteriellen Muskelzellen (PASMCs) spielen eine entscheidende Rolle in den Umbauprozessen der Pulmonalarterie.

Aktuelle Pharmakotherapien, welche für die PAH zugelassen sind, greifen auf der Grundlage der Gefäßerweiterung. Diese therapeutischen Ansätze vermindern die vasokonstriktive Komponente der Krankheit und führen zu einer Symptomlinderung sowie einer kleinen Prognoseverbesserung. Nichtsdestotrotz gibt es keine aussagekräftigen Anhaltspunkte, welche die Vasoldilatatoren im Hinblick auf einen direkten antiproliferativen Effekt auf PASMCs unterstützen und der zugrunde liegende pathologische Gefäßwandumbau und rechter Ventrikelumbau schreitet weiter voran. Deswegen müssen zukünftige medikamentöse Therapien über Vasodilatatoren hinausgehen, und Medikamente, welche in die Umbauprozesse der Lungengefäße eingreifen, haben eine potentiell großen Wert und eine vielversprechende Zukunft.

Pirfenidone und Nintedanib sind beide für die Behandlung der idiopathischen Lungenfibrose durch die FDA 2014 zugelassen worden, welches damit das Ende des Zeitalters einer fehlenden effektiven Pharmakotherapie der IPF eingeleitet hat. Auf dem antifbrotischen Effekt von Pirfenidone und Nintedanib in experimenteller Lungenfibrose und IPF Patienten zurückführend, wurde die Hypothese aufgestellt, dass Pirfenidone die Kollagensynthese und Zellproliferation von PASMCs, welche durch Wachstumsfaktoren bei Lungenhochdruck induziert werden, hemmt. Daher wurde untersucht inwieweit Pirfenidone und Nintedanib die Proliferation, Migration Kollagensynthese und Entzündung in vitro beeinflussen würden. Weiterhin wurde die Wirksamkeit von Pirfenidone/Nintedanib auf die Hämodynamik und die Umbauprozess der Lungengefäße in einem PAH Tiermodell überprüft.

In vitro Experimente zeigten, dass sowohl Pirfenidone als auch Nintedanib die PDGF induzierte Proliferation von PASMCs hemmen. Beide Substanzen hemmen auch die Migration, Entzündung, Kollagensynthese und Kollagensezernierung der PASMCs, welche durch PDGF induziert wurde. Zusätzlich wurde die durch PDGF bedingte Phosphorylierung von PDGFRβ/PI3K/AKT ebenfalls durch beide Substanzen blockiert.

ZUSAMMENFASSUNG

Im Zuge dieser vielversprechenden in vitro Effekte, wurde ein experimentelles PAH Rattenmodell (SuHx) angewendet, welches durch die Injektion von Sugen 5416, in Kombination mit 3 Wochen Hypoxie, induziert wurde um die Wirksamkeit von Pirfenidone und Nintedanib in vivo zu erproben. Die Behandlung mit Pirfenidone verminderte den erhöhten rechtsventrikulären systolischen Druck, verbesserte die beeinträchtigte RV Funktion und hemmte die RV-Hypertrophie in SuHx Ratten. Die Umbauprozesse der Lungengefäße in den SuHx Ratten wurde ebenfalls verbessert. Um den genauen Mechanismus von Pirfenidone auf den positiven Effekt bezüglich der Gefäßumbauprozesse zu untersuchen, wurde der Einfluss von Pirfenidone auf die Gefässzellen im Hinblick auf Proliferation, Kollagensezernierung und Entzündung in der Lunge überprüft. Pirfenidone verminderte die Zellproliferation, Kollagensezernierung und unterdrückte Entzündungserscheinungen durch die Hemmung der Phosphorylierung im PDGFRβ/Akt Signalweg. Nintedanib jedoch zeigte keinen therapeutischen Wert hinsichtlich der Gefäßumbauprozesse, RVSP, RV Funktion und Hypertrophie im SuHx Modell.

Schlussfolgernd lässt sich nun also sagen, dass erstmalig der erfolgreiche therapeutische Nutzen von Pirfenidone in einem gut akzeptierten Tiermodel der PAH beschrieben werden konnte. Pirfenidone verbessert signifikant den arteriellen Lungenhochdruck und die Gefäßumbauprozesse, verbessert die RV-Funktion sowie RV-Hypertrophie. Pirfenidone scheint inhibierende Wirkungen auf verschieden Signalwege, welche zur Entwicklung von PAH führen, welche die Unterdrückung von Entzündung, Proliferation, Migration und Kollagensezernierung beinhaltet, in dem es auf die PDGF und PI3k/Akt Signalkaskade wirkt, zu haben. Die klinische Entwicklung von Pirfenidone als ein neues Mittel für arteriellen Lungenhochdruck oder Lungenhochdruck welches auf Lungenerkrankungen zurückzuführen ist, könnte nun also bevorstehen. Nintedanib zeigte hemmende Effekte auf die zelluläre Funktion in vitro aber keine therapeutischen Effekte im SuHx Ratten Modell.

8 Reference

1. Romberg, E., *Ueber Sklerose der Lungen arterie.* Dtsch Archiv Klin Med, 1891 **48**: p. 197-206.
2. Dresdale, D.T., M. Schultz, and R.J. Michtom, *Primary pulmonary hypertension. I. Clinical and hemodynamic study.* Am J Med, 1951. **11**(6): p. 686-705.
3. Lau, E.M., et al., *The 2015 ESC/ERS Guidelines for the diagnosis and treatment of pulmonary hypertension: a practical chronicle of progress.* Eur Respir J, 2015. **46**(4): p. 879-82.
4. Simonneau, G., et al., *Updated clinical classification of pulmonary hypertension.* J Am Coll Cardiol, 2013. **62**(25 Suppl): p. D34-41.
5. Nazzareno Galie, M.H., Jean-Luc Vachiery, Simon Gibbs, Irene Lang, Adam Torbicki, Gerald Simonneau, Andrew Peacock, Anton Vonk Noordegraaf, Maurice Beghetti, Ardeschir Ghofrani, Miguel Angel Gomez Sanchez, Georg Hansmann, Walter Klepetko, Patrizio Lancellotti, Marco Matucci, Theresa McDonagh, Luc A. Pierard, Pedro T. Trindade, Maurizio Zompatori and Marius Hoeper, *2015 ESC/ERS Guidelines for the diagnosis and treatment of pulmonary hypertension* Eur Respir J, 2015. **46**(6): p. 1855-6.
6. Hoeper, M.M., et al., *Treatment of pulmonary hypertension.* Lancet Respir Med, 2016. **4**(4): p. 323-36.
7. Schermuly, R.T., et al., *Mechanisms of disease: pulmonary arterial hypertension.* Nat Rev Cardiol, 2011. **8**(8): p. 443-55.
8. Kim, N.H., et al., *Chronic thromboembolic pulmonary hypertension.* J Am Coll Cardiol, 2013. **62**(25 Suppl): p. D92-9.
9. Humbert, M., et al., *Advances in therapeutic interventions for patients with pulmonary arterial hypertension.* Circulation, 2014. **130**(24): p. 2189-208.
10. McLaughlin, V.V., et al., *Management of pulmonary arterial hypertension.* J Am Coll Cardiol, 2015. **65**(18): p. 1976-97.
11. D'Alonzo, G.E., et al., *Survival in patients with primary pulmonary hypertension. Results from a national prospective registry.* Ann Intern Med, 1991. **115**(5): p. 343-9.
12. Benza, R.L., et al., *An evaluation of long-term survival from time of diagnosis in pulmonary arterial hypertension from the REVEAL Registry.* Chest, 2012. **142**(2): p. 448-56.
13. Hurdman, J., et al., *ASPIRE registry: assessing the Spectrum of Pulmonary hypertension Identified at a REferral centre.* Eur Respir J, 2012. **39**(4): p. 945-55.
14. Olsson, K.M., et al., *Anticoagulation and survival in pulmonary arterial hypertension: results from the Comparative, Prospective Registry of Newly Initiated Therapies for Pulmonary Hypertension (COMPERA).* Circulation, 2014. **129**(1): p. 57-65.
15. Ventetuolo, C.E., et al., *Sex and haemodynamics in pulmonary arterial hypertension.* Eur Respir J, 2014. **43**(2): p. 523-30.
16. Rabinovitch, M., *Molecular pathogenesis of pulmonary arterial hypertension.* J Clin Invest, 2012. **122**(12): p. 4306-13.
17. Shimoda, L.A. and S.S. Laurie, *Vascular remodeling in pulmonary hypertension.* J Mol Med (Berl), 2013. **91**(3): p. 297-309.
18. Archer, S.L., E.K. Weir, and M.R. Wilkins, *Basic science of pulmonary arterial hypertension for clinicians: new concepts and experimental therapies.* Circulation, 2010. **121**(18): p. 2045-66.
19. Eddahibi, S., et al., *Cross talk between endothelial and smooth muscle cells in pulmonary hypertension: critical role for serotonin-induced smooth muscle hyperplasia.* Circulation, 2006. **113**(15): p. 1857-64.
20. Lai, Y.C., et al., *Pulmonary arterial hypertension: the clinical syndrome.* Circ Res, 2014. **115**(1): p. 115-30.
21. Giaid, A. and D. Saleh, *Reduced expression of endothelial nitric oxide synthase in the lungs of patients with pulmonary hypertension.* N Engl J Med, 1995. **333**(4): p. 214-21.
22. Fagan, K.A., et al., *The pulmonary circulation of homozygous or heterozygous eNOS-null mice is hyperresponsive to mild hypoxia.* J Clin Invest, 1999. **103**(2): p. 291-9.
23. Namba, T., et al., *cDNA cloning of a mouse prostacyclin receptor. Multiple signaling pathways and expression in thymic medulla.* J Biol Chem, 1994. **269**(13): p. 9986-92.

REFERENCE

24. Christman, B.W., et al., *An imbalance between the excretion of thromboxane and prostacyclin metabolites in pulmonary hypertension.* N Engl J Med, 1992. **327**(2): p. 70-5.
25. Hoshikawa, Y., et al., *Prostacyclin receptor-dependent modulation of pulmonary vascular remodeling.* Am J Respir Crit Care Med, 2001. **164**(2): p. 314-8.
26. Tuder, R.M., et al., *Prostacyclin synthase expression is decreased in lungs from patients with severe pulmonary hypertension.* Am J Respir Crit Care Med, 1999. **159**(6): p. 1925-32.
27. Yanagisawa, M., et al., *A novel potent vasoconstrictor peptide produced by vascular endothelial cells.* Nature, 1988. **332**(6163): p. 411-5.
28. Tabima, D.M., S. Frizzell, and M.T. Gladwin, *Reactive oxygen and nitrogen species in pulmonary hypertension.* Free Radic Biol Med, 2012. **52**(9): p. 1970-86.
29. Giaid, A., et al., *Expression of endothelin-1 in the lungs of patients with pulmonary hypertension.* N Engl J Med, 1993. **328**(24): p. 1732-9.
30. Stewart, D.J., et al., *Increased plasma endothelin-1 in pulmonary hypertension: marker or mediator of disease?* Ann Intern Med, 1991. **114**(6): p. 464-9.
31. Rubens, C., et al., *Big endothelin-1 and endothelin-1 plasma levels are correlated with the severity of primary pulmonary hypertension.* Chest, 2001. **120**(5): p. 1562-9.
32. Humbert, M., et al., *Platelet-derived growth factor expression in primary pulmonary hypertension: comparison of HIV seropositive and HIV seronegative patients.* Eur Respir J, 1998. **11**(3): p. 554-9.
33. Balasubramaniam, V., et al., *Role of platelet-derived growth factor in vascular remodeling during pulmonary hypertension in the ovine fetus.* Am J Physiol Lung Cell Mol Physiol, 2003. **284**(5): p. L826-33.
34. Perros, F., et al., *Platelet-derived growth factor expression and function in idiopathic pulmonary arterial hypertension.* Am J Respir Crit Care Med, 2008. **178**(1): p. 81-8.
35. Cohen, E.D., et al., *Wnt signaling regulates smooth muscle precursor development in the mouse lung via a tenascin C/PDGFR pathway.* J Clin Invest, 2009. **119**(9): p. 2538-49.
36. Schermuly, R.T., et al., *Reversal of experimental pulmonary hypertension by PDGF inhibition.* J Clin Invest, 2005. **115**(10): p. 2811-21.
37. Frost, A.E., et al., *Long-term safety and efficacy of imatinib in pulmonary arterial hypertension.* J Heart Lung Transplant, 2015. **34**(11): p. 1366-75.
38. Benisty, J.I., et al., *Elevated basic fibroblast growth factor levels in patients with pulmonary arterial hypertension.* Chest, 2004. **126**(4): p. 1255-61.
39. Li, P., et al., *Fibroblast growth factor mediates hypoxia-induced endothelin-- a receptor expression in lung artery smooth muscle cells.* J Appl Physiol (1985), 2003. **95**(2): p. 643-51; discussion 863.
40. Quinn, T.P., et al., *Cyclic mechanical stretch induces VEGF and FGF-2 expression in pulmonary vascular smooth muscle cells.* Am J Physiol Lung Cell Mol Physiol, 2002. **282**(5): p. L897-903.
41. Wedgwood, S., et al., *Fibroblast growth factor-2 expression is altered in lambs with increased pulmonary blood flow and pulmonary hypertension.* Pediatr Res, 2007. **61**(1): p. 32-6.
42. Kwapiszewska, G., et al., *Expression profiling of laser-microdissected intrapulmonary arteries in hypoxia-induced pulmonary hypertension.* Respir Res, 2005. **6**: p. 109.
43. Izikki, M., et al., *Endothelial-derived FGF2 contributes to the progression of pulmonary hypertension in humans and rodents.* J Clin Invest, 2009. **119**(3): p. 512-23.
44. Hayashi, S., et al., *Potential role of hepatocyte growth factor, a novel angiogenic growth factor, in peripheral arterial disease: downregulation of HGF in response to hypoxia in vascular cells.* Circulation, 1999. **100**(19 Suppl): p. Ii301-8.
45. Ono, M., et al., *Hepatocyte growth factor suppresses vascular medial hyperplasia and matrix accumulation in advanced pulmonary hypertension of rats.* Circulation, 2004. **110**(18): p. 2896-902.
46. Ono, M., et al., *Gene transfer of hepatocyte growth factor with prostacyclin synthase in severe pulmonary hypertension of rats.* Eur J Cardiothorac Surg, 2004. **26**(6): p. 1092-7.
47. Geiger, R., et al., *Enhanced expression of vascular endothelial growth factor in pulmonary plexogenic arteriopathy due to congenital heart disease.* J Pathol, 2000. **191**(2): p. 202-7.

REFERENCE

48. Tuder, R.M., et al., *Expression of angiogenesis-related molecules in plexiform lesions in severe pulmonary hypertension: evidence for a process of disordered angiogenesis.* J Pathol, 2001. **195**(3): p. 367-74.
49. Partovian, C., et al., *Heart and lung VEGF mRNA expression in rats with monocrotaline- or hypoxia-induced pulmonary hypertension.* Am J Physiol, 1998. **275**(6 Pt 2): p. H1948-56.
50. Partovian, C., et al., *Cardiac and lung VEGF mRNA expression in chronically hypoxic and monocrotaline-treated rats.* Chest, 1998. **114**(1 Suppl): p. 45s-46s.
51. Taraseviciene-Stewart, L., et al., *Inhibition of the VEGF receptor 2 combined with chronic hypoxia causes cell death-dependent pulmonary endothelial cell proliferation and severe pulmonary hypertension.* Faseb j, 2001. **15**(2): p. 427-38.
52. Klein, M., et al., *Combined tyrosine and serine/threonine kinase inhibition by sorafenib prevents progression of experimental pulmonary hypertension and myocardial remodeling.* Circulation, 2008. **118**(20): p. 2081-90.
53. Moreno-Vinasco, L., et al., *Genomic assessment of a multikinase inhibitor, sorafenib, in a rodent model of pulmonary hypertension.* Physiol Genomics, 2008. **33**(2): p. 278-91.
54. Taraseviciene-Stewart, L., et al., *Simvastatin causes endothelial cell apoptosis and attenuates severe pulmonary hypertension.* Am J Physiol Lung Cell Mol Physiol, 2006. **291**(4): p. L668-76.
55. Campbell, A.I., et al., *Cell-based gene transfer of vascular endothelial growth factor attenuates monocrotaline-induced pulmonary hypertension.* Circulation, 2001. **104**(18): p. 2242-8.
56. Farkas, L., et al., *VEGF ameliorates pulmonary hypertension through inhibition of endothelial apoptosis in experimental lung fibrosis in rats.* J Clin Invest, 2009. **119**(5): p. 1298-311.
57. Partovian, C., et al., *Adenovirus-mediated lung vascular endothelial growth factor overexpression protects against hypoxic pulmonary hypertension in rats.* Am J Respir Cell Mol Biol, 2000. **23**(6): p. 762-71.
58. Le Cras, T.D., et al., *Disrupted pulmonary vascular development and pulmonary hypertension in transgenic mice overexpressing transforming growth factor-alpha.* Am J Physiol Lung Cell Mol Physiol, 2003. **285**(5): p. L1046-54.
59. Dahal, B.K., et al., *Role of epidermal growth factor inhibition in experimental pulmonary hypertension.* Am J Respir Crit Care Med, 2010. **181**(2): p. 158-67.
60. Merklinger, S.L., et al., *Epidermal growth factor receptor blockade mediates smooth muscle cell apoptosis and improves survival in rats with pulmonary hypertension.* Circulation, 2005. **112**(3): p. 423-31.
61. Pardali, E. and P. Ten Dijke, *TGFbeta signaling and cardiovascular diseases.* Int J Biol Sci, 2012. **8**(2): p. 195-213.
62. Shi, Y. and J. Massague, *Mechanisms of TGF-beta signaling from cell membrane to the nucleus.* Cell, 2003. **113**(6): p. 685-700.
63. Harrison, R.E., et al., *Molecular and functional analysis identifies ALK-1 as the predominant cause of pulmonary hypertension related to hereditary haemorrhagic telangiectasia.* J Med Genet, 2003. **40**(12): p. 865-71.
64. Machado, R.D., et al., *Genetics and genomics of pulmonary arterial hypertension.* J Am Coll Cardiol, 2009. **54**(1 Suppl): p. S32-42.
65. Trembath, R.C., et al., *Clinical and molecular genetic features of pulmonary hypertension in patients with hereditary hemorrhagic telangiectasia.* N Engl J Med, 2001. **345**(5): p. 325-34.
66. Chaouat, A., et al., *Endoglin germline mutation in a patient with hereditary haemorrhagic telangiectasia and dexfenfluramine associated pulmonary arterial hypertension.* Thorax, 2004. **59**(5): p. 446-8.
67. Pullamsetti, S.S., et al., *Inflammation, immunological reaction and role of infection in pulmonary hypertension.* Clin Microbiol Infect, 2011. **17**(1): p. 7-14.
68. Tuder, R.M., et al., *Exuberant endothelial cell growth and elements of inflammation are present in plexiform lesions of pulmonary hypertension.* Am J Pathol, 1994. **144**(2): p. 275-85.

REFERENCE

69. Cool, C.D., et al., *Pathogenesis and evolution of plexiform lesions in pulmonary hypertension associated with scleroderma and human immunodeficiency virus infection.* Hum Pathol, 1997. **28**(4): p. 434-42.
70. Humbert, M., et al., *Increased interleukin-1 and interleukin-6 serum concentrations in severe primary pulmonary hypertension.* Am J Respir Crit Care Med, 1995. **151**(5): p. 1628-31.
71. Itoh, T., et al., *Increased plasma monocyte chemoattractant protein-1 level in idiopathic pulmonary arterial hypertension.* Respirology, 2006. **11**(2): p. 158-63.
72. Voelkel, N.F., et al., *Interleukin-1 receptor antagonist treatment reduces pulmonary hypertension generated in rats by monocrotaline.* Am J Respir Cell Mol Biol, 1994. **11**(6): p. 664-75.
73. Bhargava, A., et al., *Monocrotaline induces interleukin-6 mRNA expression in rat lungs.* Heart Dis, 1999. **1**(3): p. 126-32.
74. Miyata, M., et al., *Pulmonary hypertension in rats. 2. Role of interleukin-6.* Int Arch Allergy Immunol, 1995. **108**(3): p. 287-91.
75. Steiner, M.K., et al., *Interleukin-6 overexpression induces pulmonary hypertension.* Circ Res, 2009. **104**(2): p. 236-44, 28p following 244.
76. Savale, L., et al., *Impact of interleukin-6 on hypoxia-induced pulmonary hypertension and lung inflammation in mice.* Respir Res, 2009. **10**: p. 6.
77. Tozzi, C.A., et al., *Excess collagen in hypertensive pulmonary arteries decreases vascular distensibility.* Am J Respir Crit Care Med, 1994. **149**(5): p. 1317-26.
78. Ooi, C.Y., et al., *The role of collagen in extralobar pulmonary artery stiffening in response to hypoxia-induced pulmonary hypertension.* Am J Physiol Heart Circ Physiol, 2010. **299**(6): p. H1823-31.
79. Frumkin, L.R., *The pharmacological treatment of pulmonary arterial hypertension.* Pharmacol Rev, 2012. **64**(3): p. 583-620.
80. de Raaf, M.A., et al., *SuHx rat model: partly reversible pulmonary hypertension and progressive intima obstruction.* Eur Respir J, 2014. **44**(1): p. 160-8.
81. Firth, A.L., J. Mandel, and J.X. Yuan, *Idiopathic pulmonary arterial hypertension.* Dis Model Mech, 2010. **3**(5-6): p. 268-73.
82. Stenmark, K.R., et al., *Animal models of pulmonary arterial hypertension: the hope for etiological discovery and pharmacological cure.* Am J Physiol Lung Cell Mol Physiol, 2009. **297**(6): p. L1013-32.
83. Gomez-Arroyo, J.G., et al., *The monocrotaline model of pulmonary hypertension in perspective.* Am J Physiol Lung Cell Mol Physiol, 2012. **302**(4): p. L363-9.
84. Kay, J.M., P. Harris, and D. Heath, *Pulmonary hypertension produced in rats by ingestion of Crotalaria spectabilis seeds.* Thorax, 1967. **22**(2): p. 176-9.
85. Kasahara, Y., et al., *Inhibition of VEGF receptors causes lung cell apoptosis and emphysema.* J Clin Invest, 2000. **106**(11): p. 1311-9.
86. Nicolls, M.R., et al., *New models of pulmonary hypertension based on VEGF receptor blockade-induced endothelial cell apoptosis.* Pulm Circ, 2012. **2**(4): p. 434-42.
87. Takeda, Y., et al., *Efficacy and safety of pirfenidone for idiopathic pulmonary fibrosis.* Patient Prefer Adherence, 2014. **8**: p. 361-70.
88. Iyer, S.N., et al., *Dietary intake of pirfenidone ameliorates bleomycin-induced lung fibrosis in hamsters.* J Lab Clin Med, 1995. **125**(6): p. 779-85.
89. Macias-Barragan, J., et al., *The multifaceted role of pirfenidone and its novel targets.* Fibrogenesis Tissue Repair, 2010. **3**: p. 16.
90. Schaefer, C.J., et al., *Antifibrotic activities of pirfenidone in animal models.* Eur Respir Rev, 2011. **20**(120): p. 85-97.
91. Nagai, S., et al., *Open-label compassionate use one year-treatment with pirfenidone to patients with chronic pulmonary fibrosis.* Intern Med, 2002. **41**(12): p. 1118-23.
92. Noble, P.W., et al., *Pirfenidone in patients with idiopathic pulmonary fibrosis (CAPACITY): two randomised trials.* Lancet, 2011. **377**(9779): p. 1760-9.
93. King, T.E., Jr., et al., *A phase 3 trial of pirfenidone in patients with idiopathic pulmonary fibrosis.* N Engl J Med, 2014. **370**(22): p. 2083-92.
94. Nathan, S.D., et al., *Effect of pirfenidone on mortality: pooled analyses and meta-analyses of clinical trials in idiopathic pulmonary fibrosis.* Lancet Respir Med, 2017. **5**(1): p. 33-41.

REFERENCE

95. Karimi-Shah, B.A. and B.A. Chowdhury, *Forced vital capacity in idiopathic pulmonary fibrosis--FDA review of pirfenidone and nintedanib.* N Engl J Med, 2015. **372**(13): p. 1189-91.
96. *FDA website*. Available from: **https://www.accessdata.fda.gov/scripts/cder/daf/index.cfm?event=overview.process&ApplNo=022535.**
97. Sharma, K., et al., *Pirfenidone for diabetic nephropathy.* J Am Soc Nephrol, 2011. **22**(6): p. 1144-51.
98. Fernandez, I.E. and O. Eickelberg, *The impact of TGF-beta on lung fibrosis: from targeting to biomarkers.* Proc Am Thorac Soc, 2012. **9**(3): p. 111-6.
99. Artlett, C.M., *Inflammasomes in wound healing and fibrosis.* J Pathol, 2013. **229**(2): p. 157-67.
100. Misra, H.P. and C. Rabideau, *Pirfenidone inhibits NADPH-dependent microsomal lipid peroxidation and scavenges hydroxyl radicals.* Mol Cell Biochem, 2000. **204**(1-2): p. 119-26.
101. Hilberg, F., et al., *BIBF 1120: triple angiokinase inhibitor with sustained receptor blockade and good antitumor efficacy.* Cancer Res, 2008. **68**(12): p. 4774-82.
102. Antoniu, S.A. and M.R. Kolb, *Intedanib, a triple kinase inhibitor of VEGFR, FGFR and PDGFR for the treatment of cancer and idiopathic pulmonary fibrosis.* IDrugs, 2010. **13**(5): p. 332-45.
103. Roth, G.J., et al., *Nintedanib: from discovery to the clinic.* J Med Chem, 2015. **58**(3): p. 1053-63.
104. Jenkins, G. and A. Goodwin, *Novel approaches to pulmonary fibrosis.* Clin Med (Lond), 2014. **14 Suppl 6**: p. s45-9.
105. Richeldi, L., et al., *Efficacy and safety of nintedanib in idiopathic pulmonary fibrosis.* N Engl J Med, 2014. **370**(22): p. 2071-82.
106. Wollin, L., et al., *Mode of action of nintedanib in the treatment of idiopathic pulmonary fibrosis.* Eur Respir J, 2015. **45**(5): p. 1434-45.
107. Dimitroulis, I.A., *Nintedanib: a novel therapeutic approach for idiopathic pulmonary fibrosis.* Respir Care, 2014. **59**(9): p. 1450-5.
108. Ma, W., et al., *Calpain mediates pulmonary vascular remodeling in rodent models of pulmonary hypertension, and its inhibition attenuates pathologic features of disease.* J Clin Invest, 2011. **121**(11): p. 4548-66.
109. Lang, M., et al., *The soluble guanylate cyclase stimulator riociguat ameliorates pulmonary hypertension induced by hypoxia and SU5416 in rats.* PLoS One, 2012. **7**(8): p. e43433.
110. Schermuly, R.T., et al., *Antiremodeling effects of iloprost and the dual-selective phosphodiesterase 3/4 inhibitor tolafentrine in chronic experimental pulmonary hypertension.* Circ Res, 2004. **94**(8): p. 1101-8.
111. Humbert, M., et al., *Cellular and molecular pathobiology of pulmonary arterial hypertension.* J Am Coll Cardiol, 2004. **43**(12 Suppl S): p. 13s-24s.
112. Mandegar, M., et al., *Cellular and molecular mechanisms of pulmonary vascular remodeling: role in the development of pulmonary hypertension.* Microvasc Res, 2004. **68**(2): p. 75-103.
113. Tuder, R.M., et al., *Pathology of pulmonary hypertension.* Clin Chest Med, 2007. **28**(1): p. 23-42, vii.
114. Tajsic, T. and N.W. Morrell, *Smooth muscle cell hypertrophy, proliferation, migration and apoptosis in pulmonary hypertension.* Compr Physiol, 2011. **1**(1): p. 295-317.
115. Maarman, G., et al., *A comprehensive review: the evolution of animal models in pulmonary hypertension research; are we there yet?* Pulm Circ, 2013. **3**(4): p. 739-56.
116. Yu, Y., et al., *PDGF stimulates pulmonary vascular smooth muscle cell proliferation by upregulating TRPC6 expression.* Am J Physiol Cell Physiol, 2003. **284**(2): p. C316-30.
117. Rubin, L.J., *Primary pulmonary hypertension.* N Engl J Med, 1997. **336**(2): p. 111-7.
118. Grimminger, F. and R.T. Schermuly, *PDGF receptor and its antagonists: role in treatment of PAH.* Adv Exp Med Biol, 2010. **661**: p. 435-46.
119. Conte, E., et al., *Effect of pirfenidone on proliferation, TGF-beta-induced myofibroblast differentiation and fibrogenic activity of primary human lung fibroblasts.* Eur J Pharm Sci, 2014. **58**: p. 13-9.

REFERENCE

120. Lee, B.S., S.B. Margolin, and R.A. Nowak, *Pirfenidone: a novel pharmacological agent that inhibits leiomyoma cell proliferation and collagen production.* J Clin Endocrinol Metab, 1998. **83**(1): p. 219-23.
121. Lee, K., et al., *Antifibrotic effect of pirfenidone on human pterygium fibroblasts.* Curr Eye Res, 2014. **39**(7): p. 680-5.
122. Hewitson, T.D., et al., *Pirfenidone reduces in vitro rat renal fibroblast activation and mitogenesis.* J Nephrol, 2001. **14**(6): p. 453-60.
123. Shi, Q., et al., *In vitro effects of pirfenidone on cardiac fibroblasts: proliferation, myofibroblast differentiation, migration and cytokine secretion.* PLoS One, 2011. **6**(11): p. e28134.
124. Di Sario, A., et al., *Effect of pirfenidone on rat hepatic stellate cell proliferation and collagen production.* J Hepatol, 2002. **37**(5): p. 584-91.
125. Yang, Y., et al., *Inhibition of pirfenidone on TGF-beta2 induced proliferation, migration and epithlial-mesenchymal transition of human lens epithelial cells line SRA01/04.* PLoS One, 2013. **8**(2): p. e56837.
126. Melchers, F., A.G. Rolink, and C. Schaniel, *The role of chemokines in regulating cell migration during humoral immune responses.* Cell, 1999. **99**(4): p. 351-4.
127. Luster, A.D., R. Alon, and U.H. von Andrian, *Immune cell migration in inflammation: present and future therapeutic targets.* Nat Immunol, 2005. **6**(12): p. 1182-90.
128. Yamaguchi, H., J. Wyckoff, and J. Condeelis, *Cell migration in tumors.* Curr Opin Cell Biol, 2005. **17**(5): p. 559-64.
129. Yi, E.S., et al., *Distribution of obstructive intimal lesions and their cellular phenotypes in chronic pulmonary hypertension. A morphometric and immunohistochemical study.* Am J Respir Crit Care Med, 2000. **162**(4 Pt 1): p. 1577-86.
130. Nishimura, T., et al., *Simvastatin rescues rats from fatal pulmonary hypertension by inducing apoptosis of neointimal smooth muscle cells.* Circulation, 2003. **108**(13): p. 1640-5.
131. Li, G., et al., *Oral pirfenidone protects against fibrosis by inhibiting fibroblast proliferation and TGF-beta signaling in a murine colitis model.* Biochem Pharmacol, 2016. **117**: p. 57-67.
132. Wang, J., et al., *Pirfenidone inhibits migration, differentiation, and proliferation of human retinal pigment epithelial cells in vitro.* Mol Vis, 2013. **19**: p. 2626-35.
133. Nossaman, B.D. and P.J. Kadowitz, *The role of the RhoA/rho-kinase pathway in pulmonary hypertension.* Curr Drug Discov Technol, 2009. **6**(1): p. 59-71.
134. Shimokawa, H., S. Sunamura, and K. Satoh, *RhoA/Rho-Kinase in the Cardiovascular System.* Circ Res, 2016. **118**(2): p. 352-66.
135. Fukumoto, Y., et al., *Acute vasodilator effects of a Rho-kinase inhibitor, fasudil, in patients with severe pulmonary hypertension.* Heart, 2005. **91**(3): p. 391-2.
136. Fukumoto, Y., et al., *Double-blind, placebo-controlled clinical trial with a rho-kinase inhibitor in pulmonary arterial hypertension.* Circ J, 2013. **77**(10): p. 2619-25.
137. Li, F.H., et al., *Inhibition of rho kinase attenuates high flow induced pulmonary hypertension in rats.* Chin Med J (Engl), 2007. **120**(1): p. 22-9.
138. Choi, K., et al., *Pirfenidone inhibits transforming growth factor-beta1-induced fibrogenesis by blocking nuclear translocation of Smads in human retinal pigment epithelial cell line ARPE-19.* Mol Vis, 2012. **18**: p. 1010-20.
139. Minamino, T., et al., *Targeted expression of heme oxygenase-1 prevents the pulmonary inflammatory and vascular responses to hypoxia.* Proc Natl Acad Sci U S A, 2001. **98**(15): p. 8798-803.
140. Miyata, M., et al., *Pulmonary hypertension in rats. 1. Role of bromodeoxyuridine-positive mononuclear cells and alveolar macrophages.* Int Arch Allergy Immunol, 1995. **108**(3): p. 281-6.
141. Stow, J.L., et al., *Cytokine secretion in macrophages and other cells: pathways and mediators.* Immunobiology, 2009. **214**(7): p. 601-12.
142. Nakazato, H., et al., *A novel anti-fibrotic agent pirfenidone suppresses tumor necrosis factor-alpha at the translational level.* Eur J Pharmacol, 2002. **446**(1-3): p. 177-85.
143. Oku, H., et al., *Antifibrotic action of pirfenidone and prednisolone: different effects on pulmonary cytokines and growth factors in bleomycin-induced murine pulmonary fibrosis.* Eur J Pharmacol, 2008. **590**(1-3): p. 400-8.

REFERENCE

144. Gurujeyalakshmi, G., M.A. Hollinger, and S.N. Giri, *Pirfenidone inhibits PDGF isoforms in bleomycin hamster model of lung fibrosis at the translational level.* Am J Physiol, 1999. **276**(2 Pt 1): p. L311-8.
145. Sakao, S., et al., *VEGF-R blockade causes endothelial cell apoptosis, expansion of surviving CD34+ precursor cells and transdifferentiation to smooth muscle-like and neuronal-like cells.* Faseb j, 2007. **21**(13): p. 3640-52.
146. Hassoun, P.M., et al., *Inflammation, growth factors, and pulmonary vascular remodeling.* J Am Coll Cardiol, 2009. **54**(1 Suppl): p. S10-9.
147. Carpenter, C.L., et al., *Purification and characterization of phosphoinositide 3-kinase from rat liver.* J Biol Chem, 1990. **265**(32): p. 19704-11.
148. Chen, H.C. and J.L. Guan, *Association of focal adhesion kinase with its potential substrate phosphatidylinositol 3-kinase.* Proc Natl Acad Sci U S A, 1994. **91**(21): p. 10148-52.
149. Cantley, L.C., *The phosphoinositide 3-kinase pathway.* Science, 2002. **296**(5573): p. 1655-7.
150. Jiang, B.H., et al., *Myogenic signaling of phosphatidylinositol 3-kinase requires the serine-threonine kinase Akt/protein kinase B.* Proc Natl Acad Sci U S A, 1999. **96**(5): p. 2077-81.
151. Jiang, B.H., et al., *Phosphatidylinositol 3-kinase signaling mediates angiogenesis and expression of vascular endothelial growth factor in endothelial cells.* Proc Natl Acad Sci U S A, 2000. **97**(4): p. 1749-53.
152. Mahajan, K. and N.P. Mahajan, *PI3K-independent AKT activation in cancers: a treasure trove for novel therapeutics.* J Cell Physiol, 2012. **227**(9): p. 3178-84.
153. Hamada, K., et al., *The PTEN/PI3K pathway governs normal vascular development and tumor angiogenesis.* Genes Dev, 2005. **19**(17): p. 2054-65.
154. Chen, J., et al., *Akt1 regulates pathological angiogenesis, vascular maturation and permeability in vivo.* Nat Med, 2005. **11**(11): p. 1188-96.
155. Goncharova, E.A., et al., *PI3K is required for proliferation and migration of human pulmonary vascular smooth muscle cells.* Am J Physiol Lung Cell Mol Physiol, 2002. **283**(2): p. L354-63.
156. Furgeson, S.B., et al., *Inactivation of the tumour suppressor, PTEN, in smooth muscle promotes a pro-inflammatory phenotype and enhances neointima formation.* Cardiovasc Res, 2010. **86**(2): p. 274-82.
157. Garat, C.V., et al., *Inhibition of phosphatidylinositol 3-kinase/Akt signaling attenuates hypoxia-induced pulmonary artery remodeling and suppresses CREB depletion in arterial smooth muscle cells.* J Cardiovasc Pharmacol, 2013. **62**(6): p. 539-48.
158. Xia, X.D., et al., *Suppression of Phosphatidylinositol 3-Kinase/Akt Signaling Attenuates Hypoxia-Induced Pulmonary Hypertension Through the Downregulation of Lysyl Oxidase.* DNA Cell Biol, 2016. **35**(10): p. 599-606.
159. Tang, H., et al., *Deficiency of Akt1, but not Akt2, attenuates the development of pulmonary hypertension.* Am J Physiol Lung Cell Mol Physiol, 2015. **308**(2): p. L208-20.
160. Capdeville, R., et al., *Glivec (STI571, imatinib), a rationally developed, targeted anticancer drug.* Nat Rev Drug Discov, 2002. **1**(7): p. 493-502.
161. Chen, Z., et al., *Potent inhibition of platelet-derived growth factor-induced responses in vascular smooth muscle cells by BMS-354825 (dasatinib).* Mol Pharmacol, 2006. **69**(5): p. 1527-33.
162. Montani, D., et al., *Pulmonary arterial hypertension in patients treated by dasatinib.* Circulation, 2012. **125**(17): p. 2128-37.
163. Dumitrescu, D., et al., *Fully reversible pulmonary arterial hypertension associated with dasatinib treatment for chronic myeloid leukaemia.* Eur Respir J, 2011. **38**(1): p. 218-20.
164. Shah, N.P., et al., *Clinical features of pulmonary arterial hypertension in patients receiving dasatinib.* Am J Hematol, 2015. **90**(11): p. 1060-4.
165. Rosenkranz, S., et al., *Src family kinases negatively regulate platelet-derived growth factor alpha receptor-dependent signaling and disease progression.* J Biol Chem, 2000. **275**(13): p. 9620-7.
166. Swords, R., et al., *Nilotinib: optimal therapy for patients with chronic myeloid leukemia and resistance or intolerance to imatinib.* Drug Des Devel Ther, 2009. **3**: p. 89-101.

REFERENCE

167. Guignabert, C., et al., *Dasatinib induces lung vascular toxicity and predisposes to pulmonary hypertension.* J Clin Invest, 2016. **126**(9): p. 3207-18.
168. Gurbanov, E. and X. Shiliang, *The key role of apoptosis in the pathogenesis and treatment of pulmonary hypertension.* Eur J Cardiothorac Surg, 2006. **30**(3): p. 499-507.
169. Shihab, F.S., et al., *Effect of pirfenidone on apoptosis-regulatory genes in chronic cyclosporine nephrotoxicity.* Transplantation, 2005. **79**(4): p. 419-26.

9 Index of Tables

INDEX OF FIGURES

10 Index of Figures

INDEX OF FIGURES

11 Abbreviation

AC: adenylyl cyclase

ALK1: activin receptor-like kinase 1

APS: ammonium persulfate

ATP: adenosine triphosphate

BH2: dihydrobiopterin

BH4: tetrahydrobiopterin

BMPR2: bone morphogenic protein receptor type II

BSA: bovine serum albumin

CAV1: caveolin-1

CD68: cluster of differentiation 68

cDNA: complementary deoxyribonucleic acid

cGMP: guanosine 3’,5’-monophosphate

CI: Cardiac index

CML: chronic myeloid leukemia

CO: Cardiac output

COX: cyclooxygenase

Ct: threshold cycle

CTEPH: chronic thromboembolic pulmonary hypertension

Da: dalton

DAPI: 4', 6-diamidino-2-phenylindole

DMSO: Dimethyl sulfoxide

DPBS: Dulbecco's Phosphate-Buffered Saline

EC: endothelial cell

ECEs: endothelin-converting enzymes

ECG: Electrocardiography

ECL: Enhanced chemiluminescence

ECM: extracellular matrix

EDTA: Ethylenediaminetetraacetic acid

EGF: epidermal growth factor

endo-MT: endothelial mesenchymal transition

ENG: endoglin

eNOS: endothelial NO synthase enzyme

ET-1: endothelin-1

ETA: endothelin receptor type A

ABBREVIATION

et al.: et alii (and others)

ETB: endothelin receptor type B

FAK: focal adhesion kinase

FDA: Food and Drug Administration

FGF: fibroblast growth factor `

FGFR-1: fibroblast growth factor receptor-1

FLT3: Fms-like tyrosine kinase-3

FRS2: FGFR substrate 2

g: gram

GTP: guanosine 5'-triphosphate

Grb2: growth factor receptor-bound protein 2

Hg: hydrargyrum

HGF: hepatocyte growth factor

HIV: human immunodeficiency virus

HRP: horse radish peroxidase

HSP: heat shock protein

IFN: interferon

IPAH: idiopathic pulmonary arterial hypertension

IPF: idiopathic pulmonary fibrosis

kb: kilo base

KCNK3: potassium channel, two pore domain subfamily K, member 3

KCl: Potassium chloride

kDa: kilo dalton

KH_2PO_4M: monopotassium phosphate

IC_{50}: maximal inhibitory concentration

IL-1: interleukin-1

IL-1β: interleukin-1β

IL-6: interleukin-6

i.m.: intramuscular

i.p.: intraperitoneal

M: molar (mole/litre)

MEK1/2: mitogen-activated protein kinase kinase 1/2

MCP: monocyte chemoattractant protein

MCT: monocrotaline-treated

min: minute(s)

ABBREVIATION

miRNA: microRNA

mg: milligram

ml: milliliter

mm: millimeter

mM: millimolar

mPA: mean pulmonary artery pressure

Na_2HPO_4: disodium phosphate

NaCl: sodium chloride

NADPH: nicotinamide adenine dinucleotide phosphate

nm: nanometer

nM: nanomolar

NO: nitric oxide

NOX: normoxia

nRTKs: non-receptor tyrosine kinases

PAH: pulmonary arterial hypertension

PAP: pulmonary artery pressure

PASMCs: pulmonary artery smooth muscle cells

PAWP: pulmonary artery wedge pressure

PBS: phosphate-buffered saline

PCNA: Proliferating Cell Nuclear Antigen

PCR: polymerase chain reaction

PDE5: phosphodiesterase 5

PDGF: platelet derived growth factor

PDGFR: platelet derived growth factor receptor

PFA: paraformaldehyde

PH: pulmonary hypertension

PI3K: phosphatidylinositol-4,5-bisphosphate 3-kinase

PIP2/3: phosphatidylinositol-2/3-phosphate

PKA: protein kinase A

PKC: protein kinase C

PKG: protein kinase G

PLC-γ: phospholipase C-γ

PPARs: peroxisome proliferator-activated receptors

PTEN: phosphatase and tensin homolog

PVR: pulmonary vascular resistance

ABBREVIATION

qRT-PCR: quantitative real-time polymerase chain reaction
RIPA: radio immunoprecipitation assay
RNA: ribonucleic acid
ROS: reactive oxygen species
rpm: revolution per minute
RT: room temperature
RVSP: right ventricular systolic pressure
RVID: right ventricle internal diameter
SDS-PAGE: SDS-polyacrylamide gel electrophoresis
sGC: soluble guanylyl cyclase
SM: smooth muscle
SMAD: mothers against decapentaplegic homolog
SmBM: smooth muscle basal medium
SMC: smooth muscle cell
SmGM-2: smooth muscle growth medium-2
SOS: son of sevenless
SV: stroke volume
TBST: Tris-buffered saline and Tween 20
TEMED: tetramethylethylenediamine
TGF-α: transforming growth factor alpha
TGFβ: transforming growth factor β
TKR: tyrosine kinase receptors
TNF: tumor necrosis factor
V: volt
VEGF: vascular endothelial growth factor
VEGFR2: vascular endothelial growth factor receptor 2
WU: Wood units
µg: microgram
µl: microliter
µm: micrometer
µM: micromolar

12 ORAL AND POSTER PRESENTATIONS

12.1 Oral presentations:

- June 2015 - Annual Retreat of International Graduate Programme Molecular Biology and Medicine of the Lung, Rauischholzhausen, Germany; ‘Pirfenidone, a new candidate for pulmonary arterial hypertension’?

- July 2016 - Annual Retreat of International Graduate Programme Molecular Biology and Medicine of the Lung, Rauischholzhausen, Germany; ‘Effects of nintedanib on vessel remodeling in experimental pulmonary hypertension’.

12.2 Poster presentations:

- August 2014 - Annual Retreat of International Graduate Programme Molecular Biology and Medicine of the Lung, Rauischholzhausen, Germany; ‘Pirfenidone, a new candidate for pulmonary arterial hypertension’?

- September 2016 - European Respiratory Society International Conference, London, UK, ‘Anti-fibrotic effects of pirfenidone on pulmonary arterial vascular smooth muscle cells’.

13 Declaration

I declare that I have completed this dissertation single-handedly without the unauthorized help of a second party and only with the assistance acknowledged therein. I have appropriately acknowledged and referenced all text passages that are derived literally from, or are based on, the content of the published or unpublished work of others and all information that relates to verbal communications. I have abided by the principles of good scientific conduct outlined in the charter of the Justus Liebig University of Giessen while conducting the investigations described in this dissertation.

.....

Changwu Lu 2017, Giessen

14 Acknowledgements

I would like to take this opportunity to thank all the people, without whom this dissertation would not have existed.

First and foremost, I would like to express my sincere gratitude to my supervisor, Prof. Dr. rer. nat. Ralph Schermuly for his immense knowledge, constructive ideas, discussion, and support. It was a great honor for me to be his PhD student.

I would also like to thank Prof. Dr. rer. nat. Michael Martin for the insightful comments and advice on my thesis.

In addition, I would like to express sincere gratitude to Dr. Baktybek Kojonazarov for his initiation of this project, his guidance and support during this project, and his helpful comments and experimental advice.

A special thank you to Dr. Tatyana Novoyatleva for her experimental suggestions and many helpful comments.

I would like to thank Christina Vroom for her great effort towards the animal experiment, as well as Carina Lepper, David Dippel, and Stephie Viehmann for organizing everyday lab work.

I would also like to express gratitude to Ewa Bieniek for the help with histology work.

I sincerely thank Dr. Rory Morty, Dr. Elie El Agha, Dr. Florian Veit, and Dr. Anita Golec for their teaching talent and excellent tutoring in the Molecular Biology and Medicine of the Lung graduate program.

I would also like to give a special thank you to Prof. Dr. Werner Seeger, who provided all possible conditions for research.

My thanksThank you also to Prof. Dr. Norbert Weissmann, Prof. Dr. Ardeschir Ghofrani, Prof. Dr. Andreas Günther, and Prof. Dr. Friedrich Grimminger for the cooperative support.

I would like to take this opportunity to thank the Universities of Giessen and Marburg Lung Center (UGMLC) for the financial support.

Special thanksIn addition, a special thank you goes to Andreas Owczarek for the translation of the summary of this thesis.

I would also like to thank all my wonderful colleagues for offering experimental tips, and for the nice working atmosphere they created and all those enjoyable moments outside of work.

I would like to thank Daniela Weber, Lisa Marie Junker, and Saba Viehmann for organizing all lab meetings, research progress meetings, seminars, and conferences.

ACKNOWLEDGEMENTS

Furthermore, I greatly appreciate Dr. Xia Tian, Dr. Zhigang Lu, Dr. Kai Ni, Dr. Qingkui, Jiang, Dr, Fei Song, and all my Chinese friends for their friendship and their kind help and moral support during my study and life in Giessen.

Most importantly, I thank my beloved parents for their unconditional love and support throughout my life. This thesis is dedicated to my father in heaven. You are far away but always present in my heart.

Finally, I express my appreciation to my wife Yuanjun Ma whose dedication, love, and persistent confidence in me has taken the load off my shoulder during my studies and who has taken care of the whole family. Finally, I cannot forget my daughter Zoe Lu who has made my life full of joy and happiness during this period. Without them, I would not be at this stage in my life.